

Westinghouse Non-Proprietary Class 3

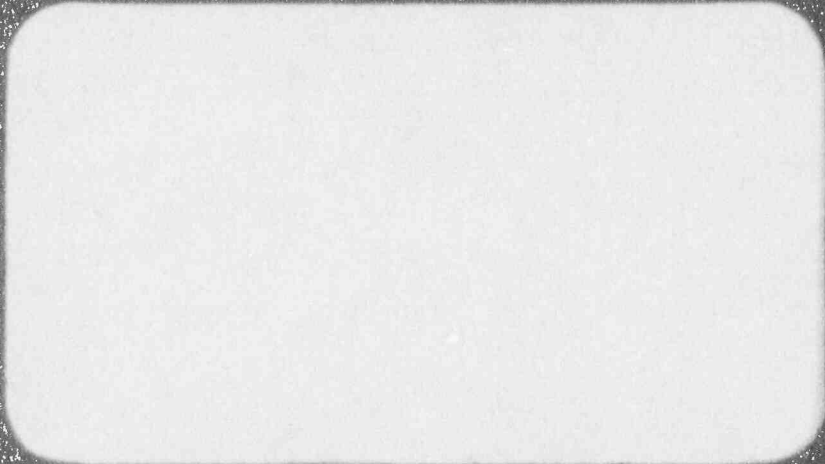


Westinghouse Energy Systems



9404120274 940404
PDR ADDCK 05000424
PDR

Westinghouse Non-Proprietary Class 3



Westinghouse Energy Systems



9404120274 940404
PDR ADOCK 05000424
P PDR

WCAP-13931

ANALYSIS OF CAPSULE Y FROM THE
GEORGIA POWER COMPANY VOGTLE UNIT 1
REACTOR VESSEL RADIATION
SURVEILLANCE PROGRAM

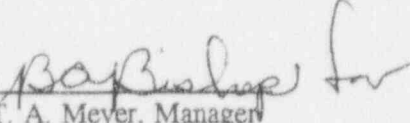
M. J. Malone
S. S. Zawalick
A. Madeyski

February 1994

Work Performed Under Shop Order GTXP-106

Prepared by Westinghouse Electric Corporation
for the Georgia Power Company

Approved by:


T. A. Meyer, Manager
Structural Reliability and
Plant Life Optimization

WESTINGHOUSE ELECTRIC CORPORATION
Nuclear and Advanced Technology Division
P.O. Box 355
Pittsburgh, Pennsylvania 15230-0355

PREFACE

This report has been technically reviewed and verified.

	Reviewer:	
Sections 1 through 5, 7, 8, and Appendix A	E. Terek	<u>Ed Terek</u>
Appendix B	B. A. Bishop	<u>B.A. Bishop</u>
Section 6	E. P. Lippincott	<u>E.P. Lippincott</u>

TABLE OF CONTENTS

<u>Section</u>	<u>Title</u>	<u>Page</u>
1.0	SUMMARY OF RESULTS	1-1
2.0	INTRODUCTION	2-1
3.0	BACKGROUND	3-1
4.0	DESCRIPTION OF PROGRAM	4-1
5.0	TESTING OF SPECIMENS FROM CAPSULE Y	5-1
	5.1 Overview	5-1
	5.2 Charpy V-Notch Impact Test Results	5-3
	5.3 Tension Test Results	5-5
	5.4 Compact Tension Specimen Tests	5-6
6.0	RADIATION ANALYSIS AND NEUTRON DOSIMETRY	6-1
	6.1 Introduction	6-1
	6.2 Discrete Ordinates Analysis	6-2
	6.3 Neutron Dosimetry	6-6
	6.4 Projections of Pressure Vessel Exposure	6-10
7.0	SURVEILLANCE CAPSULE REMOVAL SCHEDULE	7-1
8.0	REFERENCES	8-1
APPENDIX A -	LOAD-TIME RECORDS FOR CHARPY SPECIMEN TESTS	
APPENDIX B -	HEATUP AND COOLDOWN LIMIT CURVES FOR NORMAL OPERATION OF THE VOGTLE UNIT 1 REACTOR PRESSURE VESSEL	

LIST OF TABLES

<u>Table</u>	<u>Title</u>	<u>Page</u>
4-1	Chemical Composition of the Vogtle Unit 1 Reactor Vessel Intermediate Shell Plate B8805-3	4-3
4-2	Chemical Composition (wt%) of the Vogtle Unit 1 Reactor Vessel Surveillance Weld Metal	4-4
4-3	Heat Treatment of the Vogtle Unit 1 Reactor Vessel Surveillance Materials	4-5
4-4	Chemistry Results from the Low Alloy Steel NIST Certified Reference Standards	4-6
5-1	Charpy V-notch Data for the Vogtle Unit 1 Intermediate Shell Plate B8805-3 Irradiated at 550°F to a Fluence of 1.24×10^{19} n/cm ² (E > 1.0 MeV) (Longitudinal Orientation)	5-7
5-2	Charpy V-notch Data for the Vogtle Unit 1 Intermediate Shell Plate B8805-3 Irradiated at 550°F to a Fluence of 1.24×10^{19} n/cm ² (E > 1.0 MeV) (Transverse Orientation)	5-8
5-3	Charpy V-notch Data for the Vogtle Unit 1 Surveillance Weld Metal Irradiated at 550°F to a Fluence of 1.24×10^{19} n/cm ² (E > 1.0 MeV)	5-9
5-4	Charpy V-notch Data for the Vogtle Unit 1 Heat-Affected-Zone (HAZ) Metal Irradiated at 550°F to a Fluence of 1.24×10^{19} n/cm ² (E > 1.0 MeV)	5-10
5-5	Instrumented Charpy Impact Test Results for the Vogtle Unit 1 Intermediate Shell Plate B8805-3 Irradiated at 550°F to a Fluence of 1.24×10^{19} n/cm ² (E > 1.0 MeV) (Longitudinal Orientation)	5-11

LIST OF TABLES (continued)

<u>Table</u>	<u>Title</u>	<u>Page</u>
5-6	Instrumented Charpy Impact Test Results for the Vogtle Unit 1 Intermediate Shell Plate B8805-3 Irradiated at 550°F to a Fluence of 1.24×10^{19} n/cm ² (E > 1.0 MeV) (Transverse Orientation)	5-12
5-7	Instrumented Charpy Impact Test Results for the Vogtle Unit 1 Surveillance Weld Metal Irradiated at 550°F to a Fluence of 1.24×10^{19} n/cm ² (E > 1.0 MeV)	5-13
5-8	Instrumented Charpy Impact Test Results for the Vogtle Unit 1 Surveillance Heat-Affected-Zone (HAZ) Metal Irradiated at 550°F to a Fluence of 1.24×10^{19} n/cm ² (E > 1.0 MeV)	5-14
5-9	Effect of 550°F Irradiation to 1.24×10^{19} n/cm ² (E > 1.0 MeV) on the Notch Toughness Properties of the Vogtle Unit 1 Reactor Vessel Surveillance Materials	5-15
5-10	Comparison of the Vogtle Unit 1 Surveillance Material 30 ft-lb Transition Temperature Shifts and Upper Shelf Energy Decreases with Regulatory Guide 1.99 Revision 2 Predictions	5-16
5-11	Tensile Properties of the Vogtle Unit 1 Reactor Vessel Surveillance Materials Irradiated at 550°F to 1.24×10^{19} n/cm ² (E > 1.0 MeV)	5-17
6-1	Calculated Fast Neutron Exposure Rates at the Surveillance Capsule Center	6-14
6-2	Calculated Azimuthal Variation of Fast Neutron Exposure Rates at the Pressure Vessel Clad/Base Metal Interface	6-15
6-3	Relative Radial Distribution of $\phi(E > 1.0 \text{ MeV})$ within the Pressure Vessel Wall	6-16

LIST OF TABLES (continued)

<u>Table</u>	<u>Title</u>	<u>Page</u>
6-4	Relative Radial Distribution of $\phi(E > 0.1 \text{ MeV})$ within the Pressure Vessel Wall	6-17
6-5	Relative Radial Distribution of dpa/sec within the Pressure Vessel Wall	6-18
6-6	Nuclear Parameters used in the Evaluation of Neutron Sensors	6-19
6-7	Monthly Thermal Generation During the First Four Fuel Cycles of the Vogtle Unit 1 Reactor	6-20
6-8	Measured Sensor Activities and Reaction Rates Surveillance Capsule Y Saturated Activities and Derived Fast Neutron Flux	6-21
6-9	Summary of Neutron Dosimetry Results Surveillance Capsules Y and U	6-22
6-10	Comparison of Measured and Ferret Calculated Reaction Rates at the Surveillance Capsule Center Surveillance Capsule Y	6-23
6-11	Adjusted Neutron Energy Spectrum at the Center of the Surveillance Capsule Y	6-24
6-12	Comparison of Calculated and Measured Neutron Exposure Levels for Vogtle Unit 1 Surveillance Capsules Y and U	6-25
6-13	Neutron Exposure Projections at Key Locations on the Pressure Vessel Clad/Base Metal Interface	6-26
6-14	Neutron Exposure Values at the 1/4 and 3/4 depths into the Reactor Vessel Wall	6-27

LIST OF TABLES (continued)

<u>Table</u>	<u>Title</u>	<u>Page</u>
6-15	Updated Lead Factors for Vogtle Unit 1 Surveillance Capsules	6-28
7-1	Vogtle Unit 1 Reactor Vessel Surveillance Capsule Withdrawal Schedule	7-1

LIST OF ILLUSTRATIONS

<u>Figure</u>	<u>Title</u>	<u>Page</u>
4-1	Arrangement of Surveillance Capsules in the Vogtle Unit 1 Reactor Vessel	4-8
4-2	Capsule Y Diagram Showing the Location of Specimens, Thermal Monitors and Dosimeters	4-9
5-1	Charpy V-Notch Impact Properties for Vogtle Unit 1 Reactor Vessel Intermediate Shell Plate B8805-3 (Longitudinal Orientation)	5-18
5-2	Charpy V-Notch Impact Properties for Vogtle Unit 1 Reactor Vessel Intermediate Shell Plate B8805-3 (Transverse Orientation)	5-19
5-3	Charpy V-Notch Impact Properties for Vogtle Unit 1 Reactor Vessel Surveillance Weld Metal	5-20
5-4	Charpy V-Notch Impact Properties for Vogtle Unit 1 Reactor Vessel Weld Heat-Affected-Zone Metal	5-21
5-5	Charpy Impact Specimen Fracture Surfaces for Vogtle Unit 1 Reactor Vessel Intermediate Shell Plate B8805-3 (Longitudinal Orientation)	5-22
5-6	Charpy Impact Specimen Fracture Surfaces for Vogtle Unit 1 Reactor Vessel Intermediate Shell Plate B8805-3 (Transverse Orientation)	5-23
5-7	Charpy Impact Specimen Fracture Surfaces for Vogtle Unit 1 Reactor Vessel Surveillance Weld Metal	5-24
5-8	Charpy Impact Specimen Fracture Surfaces for Vogtle Unit 1 Reactor Vessel Heat-Affected-Zone Metal	5-25

LIST OF ILLUSTRATIONS (continued)

<u>Figure</u>	<u>Title</u>	<u>Page</u>
5-9	Tensile Properties for Vogtle Unit 1 Reactor Vessel Intermediate Shell Plate B8805-3 (Longitudinal Orientation)	5-26
5-10	Tensile Properties for Vogtle Unit 1 Reactor Vessel Intermediate Shell Plate B8805-3 (Transverse Orientation)	5-27
5-11	Tensile Properties for Vogtle Unit 1 Reactor Vessel Surveillance Weld Metal	5-28
5-12	Fractured Tensile Specimens from Vogtle Unit 1 Reactor Vessel Intermediate Shell Plate B8805-3 (Longitudinal Orientation)	5-29
5-13	Fractured Tensile Specimens from Vogtle Unit 1 Reactor Vessel Intermediate Shell Plate B8805-3 (Transverse Orientation)	5-30
5-14	Fractured Tensile Specimens from Vogtle Unit 1 Reactor Vessel Surveillance Weld Metal	5-31
5-15	Engineering Stress-Strain Curves for Intermediate Shell Plate B8805-3 Tensile Specimens AL13 and AL14 (Longitudinal Orientation)	5-32
5-16	Engineering Stress-Strain Curve for Intermediate Shell Plate B8805-3 Tensile Specimen AL15 (Longitudinal Orientation)	5-33
5-17	Engineering Stress-Strain Curves for Intermediate Shell Plate B8805-3 Tensile Specimens AT13 and AT14 (Transverse Orientation)	5-34
5-18	Engineering Stress-Strain Curve for Intermediate Shell Plate B8805-3 Tensile Specimen AT15 (Transverse Orientation)	5-35

LIST OF ILLUSTRATIONS (continued)

<u>Figure</u>	<u>Title</u>	<u>Page</u>
5-19	Engineering Stress-Strain Curves for Weld Metal Tensile Specimens AW13 and AW14	5-36
5-20	Engineering Stress-Strain Curve for Weld Tensile Specimen AW15	5-37
6-1	Plan View of a Dual Reactor Vessel Surveillance Capsule	6-12
6-2	Axial Distribution of Neutron Fluence ($E > 1.0$ MeV) Along the 45 Degree Azimuth	6-13

SECTION 1.0
SUMMARY OF RESULTS

The analysis of the reactor vessel materials contained in surveillance Capsule Y, the second capsule to be removed from the Vogtle Unit 1 reactor pressure vessel, led to the following conclusions:

- o The capsule received an average fast neutron fluence ($E > 1.0$ MeV) of 1.24×10^{19} n/cm² after 4.64 effective full power years (EFPY) of plant operation.
- o Irradiation of the reactor vessel intermediate shell plate B8805-3 Charpy specimens, oriented with the longitudinal axis of the specimen parallel to the major rolling direction of the plate (longitudinal orientation), to 1.24×10^{19} n/cm² ($E > 1.0$ MeV) resulted in a 30 ft-lb transition temperature increase of 40°F and a 50 ft-lb transition temperature increase of 35°F. This results in an irradiated 30 ft-lb transition temperature of 25°F and an irradiated 50 ft-lb transition temperature of 55°F for the longitudinally oriented specimens.
- o Irradiation of the reactor vessel intermediate shell plate B8805-3 Charpy specimens, oriented with the longitudinal axis of the specimen normal to the major rolling direction of the plate (transverse orientation), to 1.24×10^{19} n/cm² ($E > 1.0$ MeV) resulted in a 30 ft-lb transition temperature increase of 20°F and a 50 ft-lb transition temperature increase of 30°F. This results in an irradiated 30 ft-lb transition temperature of 35°F and an irradiated 50 ft-lb transition temperature of 95°F for transversely oriented specimens.
- o Irradiation of the weld metal Charpy specimens to 1.24×10^{19} n/cm² ($E > 1.0$ MeV) resulted in no 30 and 50 ft-lb transition temperature increases. Thus, the irradiated 30 ft-lb transition temperature remains at -40°F and the irradiated 50 ft-lb transition temperature remains at -25°F.
- o Irradiation of the weld Heat-Affected-Zone (HAZ) metal Charpy specimens to 1.24×10^{19} n/cm² ($E > 1.0$ MeV) resulted in 30 and 50 ft-lb transition temperature increases of 25°F. This results in an irradiated 30 ft-lb transition temperature of -50°F and an irradiated 50 ft-lb transition temperature of -25°F.

- o The average upper shelf energy of the intermediate shell plate B8805-3 (longitudinal orientation) resulted in no average energy decrease after irradiation to 1.24×10^{19} n/cm² (E > 1.0 MeV). Thus, the unirradiated average upper shelf energy of 122 ft-lbs for the longitudinally oriented specimens remains unchanged.
- o The average upper shelf energy of the intermediate shell plate B8805-3 (transverse orientation) resulted in no average energy decrease after irradiation to 1.24×10^{19} n/cm² (E > 1.0 MeV). Thus, the unirradiated average upper shelf energy of 96 ft-lbs for the transversely oriented specimens remains unchanged.
- o The average upper shelf energy of the weld metal Charpy specimens resulted in an average energy decrease of 1 ft-lb after irradiation to 1.24×10^{19} n/cm² (E > 1.0 MeV). This results in an irradiated average upper shelf energy of 144 ft-lbs for the weld metal specimens.
- o The average upper shelf energy of the weld HAZ metal decreased 12 ft-lbs after irradiation to 1.24×10^{19} n/cm² (E > 1.0 MeV). This results in an irradiated average upper shelf energy of 124 ft-lbs for the weld HAZ metal.
- o The surveillance Capsule Y test results indicate that the surveillance material 30 ft-lb transition temperature increases and the average upper shelf energy decreases are less than the Regulatory Guide 1.99, Revision 2⁽¹⁾ predictions.
- o The calculated end-of-license (32 EFPY) maximum neutron fluences (E > 1.0 MeV) for the Vogtle Unit 1 reactor vessel are as follows:

$$\text{Vessel inner radius}^* = 2.176 \times 10^{19} \text{ n/cm}^2$$

$$\text{Vessel 1/4 thickness} = 1.188 \times 10^{19} \text{ n/cm}^2$$

$$\text{Vessel 3/4 thickness} = 2.568 \times 10^{18} \text{ n/cm}^2$$

* Clad/base metal interface

SECTION 2.0 INTRODUCTION

This report presents the results of the examination of Capsule Y, the second capsule to be removed from the reactor in the continuing surveillance program which monitors the effects of neutron irradiation on the Georgia Power Company Alvin W. Vogtle Unit 1 reactor pressure vessel materials under actual operating conditions.

The surveillance program for the Georgia Power Company Vogtle Unit 1 reactor pressure vessel materials was designed and recommended by the Westinghouse Electric Corporation. A description of the surveillance program and the preirradiation mechanical properties of the reactor vessel materials is presented in Westinghouse Report WAP-011, "Georgia Power Company Alvin W. Vogtle Unit No. 1 Reactor Vessel Radiation Surveillance Program"^[2]. The surveillance program was planned to cover the 40-year design life of the reactor pressure vessel and was based on ASTM E185-82, "Standard Practice for Conducting Surveillance Tests for Light-Water Cooled Nuclear Power Reactor Vessels"^[3]. Capsule "Y" was removed from the reactor after less than 5 EFPY of exposure and shipped to the Westinghouse Science and Technology Center Hot Cell Facility, where the postirradiation mechanical testing of the Charpy V-notch impact and tensile surveillance specimens was performed.

This report summarizes the testing of and the postirradiation data obtained from surveillance capsule "Y" removed from the Georgia Power Company Vogtle Unit 1 reactor vessel and discusses the analysis of the data.

SECTION 3.0 BACKGROUND

The ability of the large steel pressure vessel containing the reactor core and its primary coolant to resist fracture constitutes an important factor in ensuring safety in the nuclear industry. The beltline region of the reactor pressure vessel is the most critical region of the vessel because it is subjected to significant fast neutron bombardment. The overall effects of fast neutron irradiation on the mechanical properties of low alloy, ferritic pressure vessel steels such as A533 Grade B Class 1 (base material of the Vogtle Unit 1 reactor pressure vessel) are well documented in the literature. Generally, low alloy ferritic materials show an increase in hardness and tensile properties and a decrease in ductility and toughness during high-energy irradiation.

A method for performing analyses to guard against fast fracture in reactor pressure vessels has been presented in "Protection Against Nonductile Failure," Appendix G to Section III of the ASME Boiler and Pressure Vessel Code^[4]. The method uses fracture mechanics concepts and is based on the reference nil-ductility transition temperature (RT_{NDT}).

RT_{NDT} is defined as the greater of either the drop weight nil-ductility transition temperature (NDTT per ASTM E-208^[5]) or the temperature 60°F less than the 50 ft-lb (and 35-mil lateral expansion) temperature as determined from Charpy specimens oriented normal (transverse) to the major working direction of the plate. The RT_{NDT} of a given material is used to index that material to a reference stress intensity factor curve (K_{IR} curve) which appears in Appendix G to the ASME Code^[4]. The K_{IR} curve is a lower bound of dynamic, crack arrest, and static fracture toughness results obtained from several heats of pressure vessel steel. When a given material is indexed to the K_{IR} curve, allowable stress intensity factors can be obtained for this material as a function of temperature. Allowable operating limits can then be determined using these allowable stress intensity factors.

RT_{NDT} and, in turn, the operating limits of nuclear power plants can be adjusted to account for the effects of radiation on the reactor vessel material properties. The radiation embrittlement changes in mechanical properties of a given reactor pressure vessel steel can be monitored by a reactor surveillance program, such as the Vogtle Unit 1 Reactor Vessel Radiation Surveillance Program^[2], in which a surveillance capsule is periodically removed from the operating nuclear reactor and the encapsulated specimens tested.

The increase in the average Charpy V-notch temperature (ΔRT_{NDT} at 30 ft-lbs) due to irradiation is added to the initial RT_{NDT} to adjust the RT_{NDT} (ΔRT) for radiation embrittlement. This ART (RT_{NDT} initial + ΔRT_{NDT}) is used to index the material to the K_{IR} curve and, in turn, to set operating limits for the nuclear power plant that take into account the effects of irradiation on the reactor vessel materials.

SECTION 4.0
DESCRIPTION OF PROGRAM

Six surveillance capsules for monitoring the effects of neutron exposure on the Vogtle Unit 1 reactor pressure vessel core region materials were inserted in the reactor vessel prior to initial plant start-up. The six capsules were positioned in the reactor vessel between the neutron pads and the vessel wall as shown in Figure 4-1. The vertical center of the capsules is opposite the vertical center of the core. The capsules contain specimens made from intermediate shell plate B8805-3 (Heat No. C0623-1) and weld metal fabricated with 3/16-inch Mil B-4 weld filler wire, heat number 83653 and Linde 0091 flux, lot number 3536, which is identical to that used in the actual fabrication of the intermediate to lower shell girth weld and all longitudinal weld seams of both the intermediate and lower shell plates of the pressure vessel.

Capsule Y was removed after 4.64 effective full power years (EFPY) of plant operation. This capsule contained Charpy V-notch, tensile, and 1/2T compact specimens (1/2T-CT) made from intermediate shell plate B8805-3 and submerged arc weld metal identical to the closing girth and intermediate and lower shell longitudinal seams and Charpy V-notch specimens from the weld Heat-Affected-Zone (HAZ) of intermediate shell plate B8805-1.

Test material obtained from the intermediate shell plate (after thermal heat treatment and forming of the plate) was taken at least one plate thickness from the quenched edges of the plate. All test specimens were machined from the 1/4 and 3/4 thickness locations of the plate after performing a simulated postweld, stress-relieving treatment on the test material. Specimens from weld metal and HAZ metal were machined from a stress-relieved weldment joining intermediate shell plate B8805-1 and adjacent lower shell plate B8606-3. All heat-affected-zone specimens were obtained from the weld heat-affected-zone of intermediate shell plate B8805-1.

Charpy V-notch impact and tension specimens were machined from intermediate shell plate B8805-3 in both the longitudinal orientation (longitudinal axis of the specimen parallel to the major rolling direction of the plate) and transverse orientation (longitudinal axis of the specimen normal to the major rolling direction of the plate). Charpy V-notch and tensile specimens from the weld metal were oriented such that the long dimension of the specimen was normal to the welding direction. The notch of the weld metal Charpy specimens was machined such that the direction of crack propagation in the specimen was in the welding direction.

Capsule Y, also, contained 1/2T-CT test specimens from intermediate shell plate B8805-3 machined in both the longitudinal and transverse orientations. 1/2T-CT test specimens from the weld metal were machined such that the simulated crack in the specimen would propagate in the direction of welding. All specimens were fatigue pre-cracked according to ASTM E399.

The chemical composition and heat treatment of the surveillance material is presented in Tables 4-1 through 4-3. The chemical analysis reported in Table 4-1 was obtained from unirradiated material used in the surveillance program^[1] and irradiated material from capsules U^[6] and Y.

Capsule Y contained dosimeter wires of pure copper, iron, nickel, and aluminum-0.15 weight percent cobalt wire (cadmium-shielded and unshielded). In addition, cadmium shielded dosimeters of neptunium (Np²³⁷) and uranium (U²³⁸) were placed in the capsule to measure the integrated flux at specific neutron energy levels.

The capsule contained thermal monitors made from two low-melting-point eutectic alloys and sealed in Pyrex tubes. These thermal monitors were used to define the maximum temperature attained by the test specimens during irradiation. The composition of the two eutectic alloys and their melting points are as follows:

2.5% Ag, 97.5% Pb

Melting Point: 579°F (304°C)

1.5% Ag, 1.0% Sn, 97.5% Pb

Melting Point: 590°F (310°C)

The arrangement of the various mechanical specimens, dosimeters and thermal monitors contained in capsule Y is shown in Figure 4-2.

TABLE 4-1				
Chemical Composition of the Vogtle Unit 1 Reactor Vessel Intermediate Shell Plate B8805-3				
Element	Chemical Composition (wt.%)			
	Westinghouse Analysis ⁽²⁾	CE Analysis ⁽²⁾	Capsule U ^(a) Analysis	Capsule Y ^(b) Analysis
C	0.220	0.250	--	0.225
Mn	1.320	1.320	1.262	1.277
P	0.017	0.003	0.010	<0.015
S	0.011	0.010	--	0.0139
Si	0.280	0.260	--	0.232
Ni	0.610	0.600	0.586	0.584
Mo	0.570	0.530	0.431	0.527
Cr	0.057	0.040	0.049	0.057
Cu	0.058	0.060	0.053	0.061
Al	0.030	0.029	--	0.032
Co	0.006	0.009	0.013	0.008
Pb	<0.001	<0.001	--	--
W	<0.010	<0.010	--	<0.037
Ti	0.004	<0.010	--	<0.008
Zr	<0.002	<0.001	--	<0.009
V	<0.002	0.003	<0.002	<0.001
Sn	0.019	0.017	--	<0.018
As	0.003	0.001	--	<0.015
Cb ^(c)	<0.002	<0.010	--	0.013
N	0.006	0.008	--	--
B	<0.001	<0.001	--	0.004

- a) Chemical Analysis by Westinghouse on irradiated Charpy specimen AT-5 removed from capsule U⁽⁶⁾.
b) Chemical Analysis by Westinghouse on irradiated Charpy specimen AT-64 removed from capsule Y.
c) or Nb

TABLE 4-2

Chemical Composition (wt%) of the Vogtle Unit 1 Reactor Vessel Surveillance Weld Metal

Elm.	Weld Wire Heat no. 83653, Linde 0091 Flux, Lot No. 3536 ^(a)						
	Surveillance Program ^(b) Test Weldment D	Wire Flux ^(c) Test Weld Sample	Actual Production ^(c) Weld (Intermediate To Lower Shell Girth Seam, 101-171)	Capsule U ^(d) Analysis	Capsule Y ^(e) Analysis	Capsule Y ^(f) Analysis	Capsule Y ^(g) Analysis
C	0.130	0.140	0.090	--	0.137	0.147	0.153
Mn	1.150	1.060	1.170	1.057	1.113	1.164	1.195
P	0.017	0.007	0.008	0.008	<0.014	<0.014	<0.016
S	0.010	0.009	0.009	--	0.0085	0.0112	0.0135
Si	0.190	0.160	0.170	--	0.174	0.123	0.102
Ni	0.100	--	0.100	0.091	0.101	0.117	0.105
Mo	0.610	0.520	0.630	0.475	0.553	0.561	0.584
Cr	0.052	--	0.050	0.044	0.053	0.053	0.055
Cu	0.037	0.030	0.040	0.035	0.048	0.040	0.041
Al	0.002	--	0.009	--	<0.019	<0.019	<0.021
Co	0.005	--	0.010	0.006	0.007	0.007	0.008
Pb	<0.001	--	<0.001	--	--	--	--
W	<0.010	--	0.020	--	<0.036	<0.036	<0.039
Ti	0.006	--	<0.010	--	0.011	0.011	0.012
Zr	<0.002	--	0.001	--	<0.009	<0.009	<0.010
V	0.003	0.005	0.007	0.006	0.001	0.001	0.001
Sn	<0.002	--	0.003	--	<0.019	<0.019	<0.020
As	0.004	--	0.006	--	<0.015	<0.015	<0.016
Cb ^(b)	<0.002	--	0.010	--	0.013	0.013	0.014
N	0.003	--	0.021	--	--	--	--
B	<0.001	--	<0.001	--	0.004	0.004	0.003

- a) Surveillance weldment was made using the same wire and flux as was used for all beltline weld seams.⁽²⁾
b) Chemical analysis by Westinghouse.⁽²⁾
c) Chemical analysis by Combustion Engineering, Inc.⁽²⁾
d) Chemical analysis by Westinghouse on irradiated Charpy specimen AW-12 removed from capsule U⁽⁶⁾.
e) Chemical analysis by Westinghouse on irradiated Charpy specimen AW-62 removed from capsule Y.
f) Chemical analysis by Westinghouse on irradiated Charpy specimen AW-65 removed from capsule Y.
g) Chemical analysis by Westinghouse on irradiated Charpy specimen AW-66 removed from capsule Y.
h) or Nb

TABLE 4-3			
Heat Treatment of the Vogtle Unit 1 Reactor Vessel Surveillance Materials ^[2]			
Material	Temperature (°F)	Time (hr)	Coolant
Surveillance Program Test Plate B8805-3	Austenitizing: 1600 ± 25	4	Water quenched
	Tempered: 1225 ± 25	4	Air cooled
	Stress Relief: ^(a) 1150 ± 50	17.5	Furnace cooled
Weldment	Stress Relief: ^(a) 1150 ± 50	12.75	Furnace cooled

- a) The stress relief heat treatment received by the surveillance test plate and weldment have been simulated.

TABLE 4-4

Chemistry Results from the Low Alloy Steel NIST Certified Reference Standards

Metals	Concentration in Weight Percent					
	NIST 361		NIST 362		NIST 363	
	Certified	Measured	Certified	Measured	Certified	Measured
Fe	95.600	95.793	95.300	95.758	94.400	94.577
Co	0.032	0.030	0.300	0.297	0.048	0.044
Cr	0.694	0.664	0.300	0.291	1.310	1.262
Cu	0.042	0.041	0.500	0.487	0.100	0.094
Mn	0.660	0.625	1.040	1.025	1.500	1.447
Mo	0.190	0.186	0.068	0.061	0.028	0.021
Ni	2.000	1.844	0.590	0.543	0.300	0.282
P	0.014	0.017	0.041	0.041	0.029	0.031
Ti	0.020	0.016	0.084	0.024	0.050	0.045
V	0.011	0.006	0.040	0.037	0.310	0.301
Al	0.021	0.019	0.095	0.080	0.240	0.234
As	0.017	0.018	0.092	0.082	0.010	<0.015
B	0.000	<0.002	0.003	0.004	0.001	<0.002
Nb	0.022	0.021	0.290	0.016	0.049	0.042
Sn	0.010	<0.019	0.016	<0.015	0.104	0.102
W	0.017	0.047	0.200	0.202	0.046	<0.037
Zr	0.009	0.010	0.190	<0.187	0.049	0.038
C	0.383	0.383	0.160	0.161	0.620	NA
S	0.0140	NA	0.0360	0.0358	0.0068	NA
Si	0.222	0.208	0.390	0.414	0.740	NA

NA represents elements not requested for analysis

TABLE 4-4 cont.

Chemistry Results from the Low Alloy Steel NIST Certified Reference Standards

Metals	Concentration in Weight Percent					
	NIST 364		NIST 4H		NIST 5J	
	Certified	Measured	Certified	Measured	Certified	Measured
Fe	96.700	96.937	94.680	94.589	93.030	93.000
Co	0.150	0.146	--	0.007	--	0.009
Cr	0.063	0.062	0.117	0.113	0.021	0.021
Cu	0.249	0.238	0.243	0.243	0.990	0.943
Mn	0.255	0.237	0.840	0.829	0.700	0.672
Mo	0.490	0.468	0.017	0.015	0.005	<0.005
Ni	0.144	0.128	0.065	0.065	0.018	0.019
P	0.010	<0.014	0.124	0.143	0.241	0.244
Ti	0.240	0.262	0.024	0.030	0.044	0.057
V	0.105	0.102	0.011	0.006	0.012	0.009
Al	0.008	<0.019	--	<0.020	--	<0.019
As	0.052	0.037	0.015	<0.016	0.026	0.019
B	0.011	0.011	--	<0.002	--	<0.003
Nb	0.157	0.034	--	0.014	--	0.014
Sn	0.008	<0.019	--	<0.019	--	<0.018
W	0.100	0.036	--	<0.037	--	<0.035
Zr	0.068	<0.059	--	<0.002	--	<0.002
C	0.870	NA	2.440	NA	2.370	NA
S	0.0250	0.0242	0.0700	NA	0.1000	NA
Si	0.065	NA	1.34	NA	2.44	NA

NA represents elements not requested for analysis

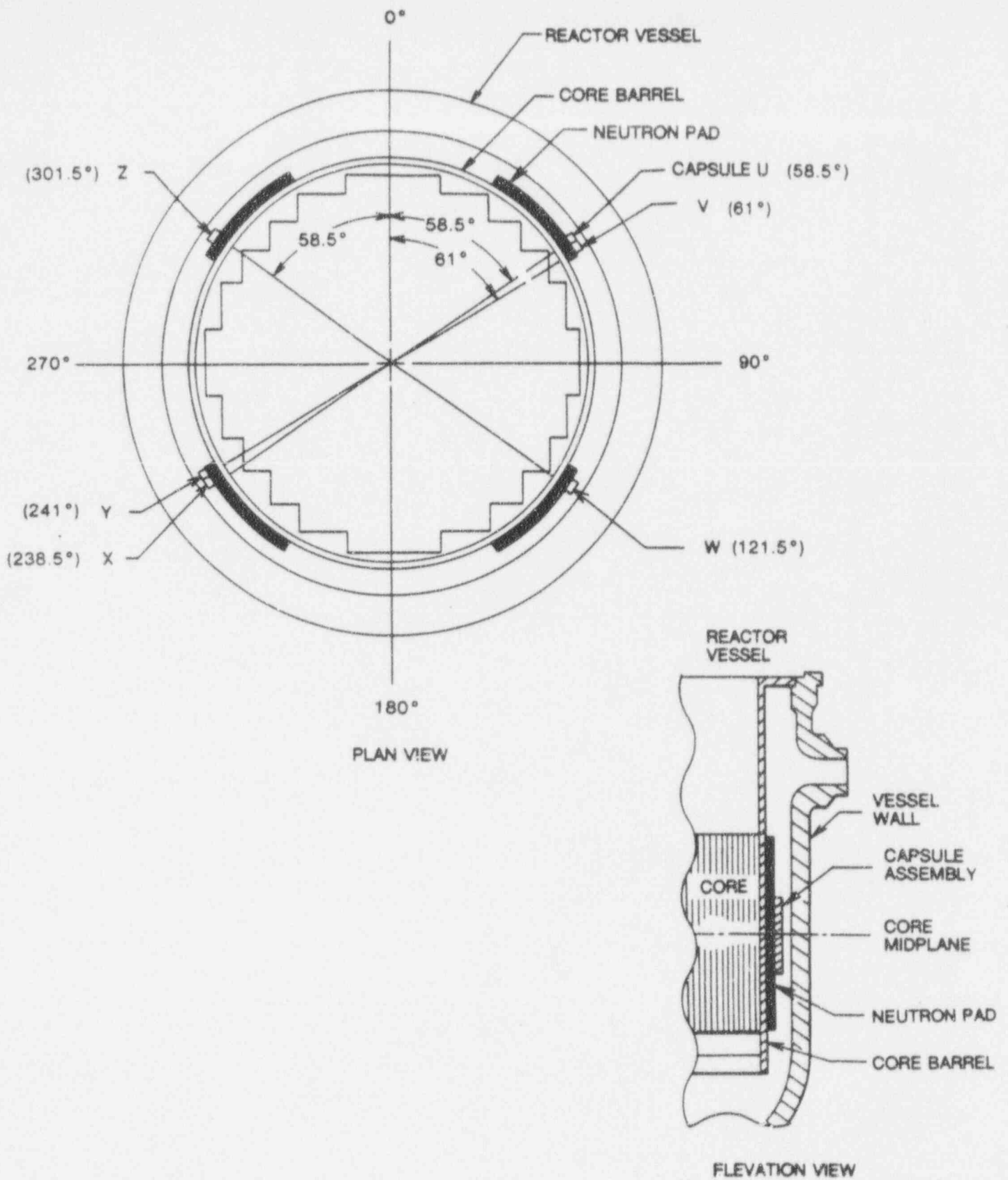
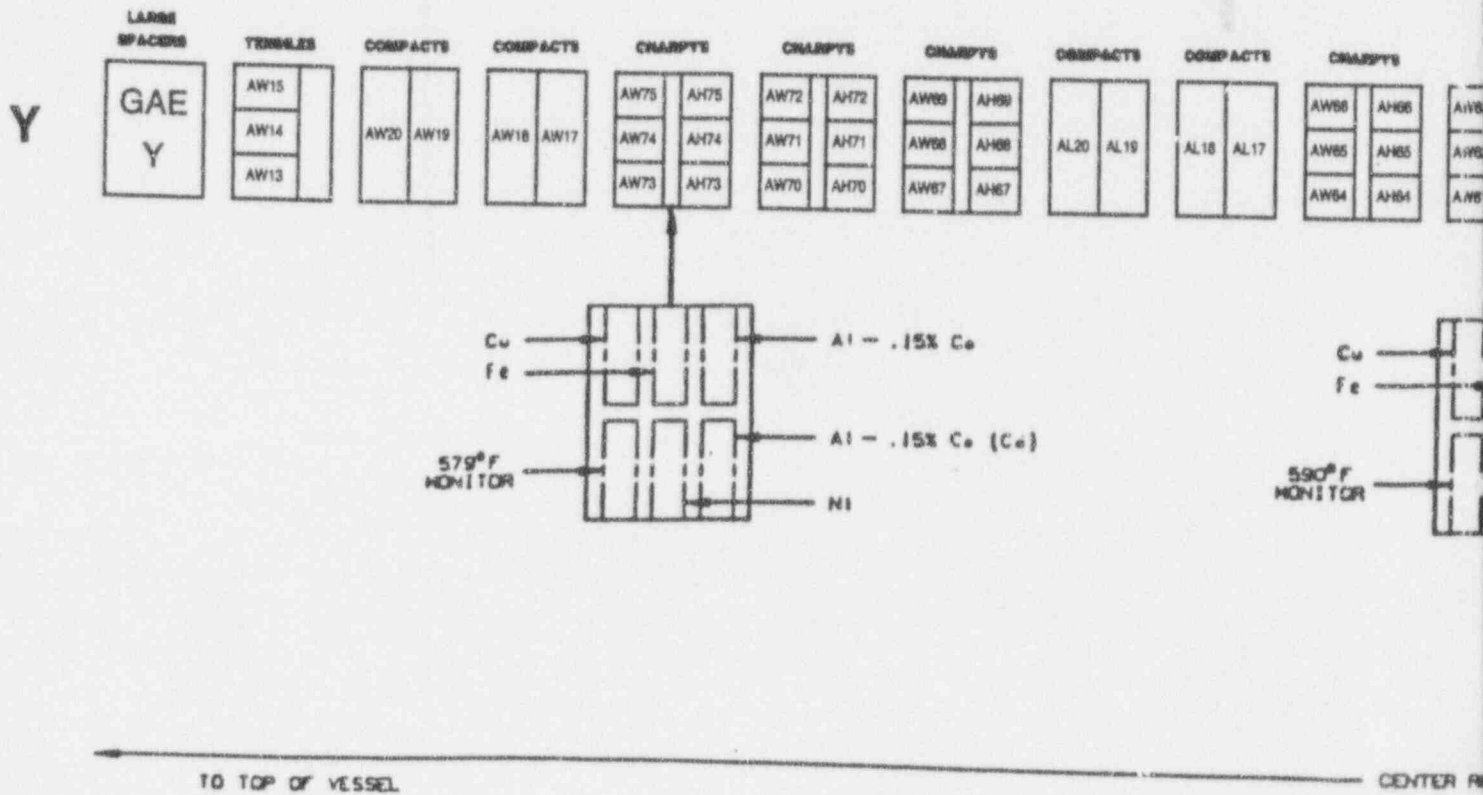


Figure 4-1. Arrangement of Surveillance Capsules in the Vogtle Unit 1 Reactor Vessel ^[2]

- LEGEND: AL - INTERMEDIATE SHELL PLATE B8805-3 (LONGITUDINAL)
 AT - INTERMEDIATE SHELL PLATE B8805-3 (TRANSVERSE)
 AW - WELD METAL
 AH - HEAT-AFFECTED-ZONE MATERIAL



ANSTEC APERTURE CARD

Also Available on
Aperture Card

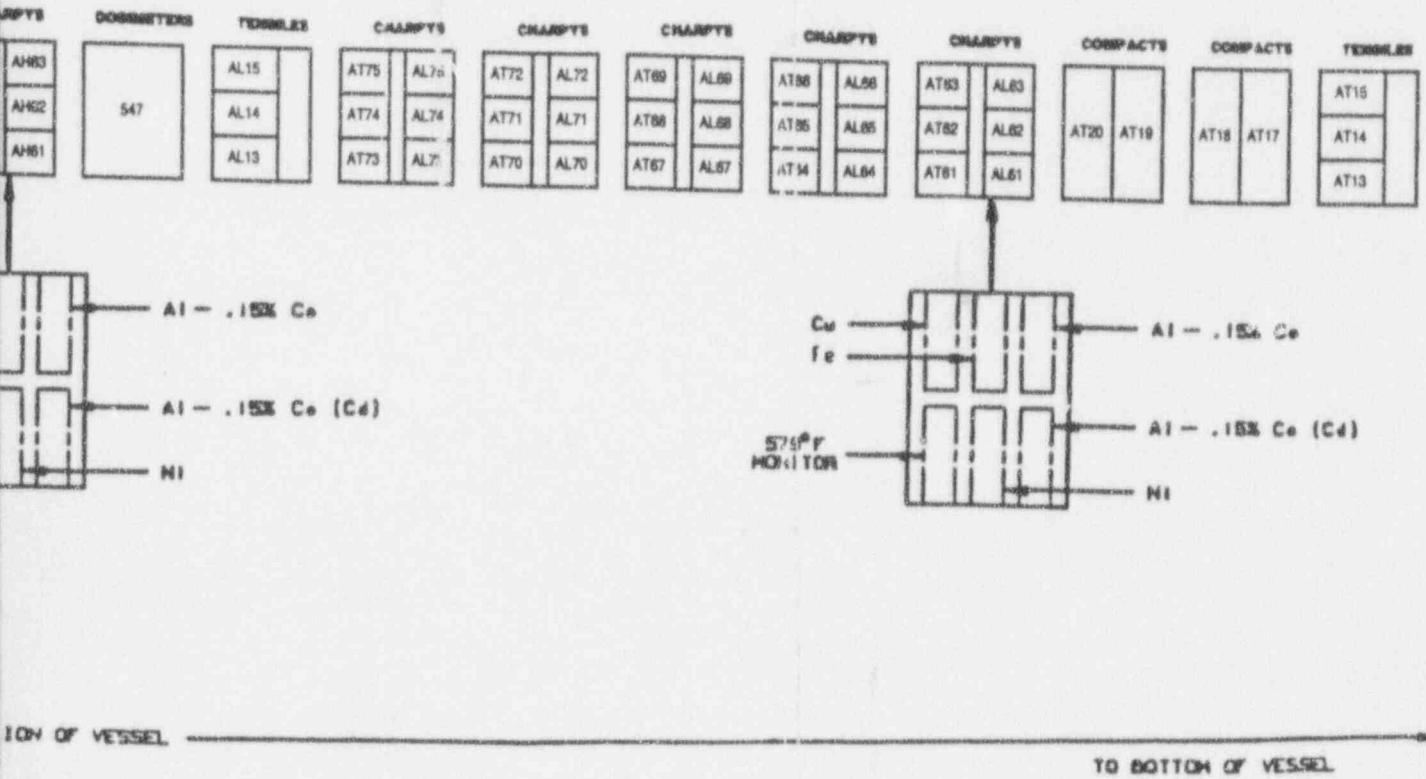


Figure 4-2. Capsule Y Diagram Showing the Location of Specimens, Thermal Monitors, and Dosimeters ^[2]

9404/2027-01

SECTION 5.0
TESTING OF SPECIMENS FROM CAPSULE Y

5.1 Overview

The post-irradiation mechanical testing of the Charpy V-notch impact specimens and tensile specimens was performed in the Remote Metallographic Facility at the Westinghouse Science and Technology Center. Testing was performed in accordance with 10CFR50, Appendices G and H⁽⁷⁾, ASTM Specification E185-82⁽³⁾ and Westinghouse Procedure MHL 8402, Revision 2 as modified by Westinghouse RMF Procedures 8102, Revision 1, and 8103, Revision 1.

Upon receipt of the capsule at the hot cell laboratory, the specimens and spacer blocks were carefully removed, inspected for identification number, and checked against the master list in WCAP-11011⁽²⁾. No discrepancies were found.

Examination of the two low-melting point 579°F (304°C) and 590°F (310°C) eutectic alloys indicated no melting of either type of thermal monitor. Based on this examination, the maximum temperature to which the test specimens were exposed was less than 579°F (304°C).

The Charpy impact tests were performed per ASTM Specification E23-92⁽⁸⁾ and RMF Procedure 8103, Revision 1, on a Tinius-Olsen Model 74, 358J machine. The tup (striker) of the Charpy impact test machine is instrumented with a GRC 8301 instrumentation system, feeding information into an IBM XT Computer. With this system, load-time and energy-time signals can be recorded in addition to the standard measurement of Charpy energy (E_D). From the load-time curve, the load of general yielding (P_{GY}), the time to general yielding (t_{GY}), the maximum load (P_M), and the time to maximum load (t_M) can be determined. Under some test conditions, a sharp drop in load indicative of fast fracture was observed. The load at which fast fracture was initiated is identified as the fast fracture load (P_F), and the load at which fast fracture terminated is identified as the arrest load (P_A). The energy at maximum load (E_M) was determined by comparing the energy-time record and the load-time record. The energy at maximum load is approximately equivalent to the energy required to initiate a crack in the specimen. Therefore, the propagation energy for the crack (E_p) is the difference between the total energy to fracture (E_D) and the energy at maximum load (E_M).

The yield stress (σ_Y) was calculated from the three-point bend formula having the following expression:

$$\sigma_Y = (P_{GY} * L) / [B * (W - a)^2 * C] \quad (1)$$

where: L = distance between the specimen supports in the impact machine
B = the width of the specimen measured parallel to the notch
W = height of the specimen, measured perpendicularly to the notch
a = notch depth

The constant C is dependent on the notch flank angle (ϕ), notch root radius (ρ) and the type of loading (ie. pure bending or three-point bending). In three-point bending, for a Charpy specimen in which $\phi = 45^\circ$ and $\rho = 0.010"$, Equation 1 is valid with $C = 1.21$. Therefore, (for $L = 4W$),

$$\sigma_Y = (P_{GY} * L) / [B * (W - a)^2 * 1.21] = (3.3 * P_{GY} * W) / [B * (W - a)^2] \quad (2)$$

For the Charpy specimen, $B = 0.394"$, $W = 0.394"$ and $a = 0.079"$ Equation 2 then reduces to:

$$\sigma_Y = 33.3 * P_{GY} \quad (3)$$

where σ_Y is in units of psi and P_{GY} is in units of lbs. The flow stress was calculated from the average of the yield and maximum loads, also using the three-point bend formula.

Percent shear was determined from post-fracture photographs using the ratio-of-areas methods in compliance with ASTM Specification A370-92^[9]. The lateral expansion was measured using a dial gage rig similar to that shown in the same specification.

Tensile tests were performed on a 20,000-pound Instron, split-console test machine (Model 1115) per ASTM Specification E8-91^[10] and E21-79(1988)^[11], and RMF Procedure 8102, Revision 1. All pull rods, grips, and pins were made of Inconel 718. The upper pull rod was connected through a universal joint to improve axially of loading. The tests were conducted at a constant crosshead speed of 0.05 inches per minute throughout the test.

Extension measurements were made with a linear variable displacement transducer extensometer. The extensometer knife edges were spring-loaded to the specimen and operated through specimen failure. The extensometer gage length was 1.00 inch. The extensometer is rated as Class B-2 per ASTM E83-92^[12].

Elevated test temperatures were obtained with a three-zone electric resistance split-tube furnace with a 9-inch hot zone. All tests were conducted in air. Because of the difficulty in remotely attaching a thermocouple directly to the specimen, the following procedure was used to monitor specimen temperatures. Chromel-alumel thermocouples were positioned at center and each end of the gage section of a dummy specimen in each grip. In the test configuration, with a slight load on the specimen, a plot of specimen temperature versus upper and lower grip and controller temperatures was developed over the range from room temperature to 550°F (288°C). During the actual testing, the grip temperatures were used to obtain desired specimen temperatures. Experiments indicated that this method is accurate to $\pm 2^\circ\text{F}$.

The yield load, ultimate load, fracture load, total elongation, and uniform elongation were determined directly from the load-extension curve. The yield strength, ultimate strength, and fracture strength were calculated using the original cross-sectional area. The final diameter and final gage length were determined from post-fracture photographs. The fracture area used to calculate the fracture stress (true stress at fracture) and percent reduction in area was computed using the final diameter measurement.

5.2 Charpy V-Notch Impact Test Results

The results of the Charpy V-notch impact tests performed on the various materials contained in Capsule Y, which was irradiated to 1.24×10^{19} n/cm² ($E > 1.0$ MeV), are presented in Tables 5-1 through 5-8 and are compared with unirradiated results^[2] as shown in Figures 5-1 through 5-4. The transition temperature increases and upper shelf energy decreases for the Capsule Y materials are summarized in Table 5-9.

Irradiation of the reactor vessel intermediate shell plate B8805-3 Charpy specimens oriented with the longitudinal axis of the specimen parallel to the major rolling direction of the plate (longitudinal orientation) to 1.24×10^{19} n/cm² ($E > 1.0$ MeV) at 550°F (Figure 5-1) resulted in a 30 ft-lb transition temperature increase of 40°F and a 50 ft-lb transition temperature increase of 55°F. This results in an irradiated 30 ft-lb transition temperature of 25°F and an irradiated 50 ft-lb transition temperature of

55°F (longitudinal orientation).

The average upper shelf energy (USE) of the intermediate shell plate B8805-3 Charpy specimens (longitudinal orientation) resulted in no energy decrease after irradiation to 1.24×10^{19} n/cm² (E > 1.0 MeV) at 550°F. This results in an irradiated average USE of 122 ft-lbs (Figure 5-1).

Irradiation of the reactor vessel intermediate shell plate B8805-3 Charpy specimens oriented with the longitudinal axis of the specimen normal to the major rolling direction of the plate (transverse orientation) to 1.24×10^{19} n/cm² (E > 1.0 MeV) at 550°F (Figure 5-2) resulted in a 30 ft-lb transition temperature increase of 20°F and a 50 ft-lb transition temperature increase of 30°F. This results in an irradiated 30 ft-lb transition temperature of 35°F and an irradiated 50 ft-lb transition temperature of 95°F (transverse orientation).

The average USE of the intermediate shell plate B8805-3 Charpy specimens (transverse orientation) resulted in no energy decrease after irradiation to 1.24×10^{19} n/cm² (E > 1.0 MeV) at 550°F. This results in an irradiated average USE of 96 ft-lbs (Figure 5-2).

Irradiation of the surveillance weld metal Charpy specimens to 1.24×10^{19} n/cm² (E > 1.0 MeV) at 550°F (Figure 5-3) resulted in no 30 ft-lb and 50 ft-lb transition temperature increases. This results in an irradiated 30 ft-lb transition temperature of -40°F and an irradiated 50 ft-lb transition temperature of 25°F.

The average USE of the surveillance weld metal resulted in an energy decrease of 1 ft-lb after irradiation to 1.24×10^{19} n/cm² (E > 1.0 MeV) at 550°F. This results in an irradiated average USE of 144 ft-lbs (Figure 5-3).

Irradiation of the reactor vessel weld HAZ metal Charpy specimens to 1.24×10^{19} n/cm² (E > 1.0 MeV) at 550°F (Figure 5-4) resulted in 30 ft-lb and 50 ft-lb transition temperature increases of 25°F. This results in an irradiated 30 ft-lb transition temperature of -50°F and an irradiated 50 ft-lb transition temperature of -25°F.

The average USE of the weld HAZ metal resulted in an energy decrease of 12 ft-lbs after irradiation to 1.24×10^{19} n/cm² (E > 1.0 MeV) at 550°F. This results in an irradiated average USE of 124 ft-lbs (Figure 5-4).

The fracture appearance of each irradiated Charpy specimen from the various materials is shown in Figures 5-5 through 5-8 and show an increasingly ductile or tougher appearance with increasing test temperature.

A comparison of the 30 ft-lb transition temperature increases and upper shelf energy decreases for the various Vogtle Unit 1 surveillance materials with predicted values using the methods of NRC Regulatory Guide 1.99, Revision 2^[1] is presented in Table 5-10 and led to the following conclusions:

- o The 30 ft-lb transition temperature increases for the capsule Y surveillance materials are less than the Regulatory Guide 1.99, Revision 2 predictions.
- o The Upper Shelf Energy decreases of the capsule Y surveillance materials are less than the Regulatory Guide 1.99, Revision 2 predictions.

The load-time records for the Charpy tests are provided in Appendix A.

5.3 Tension Test Results

The results of the tension tests performed on the various materials contained in capsule Y irradiated to 1.24×10^{19} n/cm² (E > 1.0 MeV) are presented in Table 5-11 and are compared with unirradiated results^[2] as shown in Figures 5-9 through 5-11.

The results of the tension tests performed on the intermediate shell plate B8805-3 (longitudinal orientation) indicated that irradiation to 1.24×10^{19} n/cm² (E > 1.0 MeV) at 550°F caused a 0 to 4 ksi increase in the 0.2 percent offset yield strength and a 0 to 6 ksi increase in the ultimate tensile strength when compared to unirradiated data^[2] (Figure 5-9).

The results of the tension tests performed on the intermediate shell plate B8805-3 (transverse orientation) indicated that irradiation to 1.24×10^{19} n/cm² (E > 1.0 MeV) at 550°F caused a 0 to 3 ksi increase in the 0.2 percent offset yield strength and a 0 to 3 ksi increase in the ultimate tensile strength when compared to unirradiated data^[2] (Figure 5-10).

The results of the tension tests performed on the surveillance weld metal indicated that irradiation to 1.24×10^{19} n/cm² (E > 1.0 MeV) at 550°F caused a 1 to 4 ksi increase in the 0.2 percent offset yield

strength and a 2 to 5 ksi increase in the ultimate tensile strength when compared to unirradiated data^[2] (Figure 5-11).

The fractured tension specimens for the intermediate shell plate B8805-3 material are shown in Figures 5-12 and 5-13, while the fractured specimens for the surveillance weld metal are shown in Figure 5-14. The engineering stress-strain curves for the tension tests are shown in Figures 5-15 through 5-20.

5.4 Compact Tension Specimen Tests

Per the surveillance capsule testing contract, the 1/2T compact tension (CT) specimens were not tested. The 1/2T CT specimens are being stored at the Westinghouse Science and Technology Center Hot Cell facility.

TABLE 5-1

Charpy V-notch Data for the Vogtle Unit 1 Intermediate Shell Plate B8805-3
Irradiated at 550°F to a Fluence of 1.24×10^{19} n/cm² (E > 1.0 MeV)
(Longitudinal Orientation)

Sample Number	Temperature		Impact Energy		Lateral Expansion		Shear (%)
	(°F)	(°C)	(ft-lb)	(J)	(mils)	(mm)	
AL67	-25	-32	6	8	5	0.13	10
AL69	0	-18	23	31	18	0.46	15
AL74	25	-4	17	23	17	0.43	20
AL61	25	-4	23	31	20	0.51	20
AL65	35	2	53	72	39	0.99	35
AL64	50	10	57	77	44	1.12	40
AL62	60	16	41	56	31	0.79	30
AL71	75	24	82	111	51	1.30	60
AL73	100	38	74	100	56	1.42	70
AL72	125	52	79	107	60	1.52	80
AL75	150	66	96	130	62	1.57	90
AL66	175	79	94	127	69	1.75	95
AL68	225	107	132	179	78	1.98	100
AL63	275	135	130	176	80	2.03	100
AL70	300	149	133	180	88	2.24	100

TABLE 5-2

Charpy V-notch Data for the Vogtle Unit 1 Intermediate Shell Plate B8805-3
 Irradiated at 550°F to a Fluence of 1.24×10^{19} n/cm² (E > 1.0 MeV)
 (Transverse Orientation)

Sample Number	Temperature		Impact Energy		Lateral Expansion		Shear (%)
	(°F)	(°C)	(ft-lb)	(J)	(mils)	(mm)	
AT65	-50	-46	17	23	12	0.30	5
AT64	-25	-32	28	38	20	0.51	15
AT66	-20	-29	21	28	15	0.38	10
AT72	0	-18	24	33	20	0.51	10
AT75	25	-4	20	27	18	0.46	15
AT70	35	2	33	45	26	0.66	15
AT68	75	24	45	61	34	0.86	45
AT63	100	38	47	64	40	1.02	45
AT73	110	43	55	75	48	1.22	70
AT69	125	52	65	88	50	1.27	70
AT71	150	66	67	91	53	1.35	75
AT74	175	79	81	110	66	1.68	90
AT67	225	107	100	136	73	1.85	100
AT61	275	135	109	148	66	1.68	100
AT62	300	149	109	148	75	1.91	100

TABLE 5-3

Charpy V-notch Data for the Vogtle Unit 1 Surveillance Weld Metal
Irradiated at 550°F to a Fluence of 1.24×10^{19} n/cm² (E > 1.0 MeV)

Sample Number	Temperature		Impact Energy		Lateral Expansion		Shear (%)
	(°F)	(°C)	(ft-lb)	(J)	(mils)	(mm)	
AW66	-50	-46	13	18	11	0.28	10
AW68	-35	-37	17	23	14	0.36	15
AW65	-25	-32	15	20	14	0.36	20
AW74	-25	-32	67	91	52	1.32	50
AW62	-10	-23	98	133	67	1.70	70
AW67	-5	-21	80	108	57	1.45	60
AW61	0	-18	94	127	68	1.73	70
AW63	5	-15	114	155	71	1.80	80
AW70	25	-4	70	95	52	1.32	55
AW72	40	4	109	148	72	1.83	80
AW71	60	16	112	152	74	1.88	80
AW69	100	38	124	168	86	2.18	95
AW75	175	79	134	182	87	2.21	100
AW73	275	135	153	207	76	1.93	100
AW64	300	149	145	197	81	2.06	100

TABLE 5-4

Charpy V-notch Data for the Vogtle Unit 1 Heat-Affected-Zone (HAZ) Metal Irradiated
at 550°F to a Fluence of 1.24×10^{19} n/cm² (E > 1.0 MeV)

Sample Number	Temperature		Impact Energy		Lateral Expansion		Shear (%)
	(°F)	(°C)	(ft-lb)	(J)	(mils)	(mm)	
AH75	-100	-73	19	26	14	0.36	5
AH68	-50	-46	28	38	21	0.53	15
AH63	-35	-37	15	20	22	0.56	20
AH67	-30	-34	75	102	49	1.24	55
AH72	-25	-32	78	106	52	1.32	60
AH66	-25	-32	89	121	55	1.40	65
AH71	0	-18	65	88	43	1.09	50
AH74	25	-4	121	164	69	1.75	85
AH65	45	7	114	155	69	1.75	85
AH61	60	16	78	106	51	1.30	65
AH73	100	38	134	182	77	1.96	100
AH69	150	66	109	148	71	1.80	100
AH62	200	93	114	155	71	1.80	100
AH70	250	121	141	191	77	1.96	100
AH64	300	149	123	167	75	1.91	100

TABLE 5-5

Instrumented Charpy Impact Test Results for the Vogtle Unit 1 Intermediate Shell Plate B8805-3
Irradiated at 550°F to a Fluence of 1.24×10^{19} n/cm² (E > 1.0 MeV) (Longitudinal Orientation)

Sample No.	Test Temp. (°F)	Charpy Energy E _D (ft-lb)	Normalized Energies (ft-lb/in ²)			Yield Load P _{GY} (lbs)	Time to Yield t _{GY} (μsec)	Max. Load P _M (lbs)	Time to Max. t _M (μsec)	Fast Fract. Load P _F (lbs)	Arrest Load P _A (lbs)	Yield Stress σ _Y (ksi)	Flow Stress (ksi)
			Charpy E _D /A	Max. E _M /A	Prop. E _P /A								
AL67	-25	6	48	25	24	2817	0.12	3043	0.14	3013	0	94	97
AL69	0	23	185	141	44	3408	0.16	4074	0.37	4067	169	113	124
AL74	25	17	137	67	70	3292	0.16	3495	0.23	3479	318	109	113
AL61	25	23	185	130	55	3327	0.17	3950	0.36	3944	229	111	121
AL65	35	53	427	304	123	3316	0.16	4301	0.68	4246	158	110	126
AL64	50	57	459	297	162	3155	0.15	4217	0.67	4081	526	105	122
AL62	60	41	330	241	89	3112	0.15	4138	0.57	4135	784	103	120
AL71	75	82	660	298	363	3234	0.16	4233	0.67	3706	456	107	124
AL73	100	74	596	294	302	3187	0.17	4195	0.69	3820	1708	106	123
AL72	125	79	636	281	355	2894	0.14	4067	0.67	3584	2014	96	116
AL75	150	96	773	351	422	2840	0.14	4059	0.82	3455	1938	94	115
AL66	175	94	757	279	477	2802	0.15	3970	0.69	3021	1791	93	112
AL68	225	132	1063	284	778	2766	0.14	4054	0.68	**	**	92	113
AL63	275	130	1047	278	769	2742	0.14	3954	0.68	**	**	91	111
AL70	300	133	1071	262	809	2634	0.15	3797	0.67	**	**	87	107

** Fully ductile fracture.

TABLE 5-6

Instrumented Charpy Impact Test Results for the Vogtle Unit 1 Intermediate Shell Plate B8805-3
Irradiated at 550°F to a Fluence of 1.24×10^{19} n/cm² (E > 1.0 MeV) (Transverse Orientation)

Sample No.	Test Temp. (°F)	Charpy Energy E _p (ft-lb)	Normalized Energies (ft-lb/in ²)			Yield Load P _{GY} (lbs)	Time to Yield t _{GY} (μsec)	Max. Load P _M (lbs)	Time to Max. t _M (μsec)	Fast Fract. Load P _F (lbs)	Arrest Load P _A (lbs)	Yield Stress σ _Y (ksi)	Flow Stress (ksi)
			Charpy E _p /A	Max. E _M /A	Prop. E _p /A								
AT65	-50	17	137	100	37	3738	0.17	4070	0.28	4054	0	124	130
AT64	-25	28	225	200	25	3677	0.17	4354	0.47	4335	0	122	133
AT66	-20	21	169	129	40	3553	0.17	4066	0.34	4040	0	118	127
AT72*	0	24	193	-	-	-	-	-	-	-	-	-	-
AT75	25	20	161	93	68	3319	0.16	3704	0.28	3685	446	110	117
AT70	35	33	266	206	60	3425	0.17	4250	0.49	4237	181	114	127
AT68	75	45	362	244	118	3268	0.16	4237	0.57	4233	680	109	125
AT63	100	47	378	235	144	3070	0.15	4043	0.57	4008	1573	102	118
AT73	110	55	443	231	212	3147	0.16	4040	0.56	4002	1545	105	119
AT69	125	65	523	235	288	3147	0.16	4078	0.57	3721	1865	105	120
AT71	150	67	540	262	278	2895	0.15	4027	0.63	3720	2290	96	115
AT74	175	81	652	268	384	2892	0.14	3972	0.65	3150	1950	96	114
AT67	225	100	805	282	523	2829	0.14	4056	0.67	**	**	94	114
AT61	275	109	878	269	609	2724	0.14	3860	0.67	**	**	90	109
AT62	300	109	878	272	606	2811	0.17	3884	0.69	**	**	93	111

* Data not available due to machine malfunction.

** Fully ductile fracture.

TABLE 5-7

Instrumented Charpy Impact Test Results for the Vogtle Unit 1 Surveillance Weld Metal
Irradiated at 550°F to a Fluence of 1.24×10^{19} n/cm² (E > 1.0 MeV)

Sample No.	Test Temp. (°F)	Charpy Energy E _D (ft-lb)	Normalized Energies (ft-lb/in ²)			Yield Load P _{GY} (lbs)	Time to Yield t _{GY} (μsec)	Max. Load P _M (lbs)	Time to Max. t _M (μsec)	Fast Fract. Load P _F (lbs)	Arrest Load P _A (lbs)	Yield Stress σ _Y (ksi)	Flow Stress (ksi)
			Charpy E _D /A	Max. E _M /A	Prop. E _P /A								
AW66	-50	13	105	48	57	3815	0.16	3958	0.18	3935	314	127	129
AW68	-35	17	137	67	70	3811	0.17	3885	0.22	3879	519	127	128
AW65	-25	15	121	46	75	3605	0.16	3727	0.18	3705	754	120	122
AW74	-25	67	540	322	217	3737	0.17	4442	0.68	4229	1030	124	136
AW62	-10	98	789	225	564	3562	0.17	4244	0.52	3160	1535	118	130
AW67	-5	80	644	313	331	3676	0.17	4410	0.67	4022	2095	122	134
AW61	0	94	757	315	442	3554	0.16	4318	0.69	3892	2377	118	131
AW63	5	114	918	310	608	3499	0.18	4223	0.69	2837	1512	116	128
AW70	25	70	564	310	253	3503	0.16	4310	0.68	4297	2571	116	130
AW72	40	109	878	309	568	3399	0.16	4265	0.69	3331	2013	113	127
AW71	60	112	902	304	597	3366	0.16	4208	0.69	3389	2459	112	126
AW69	100	124	998	294	704	3306	0.17	4125	0.68	3112	2451	110	123
AW75	175	134	1079	357	722	2965	0.15	4043	0.82	**	**	98	116
AW73	275	153	1232	341	891	2716	0.14	3898	0.81	**	**	90	110
AW64	300	145	1168	266	902	2701	0.15	3747	0.69	**	**	90	107

** Fully ductile fracture.

TABLE 5-8

Instrumented Charpy Impact Test Results for the Vogtle Unit 1 Surveillance Heat-Affected-Zone (HAZ) Metal
Irradiated at 550°F to a Fluence of 1.24×10^{19} n/cm² (E > 1.0 MeV)

Sample No.	Test Temp. (°F)	Charpy Energy E _D (ft-lb)	Normalized Energies (ft-lb/in ²)			Yield Load P _{GY} (lbs)	Time to Yield t _{GY} (μsec)	Max. Load P _M (lbs)	Time to Max. t _M (μsec)	Fast Fract. Load P _F (lbs)	Arrest Load P _A (lbs)	Yield Stress σ _Y (ksi)	Flow Stress (ksi)
			Charpy E _D /A	Max. E _M /A	Prop. E _P /A								
AH75	-100	19	153	91	62	4195	0.17	4296	0.25	4283	314	139	141
AH68	-50	28	225	110	115	3916	0.17	4152	0.30	4149	1650	130	134
AH63	-35	15	121	110	11	3737	0.17	4137	0.30	4133	1500	124	131
AH67	-30	75	604	231	373	3709	0.16	4423	0.51	3763	979	123	135
AH72	-25	78	628	321	307	3682	0.17	4476	0.69	4409	3147	122	135
AH66	-25	89	717	324	393	3732	0.17	4515	0.68	3761	1094	124	137
AH71	0	65	523	291	233	3689	0.17	4431	0.63	4163	1268	123	135
AH74	25	121	974	316	659	3481	0.16	4352	0.69	3054	1818	116	130
AH65	45	114	918	300	618	3337	0.16	4210	0.68	2535	1499	111	125
AH61	60	78	628	218	410	3369	0.16	4160	0.52	3321	2004	112	125
AH73	100	134	1079	331	748	3257	0.17	4202	0.75	**	**	108	124
AH69	150	109	878	288	590	3315	0.17	4089	0.68	**	**	104	120
AH62	200	114	918	277	641	2883	0.16	3957	0.68	**	**	96	114
AH70	250	141	1135	351	784	2980	0.17	4049	0.82	**	**	99	117
AH64	300	123	990	274	716	2839	0.16	3885	0.68	**	**	94	112

** Fully ductile fracture.

TABLE 5-9

Effect of 550°F Irradiation to 1.24×10^{19} n/cm² (E > 1.0 MeV) on the Notch Toughness Properties of the Vogtle Unit 1
Reactor Vessel Surveillance Materials

Material	Average 30 (ft-lb) ^(a) Transition Temperature (°F)			Average 35 mil Lateral ^(a) Expansion Temperature (°F)			Average 50 ft-lb ^(a) Transition Temperature (°F)			Average Energy Absorption ^(a) at Full Shear (ft-lb)		
	Unirradiated	Irradiated	ΔT	Unirradiated	Irradiated	ΔT	Unirradiated	Irradiated	ΔT	Unirradiated	Irradiated	ΔE
Plate B8805-3 (longitudinal)	- 15	25	40	10	45	35	20	55	35	122	132	+ 10
Plate B8805-3 (transverse)	15	35	20	55	75	20	65	95	30	96	106	+ 10
Weld Metal	- 40	- 40	0	- 35	- 25	10	- 25	- 25	0	145	144	- 1
HAZ Metal	- 75	- 50	25	- 45	- 45	0	- 50	- 25	25	136	124	- 12

(a) "Average" is defined as the value read from the curve fit through the data points of the Charpy tests (see Figures 5-1 through 5-4)

TABLE 5-10						
Comparison of the Vogtle Unit 1 Surveillance Material 30 ft-lb Transition Temperature Shifts and Upper Shelf Energy Decreases with Regulatory Guide 1.99 Revision 2 Predictions						
Material	Capsule	Fluence ($\times 10^{19}$ n/cm ²)	30 ft-lb Transition Temperature Shift		Upper Shelf Energy Decrease	
			Predicted ^(a) (°F)	Measured (°F)	Predicted ^(a) (%)	Measured (%)
Intermediate Shell Plate B8805-3 (longitudinal)	U	0.344	27	15	15	0
	Y	1.24	41	40	20	0
Intermediate Shell Plate B8805-3 (transverse)	U	0.344	27	0	15	0
	Y	1.24	41	20	20	0
Weld Metal	U	0.344	23	15	15	0
	Y	1.24	35	0	20	- 1
HAZ Metal	U	0.344	-	0	-	- 6
	Y	1.24	-	25	-	- 9

(a) Based on Regulatory Guide 1.99, Revision 2 methodology using Mean wt. % values of Cu and Ni.

TABLE 5-11

Tensile Properties of the Vogtle Unit 1 Reactor Vessel Surveillance Materials Irradiated at 550°F to 1.24×10^{19} n/cm² (E > 1.0 MeV)

Material	Sample Number	Test Temp. (°F)	0.2% Yield Strength (ksi)	Ultimate Strength (ksi)	Fracture Load (kip)	Fracture Stress (ksi)	Fracture Strength (ksi)	Uniform Elongation (%)	Total Elongation (%)	Reduction in Area (%)
Plate B8805-3 (longitudinal)	AL13	85	72.8	96.8	3.00	182.3	61.1	10.5	24.9	66
Plate B8805-3 (longitudinal)	AL14	200	70.3	88.6	2.80	153.0	57.0	9.9	22.5	63
Plate B8805-3 (Longitudinal)	AL15	550	64.2	90.1	3.25	137.2	66.2	10.5	20.9	52
Plate B8805-3 (transverse)	AT13	100	70.3	95.3	3.20	163.4	65.2	10.3	23.2	60
Plate B8805-3 (transverse)	AT14	225	68.8	88.6	3.00	169.8	61.1	9.9	21.8	64
Plate B8805-3 (transverse)	AT15	550	67.2	90.7	3.34	149.7	67.9	10.5	19.4	55
Weld Metal	AW13	175	72.8	85.6	2.50	170.0	50.9	9.0	23.4	70
Weld Metal	AW14	25	74.9	91.3	2.65	180.2	54.0	11.1	30.0	70
Weld Metal	AW15	550	67.5	85.6	2.60	158.0	53.0	9.6	23.1	66

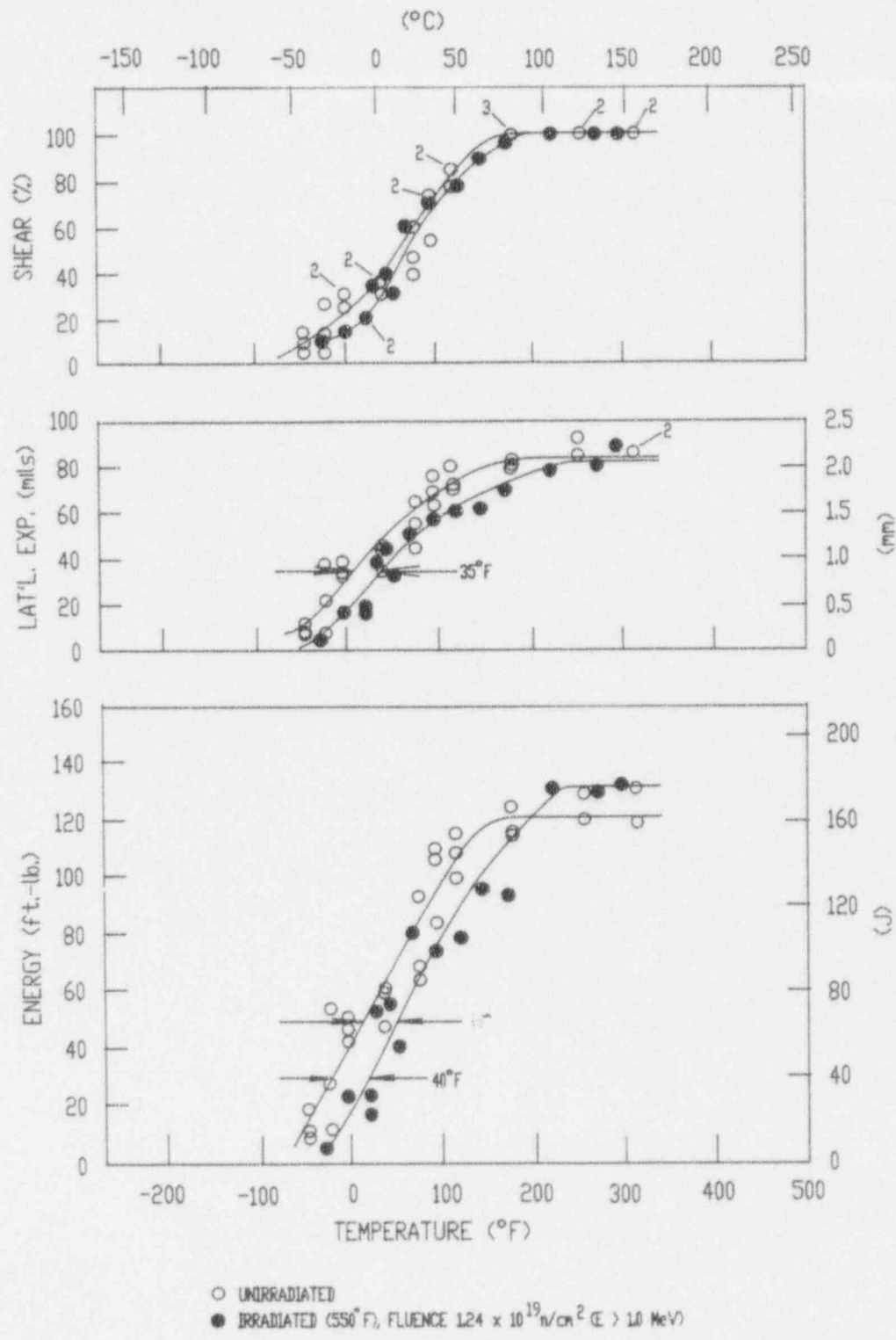


Figure 5-1 Charpy V-Notch Impact Properties for Vogtle Unit 1 Reactor Vessel Intermediate Shell Plate B8805-3 (Longitudinal Orientation)

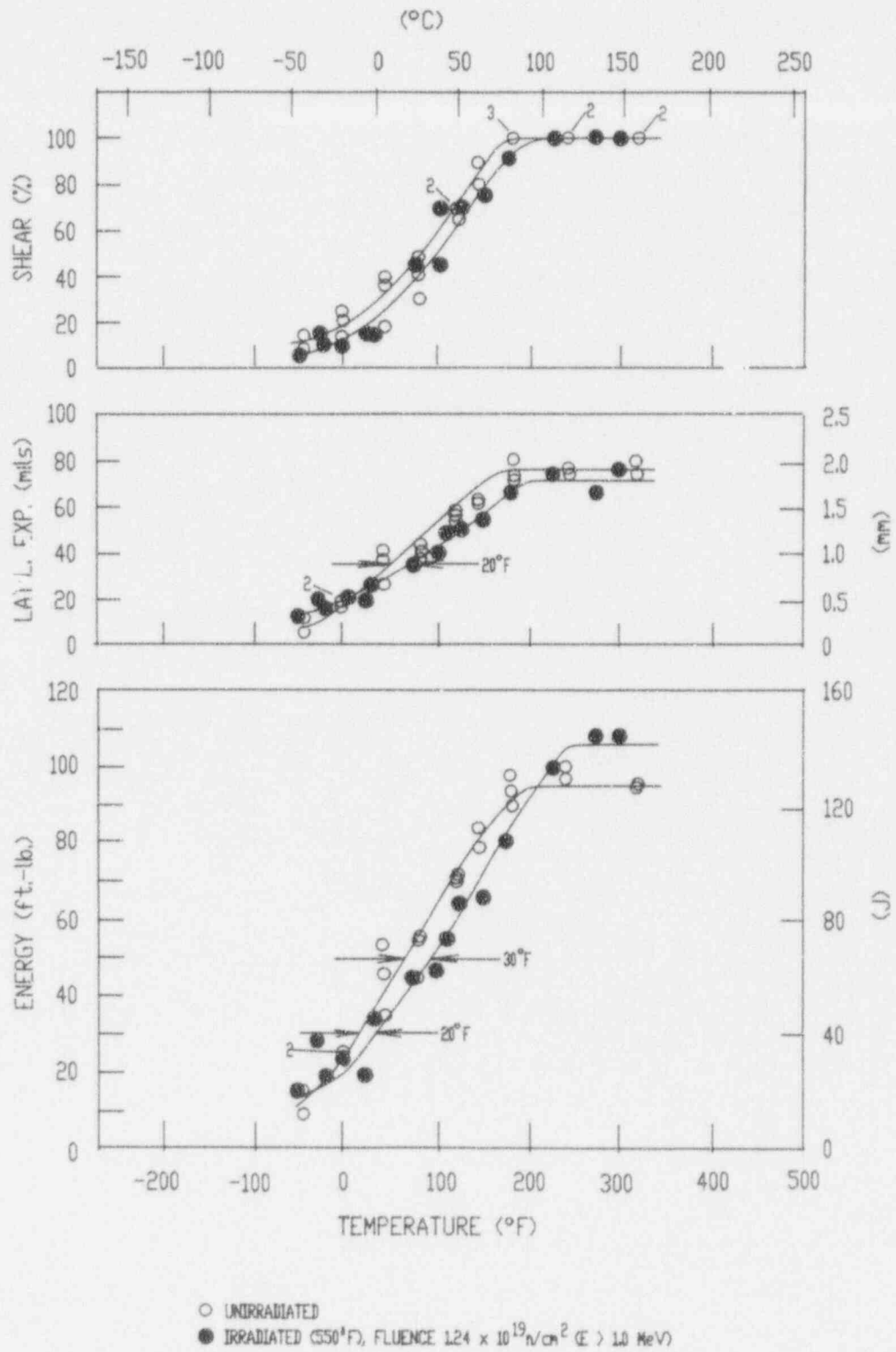


Figure 5-2 Charpy V-Notch Impact Properties for Vogtle Unit 1 Reactor Vessel Intermediate Shell Plate B8805-3 (Transverse Orientation)

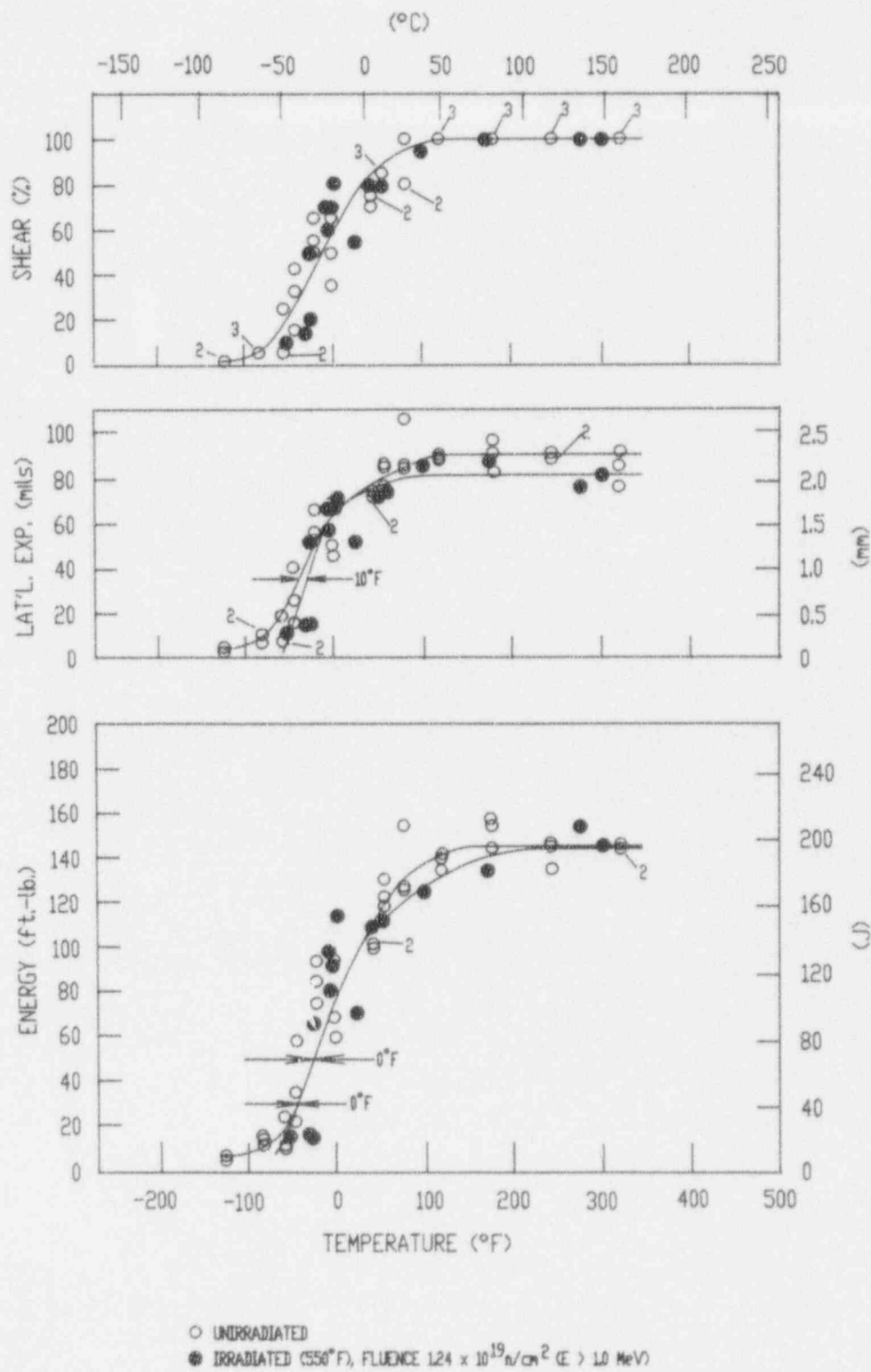


Figure 5-3 Charpy V-Notch Impact Properties for Vogtle Unit 1 Reactor Vessel Surveillance Weld Metal

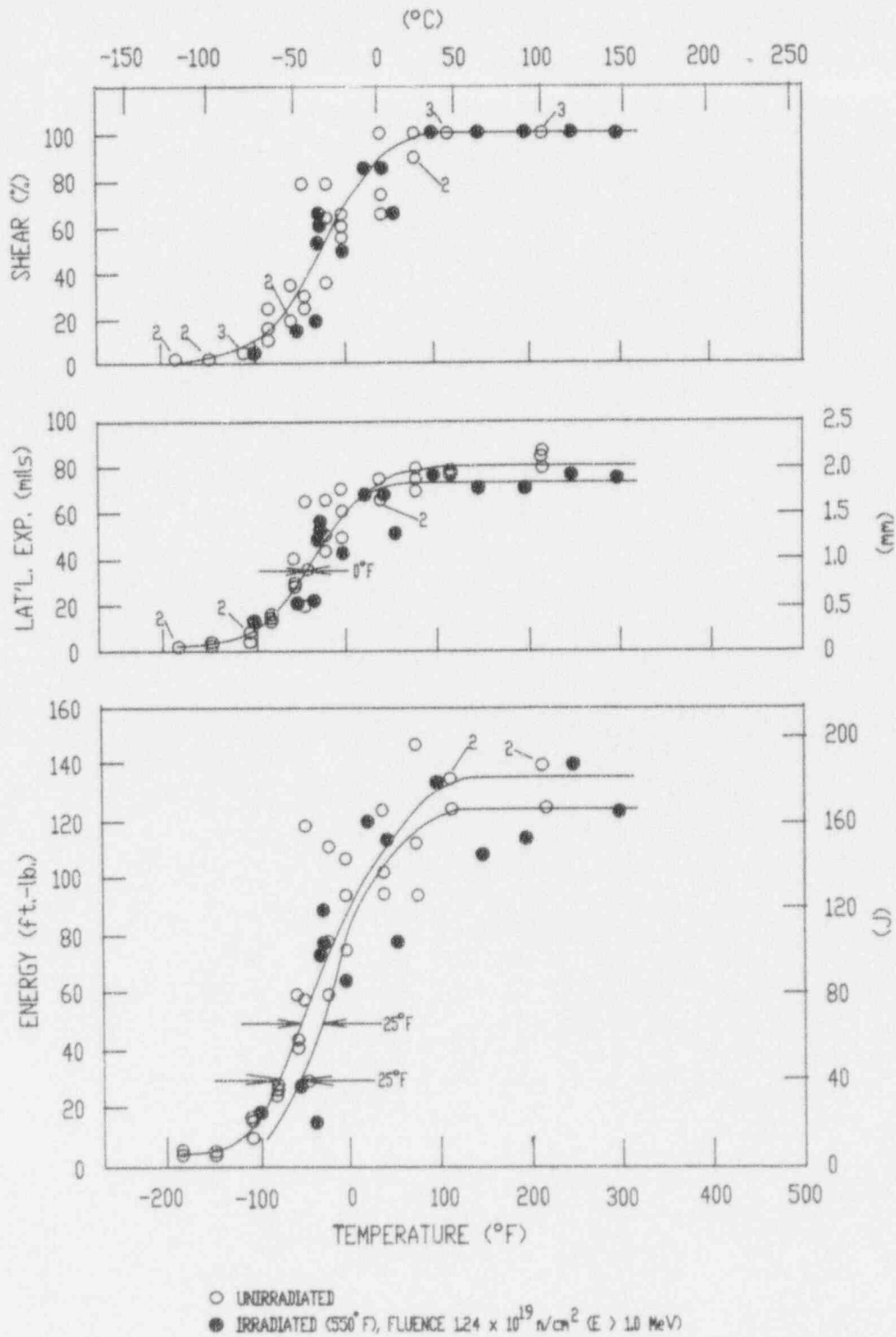


Figure 5-4 Charpy V-Notch Impact Properties for Vogtle Unit 1 Reactor Vessel Weld Heat-Affected-Zone Metal

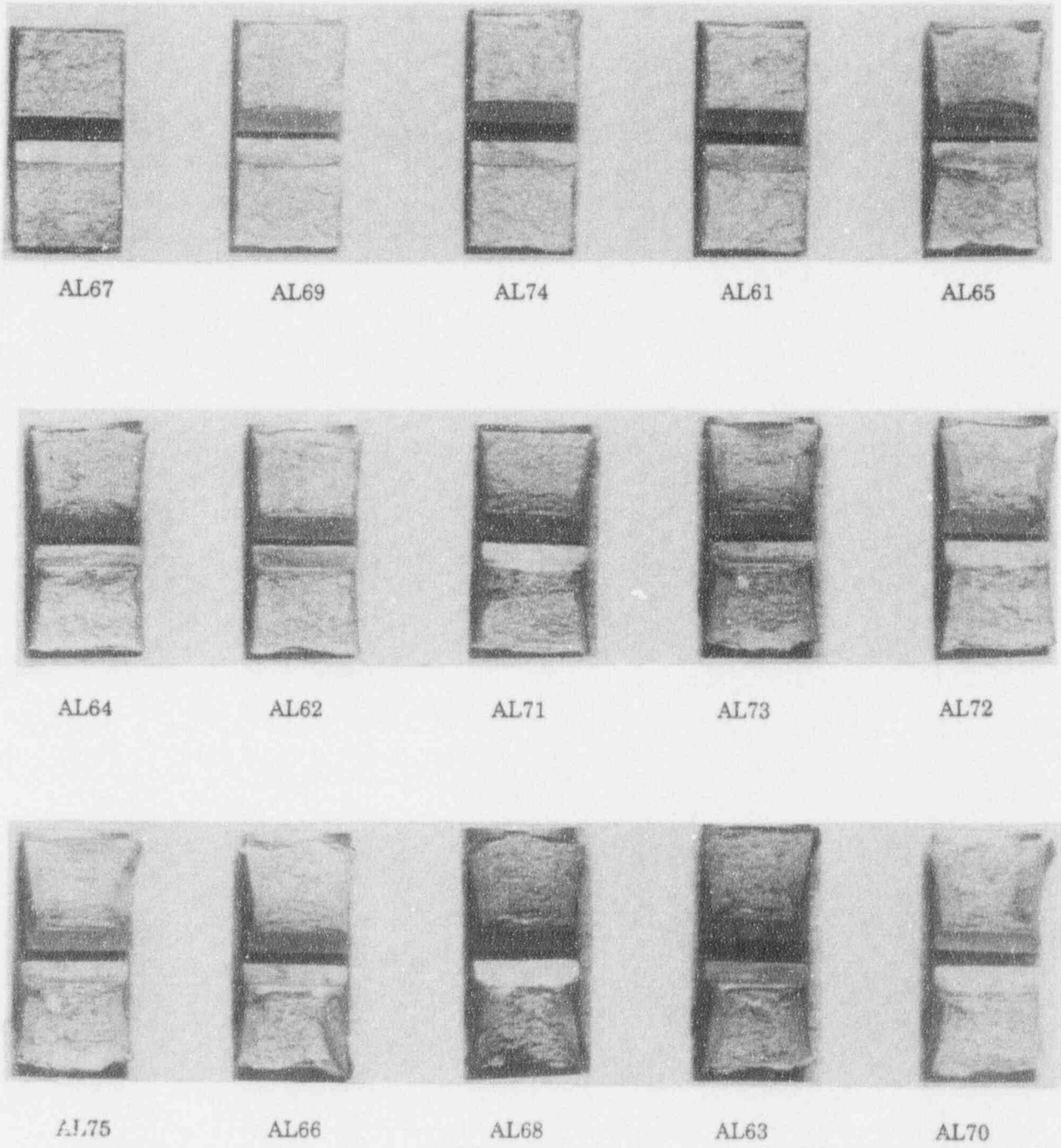


Figure 5-5 Charpy Impact Specimen Fracture Surfaces for Vogtle Unit 1 Reactor Vessel Intermediate Shell Plate B8805-3 (Longitudinal Orientation)

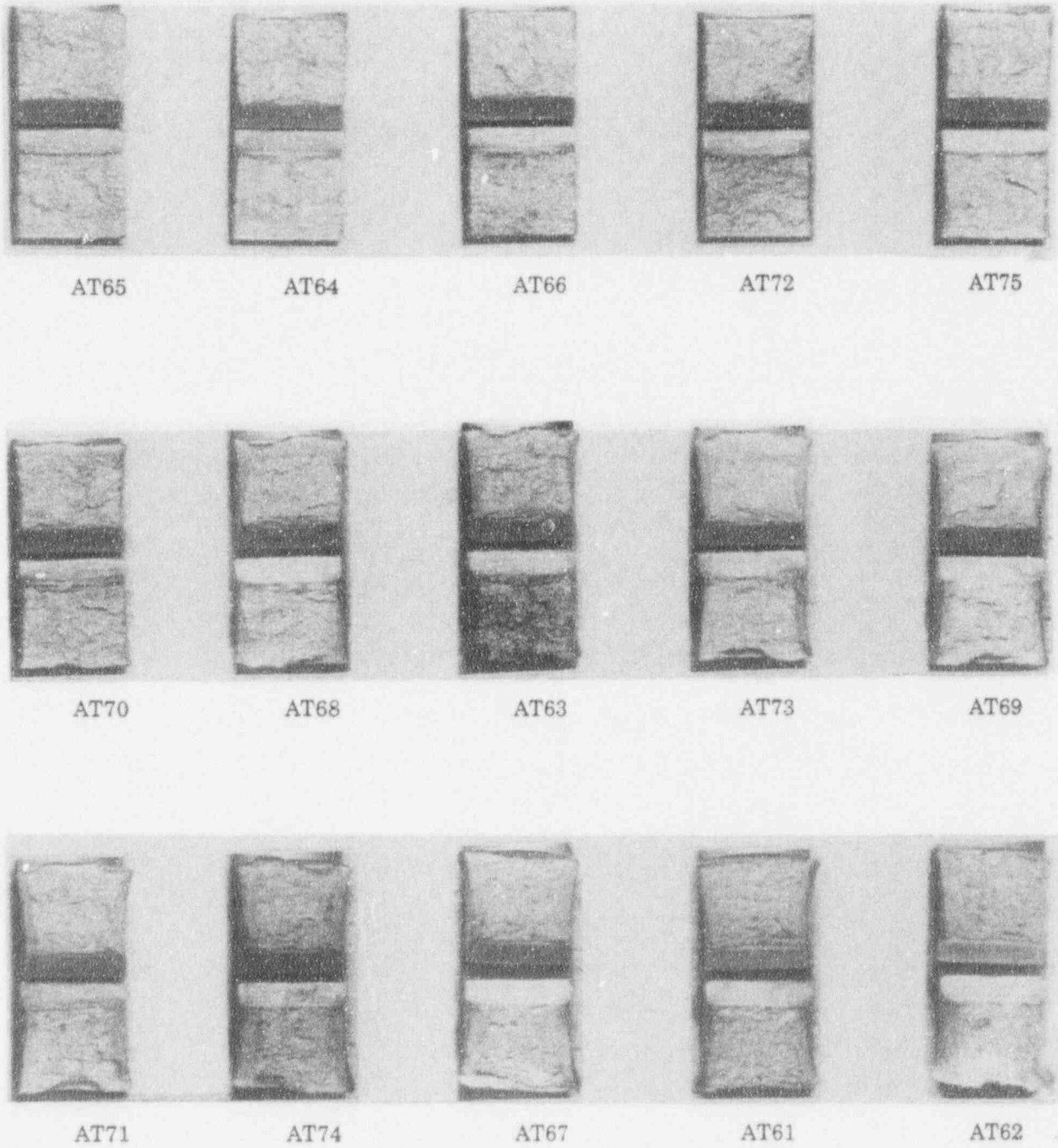
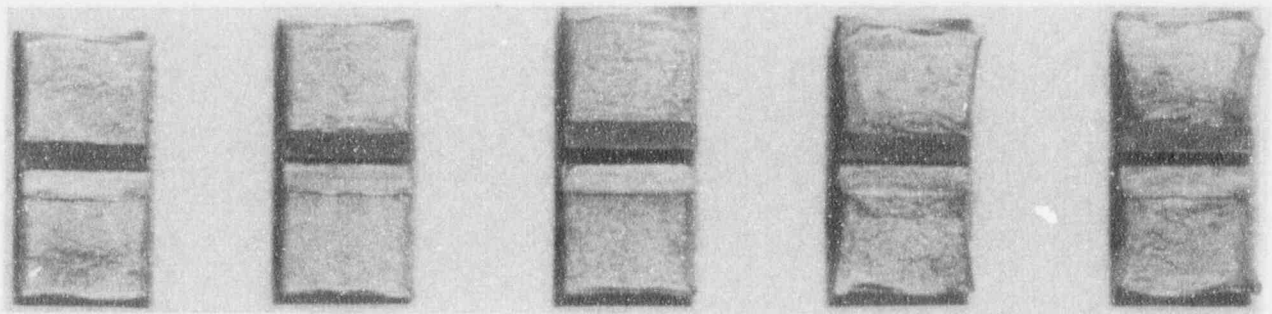


Figure 5-6 Charpy Impact Specimen Fracture Surfaces for Vogtle Unit 1 Reactor Vessel Intermediate Shell Plate B8805-3 (Transverse Orientation)



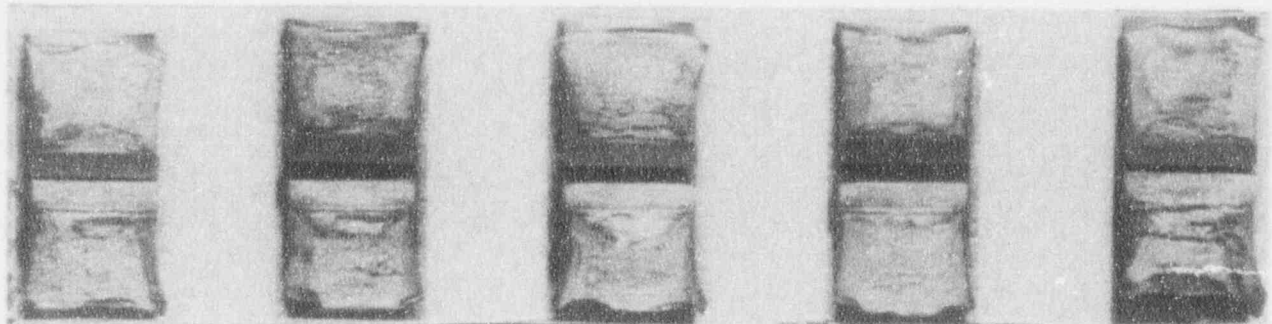
AW66

AW68

AW65

AW74

AW62



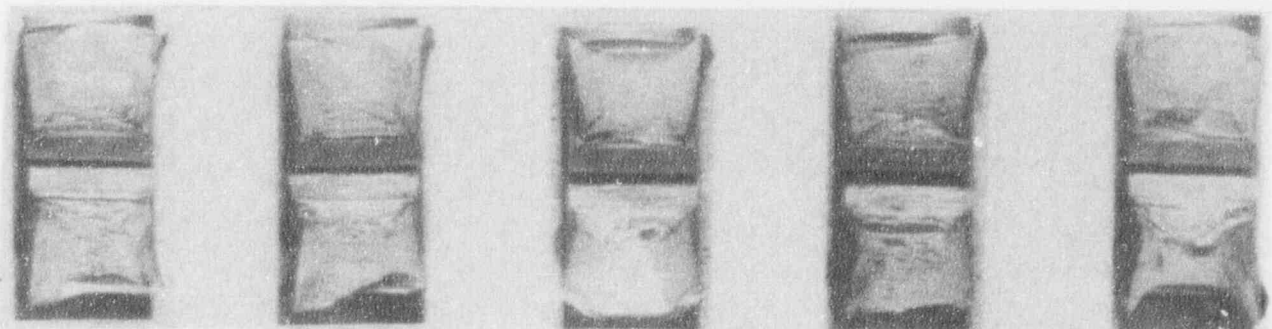
AW67

AW61

AW63

AW70

AW72



AW71

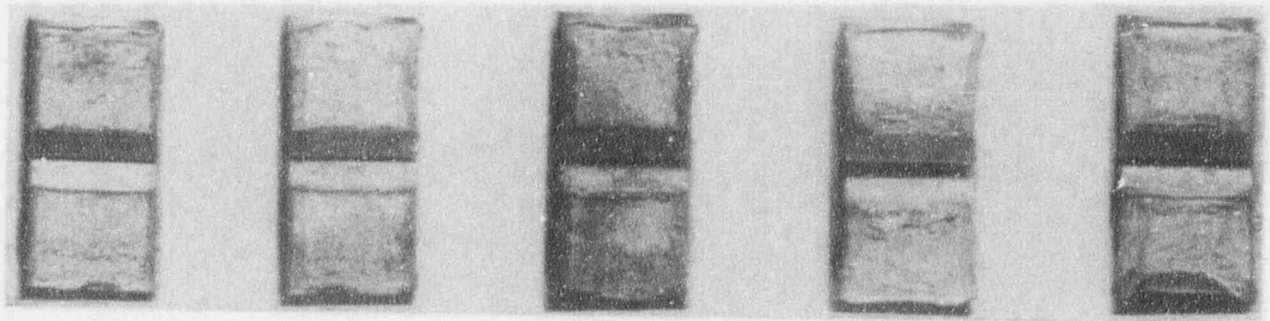
AW69

AW75

AW73

AW64

Figure 5-7 Charpy Impact Specimen Fracture Surfaces for Vogtle Unit 1 Reactor Vessel Surveillance Weld Metal



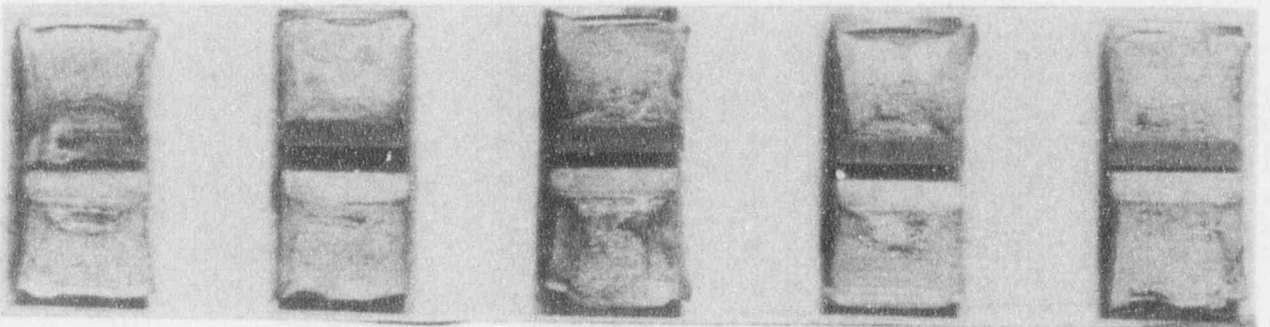
AH75

AH68

AH63

AH67

AH72



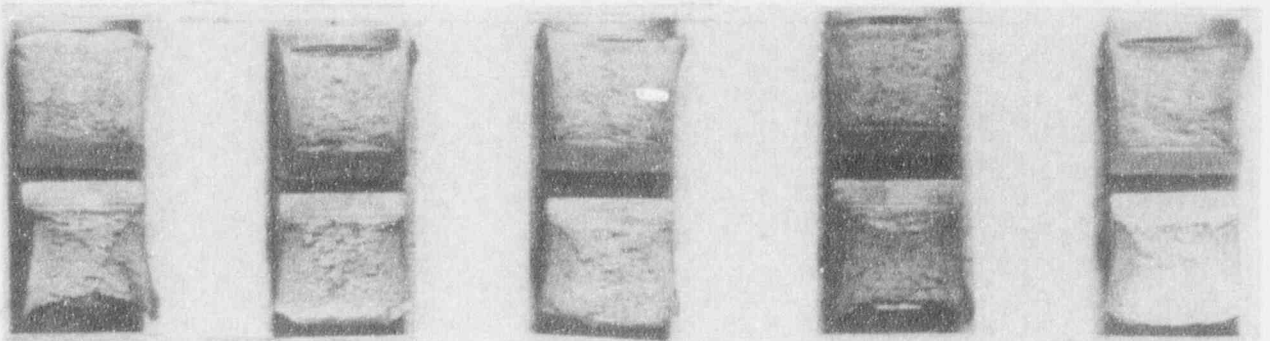
AH66

AH71

AH74

AH65

AH61



AH73

AH69

AH62

AH70

AH64

Figure 5-8 Charpy Impact Specimen Fracture Surfaces for Vogtle Unit 1 Reactor Vessel Heat-Affected-Zone Metal

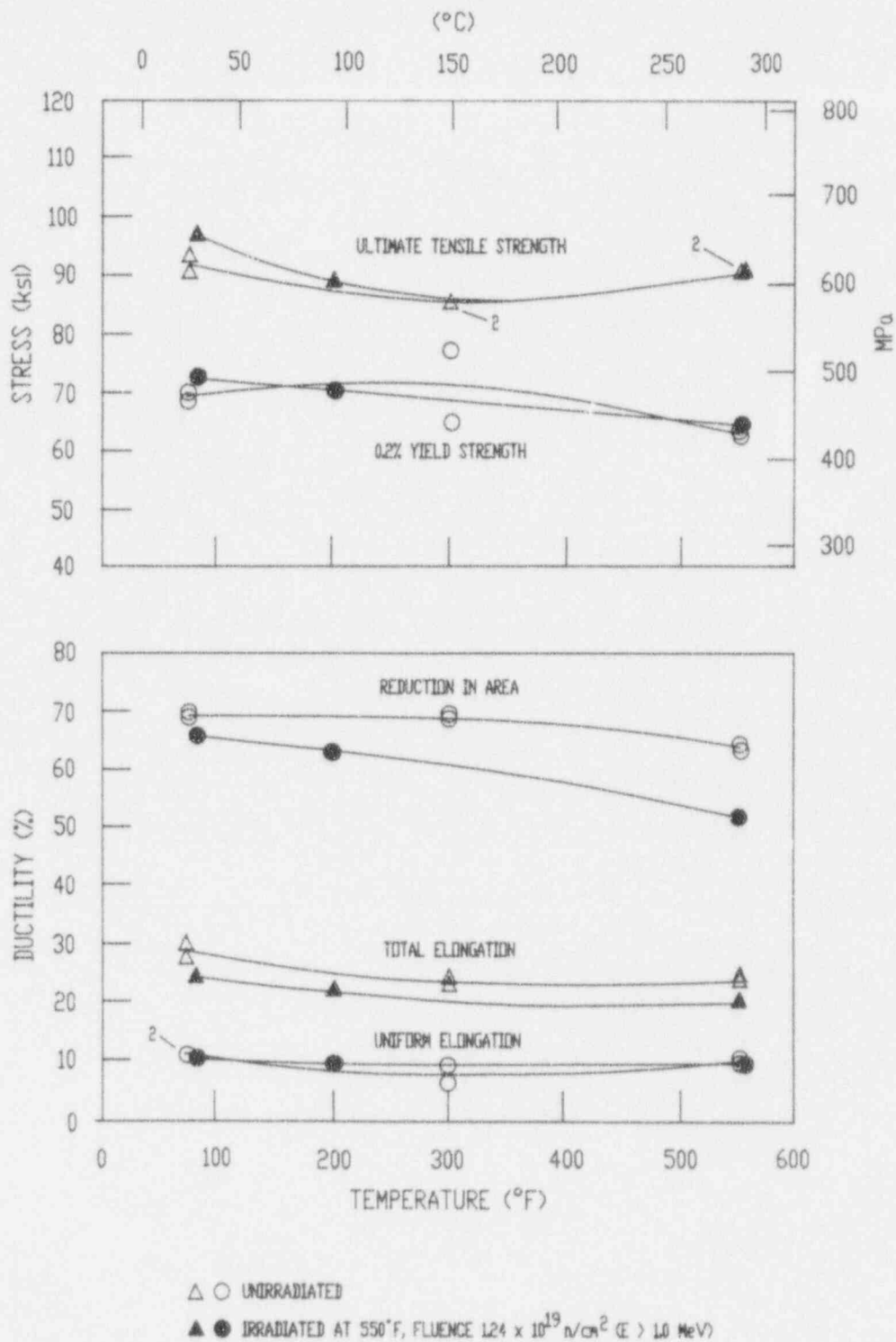


Figure 5-9 Tensile Properties for Vogtle Unit 1 Reactor Vessel Intermediate Shell Plate B8805-3 (Longitudinal Orientation)

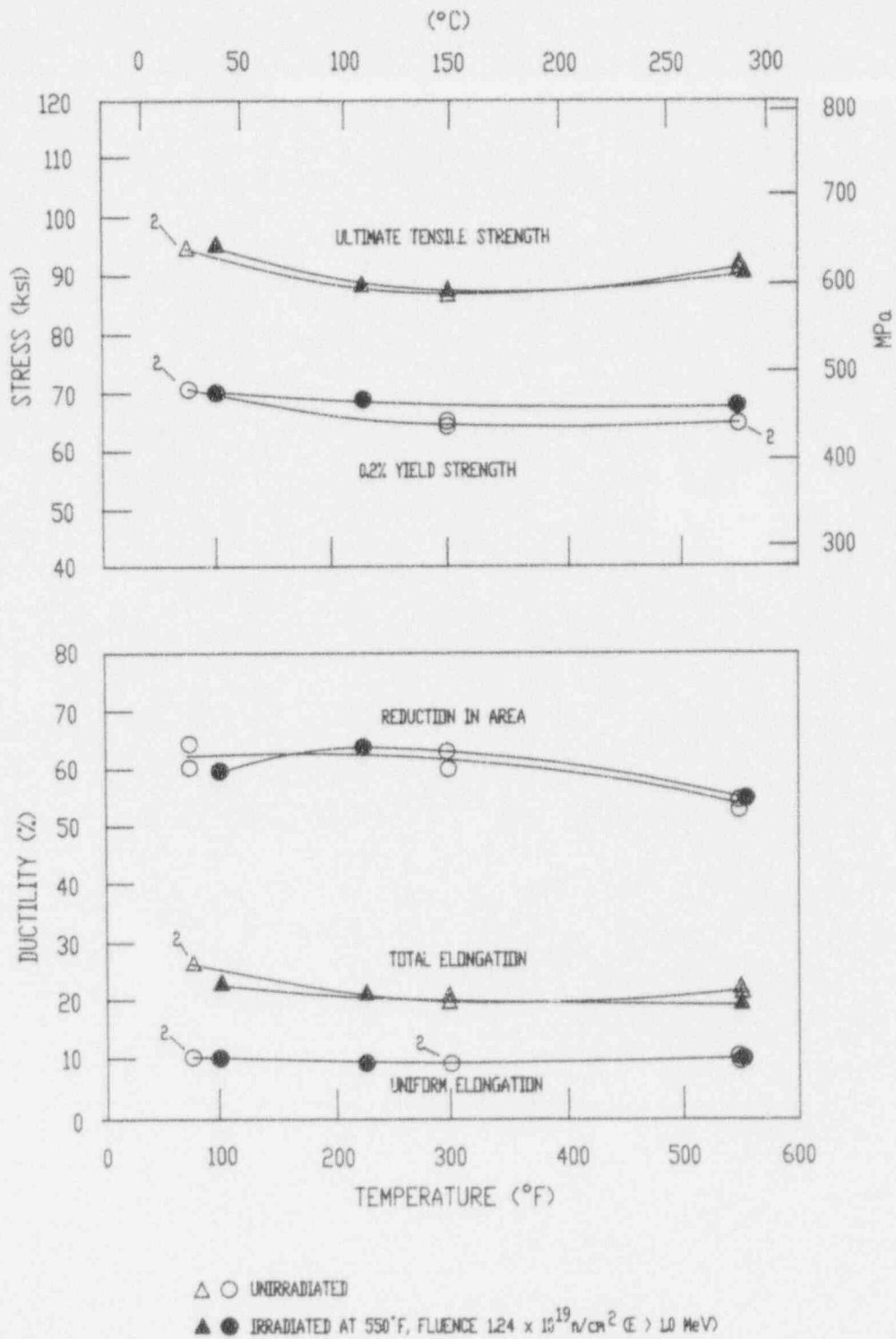


Figure 5-10 Tensile Properties for Vogtle Unit 1 Reactor Vessel Intermediate Shell Plate B8805-3 (Transverse Orientation)

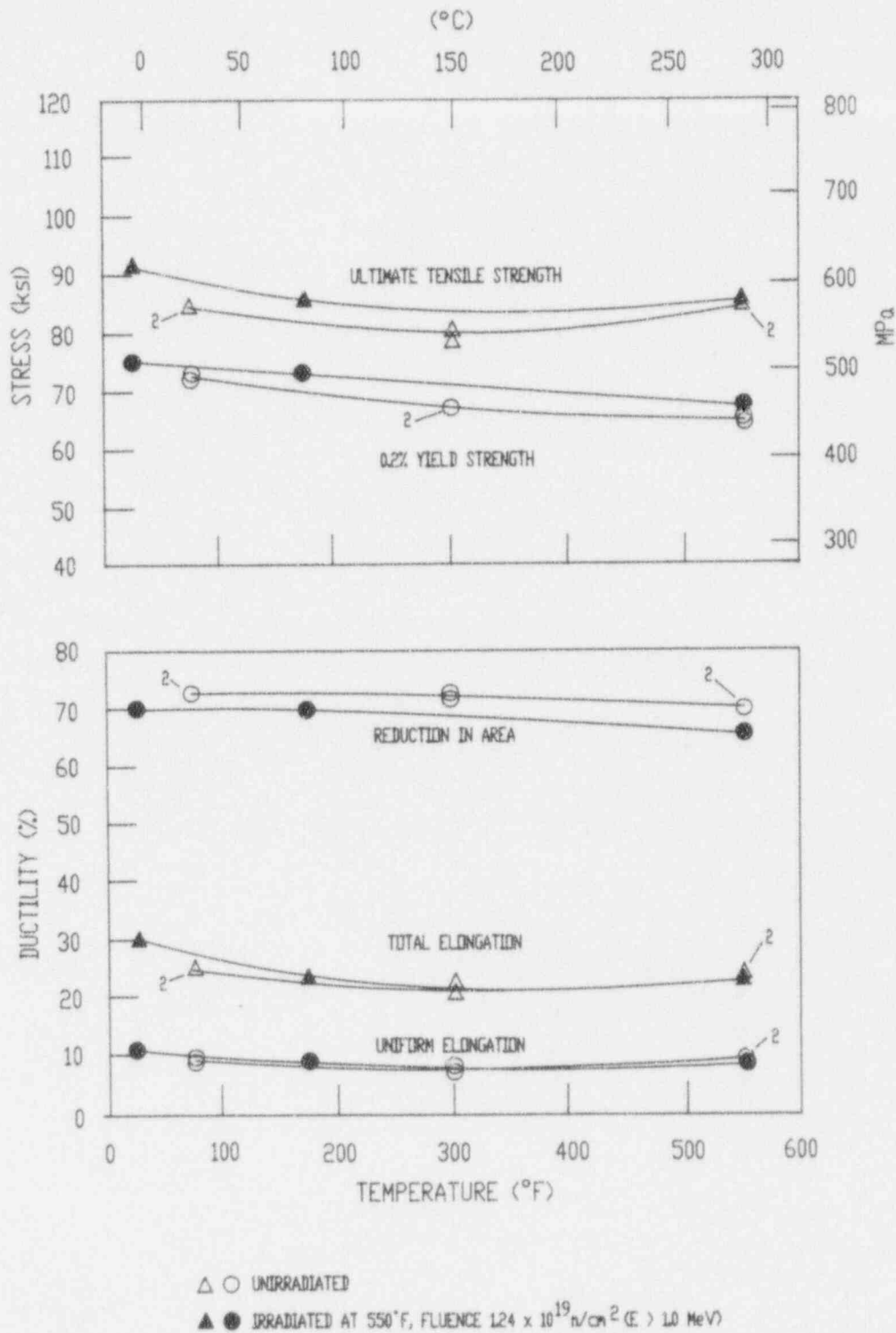
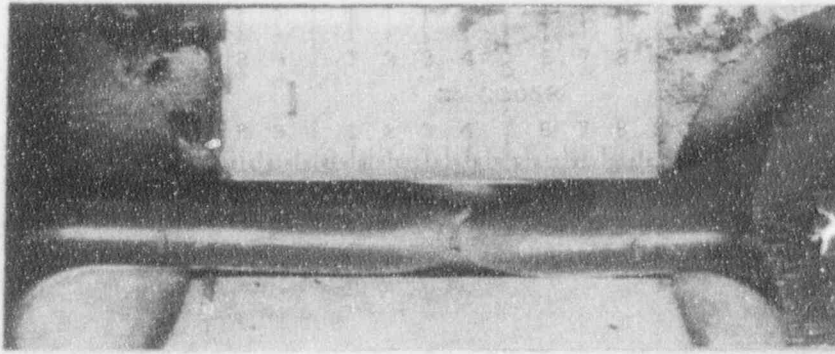
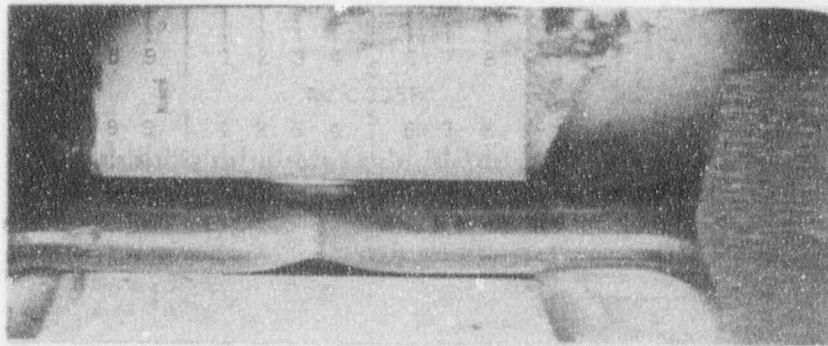


Figure 5-11 Tensile Properties for Vogtle Unit 1 Reactor Vessel Surveillance Weld Metal



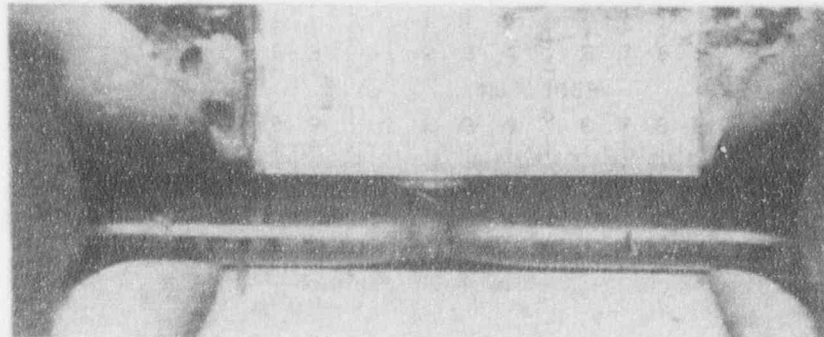
Specimen AL13

85° F



Specimen AL14

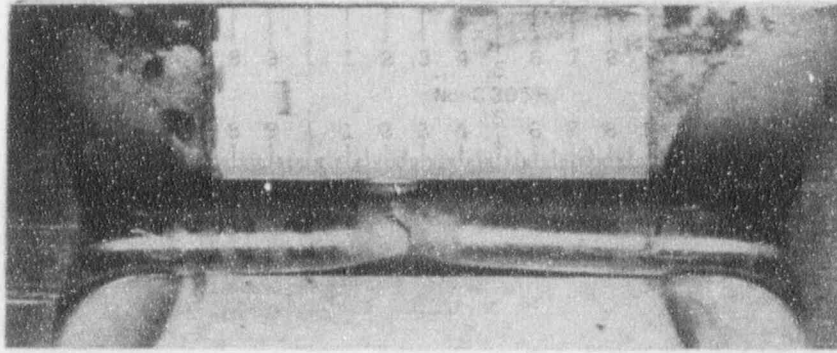
200° F



Specimen AL15

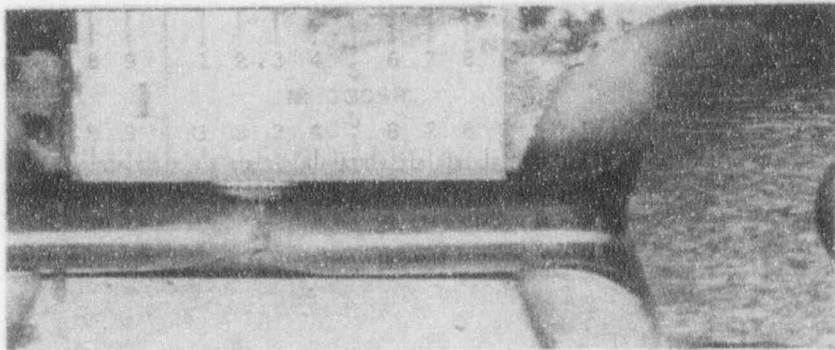
550° F

Figure 5-12 Fractured Tensile Specimens from Vogtle Unit 1 Reactor Vessel Intermediate Shell Plate B8805-3 (Longitudinal Orientation)



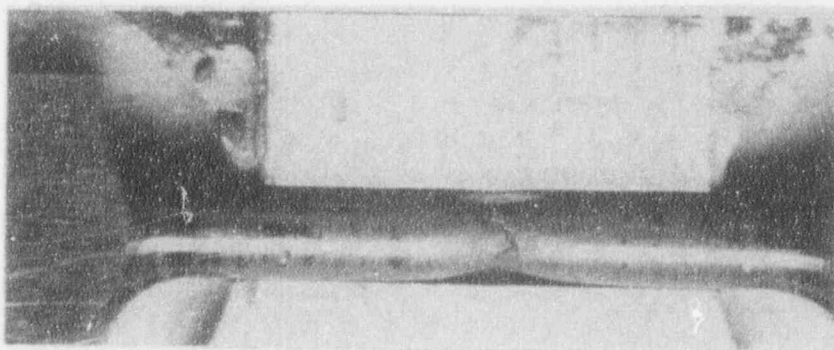
Specimen AT13

100° F



Specimen AT14

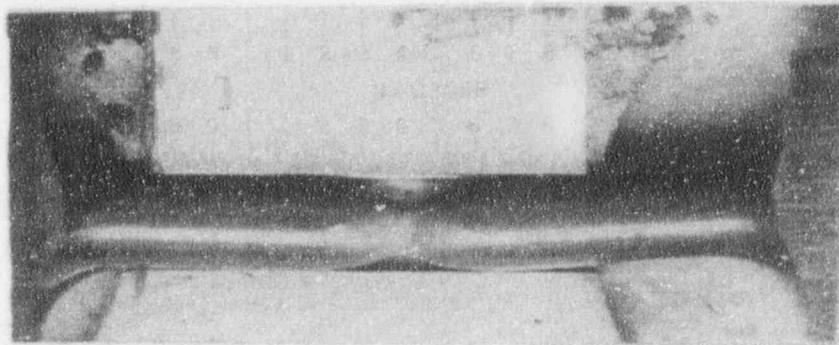
225° F



Specimen AT15

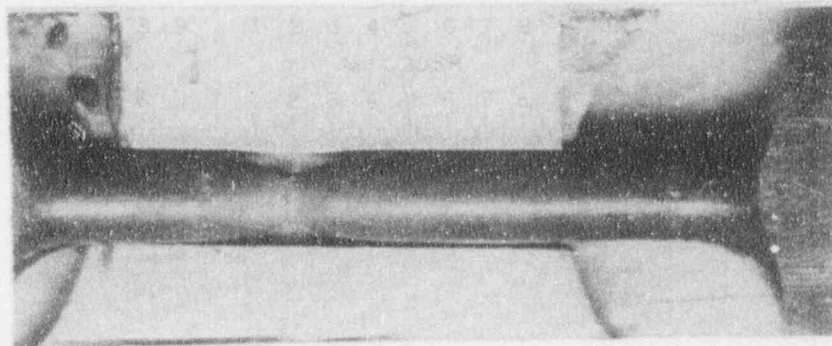
550° F

Figure 5-13 Fractured Tensile Specimens from Vogtle Unit 1 Reactor Vessel Intermediate Shell Plate B8805-3 (Transverse Orientation)



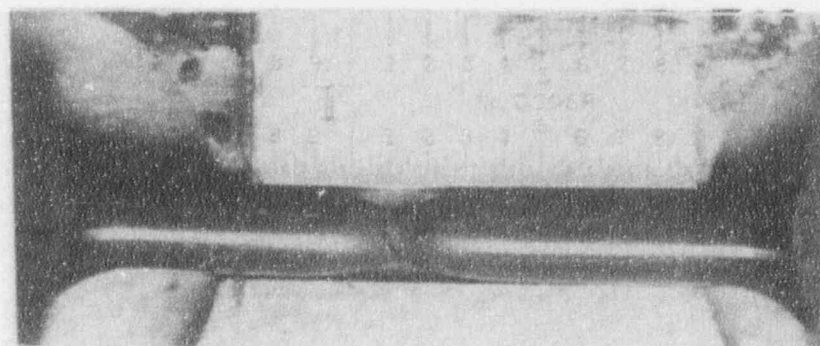
Specimen AW13

175°F



Specimen AW14

25°F



Specimen AW15

550°F

Figure 5-14 Fractured Tensile Specimens from Vogtle Unit 1 Reactor Vessel Surveillance Weld Metal

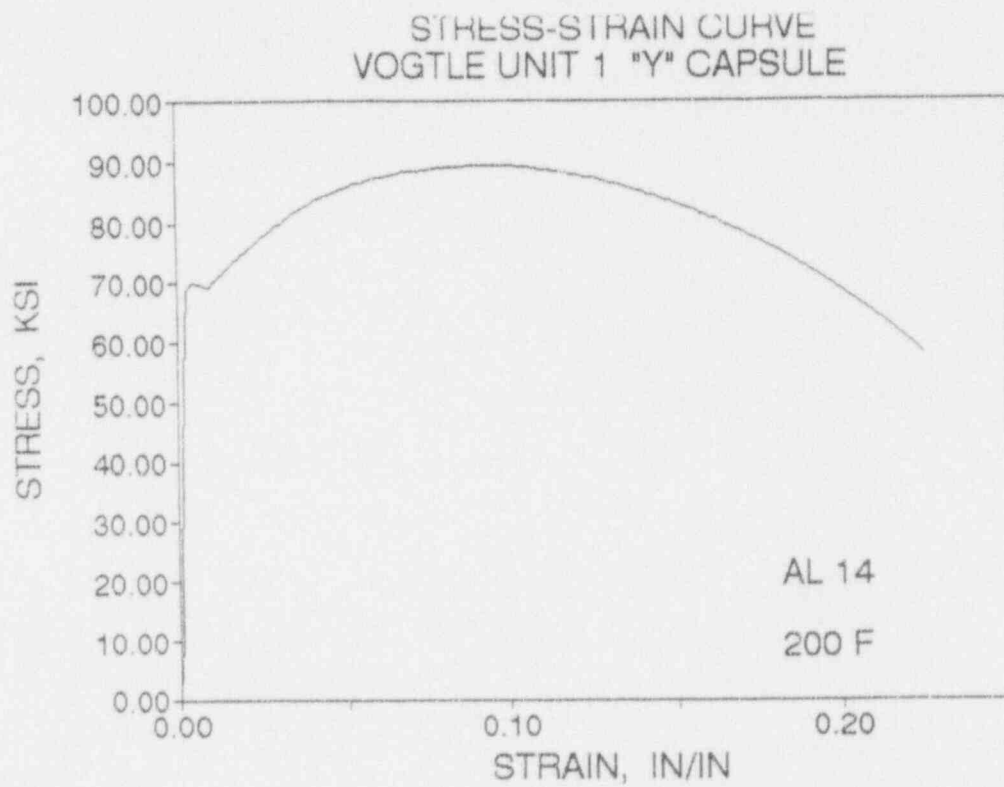
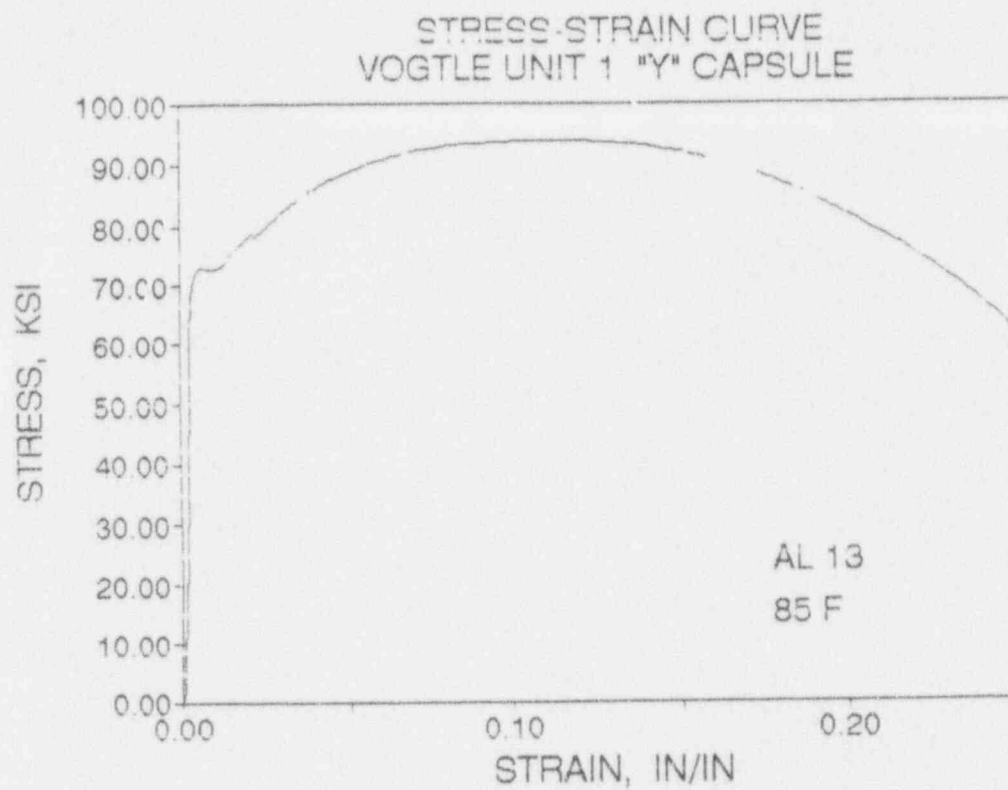


Figure 5-15 Engineering Stress-Strain Curves for Intermediate Shell Plate B8805-3 Tensile Specimens AL13 and AL14 (Longitudinal Orientation)

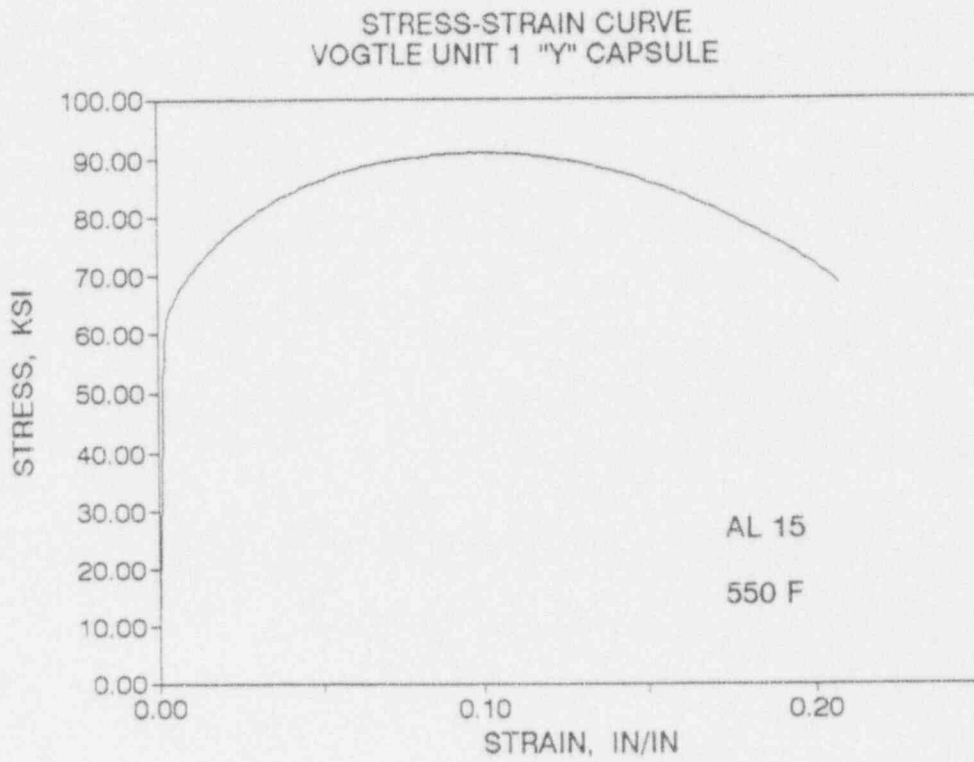


Figure 5-16 Engineering Stress-Strain Curve for Intermediate Shell Plate B8805-3
Tensile Specimen AL15 (Longitudinal Orientation)

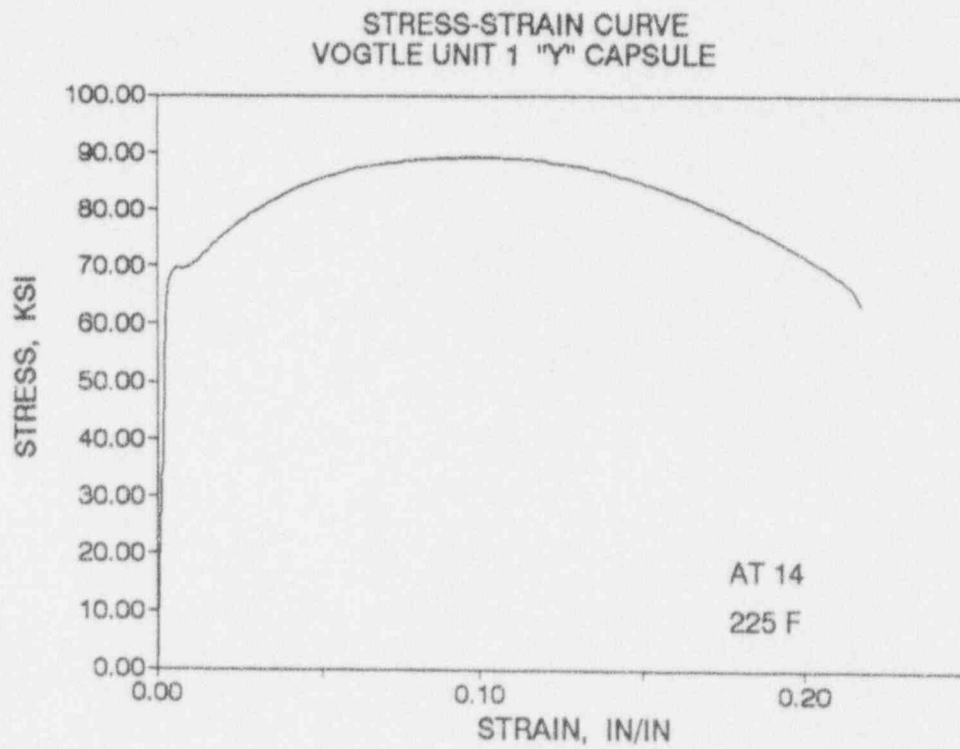
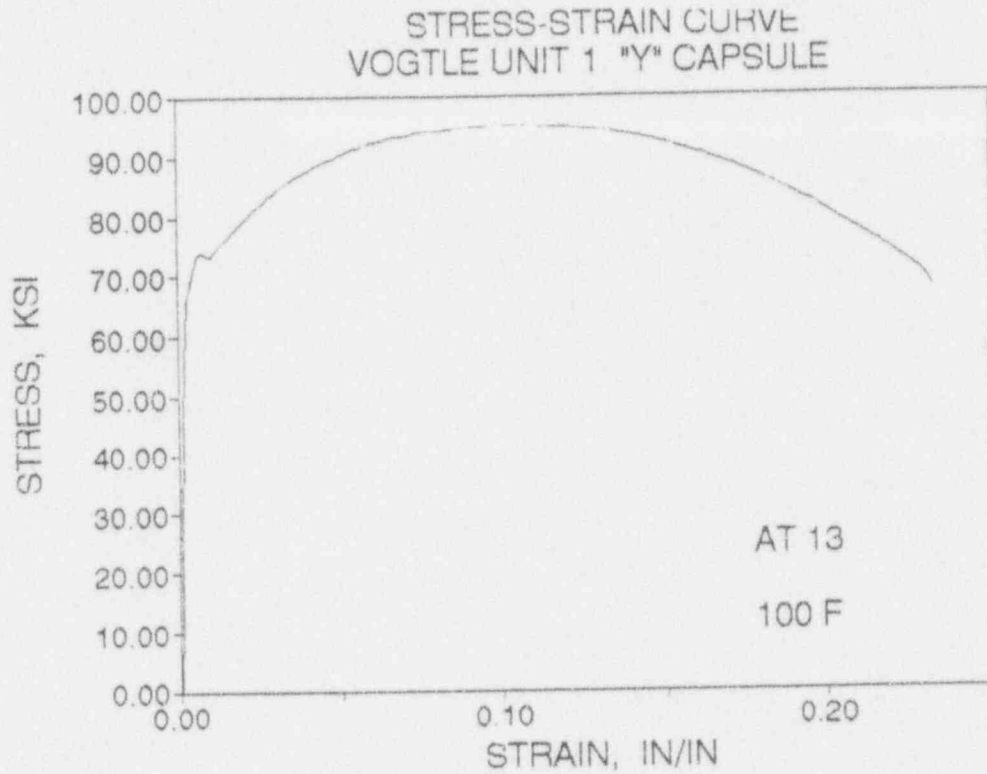


Figure 5-17 Engineering Stress-Strain Curves for Intermediate Shell Plate B8805-3 Tensile Specimens AT13 and AT14 (Transverse Orientation)

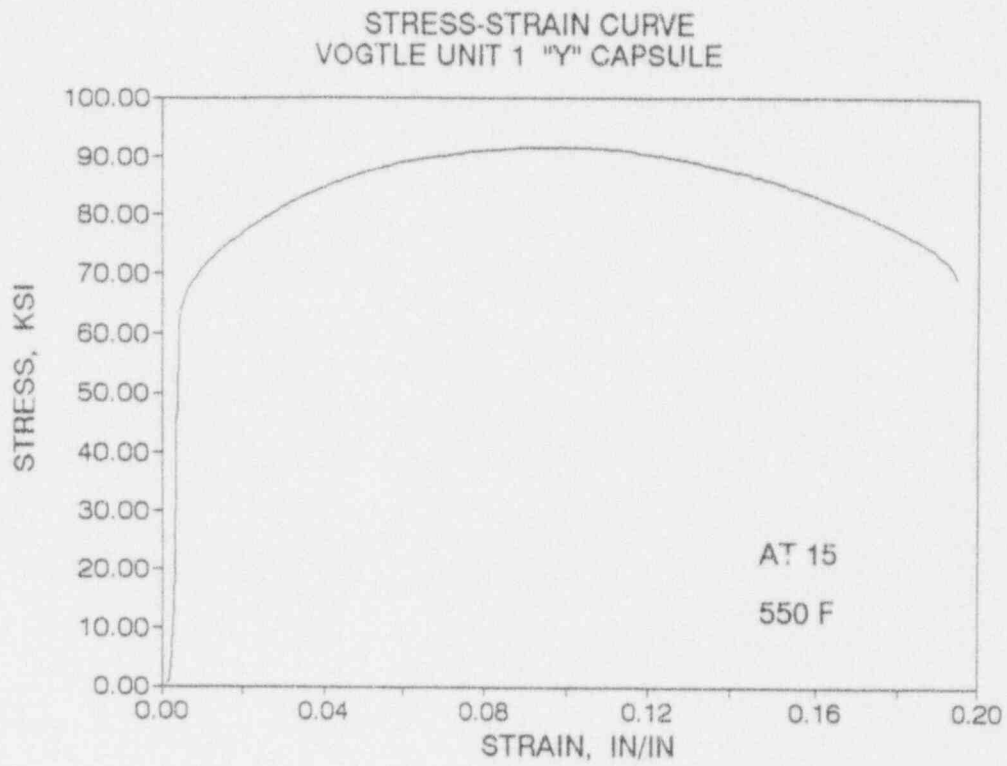


Figure 5-18 Engineering Stress-Strain Curve for Intermediate Shell Plate B8805-3
Tensile Specimen AT15 (Transverse Orientation)

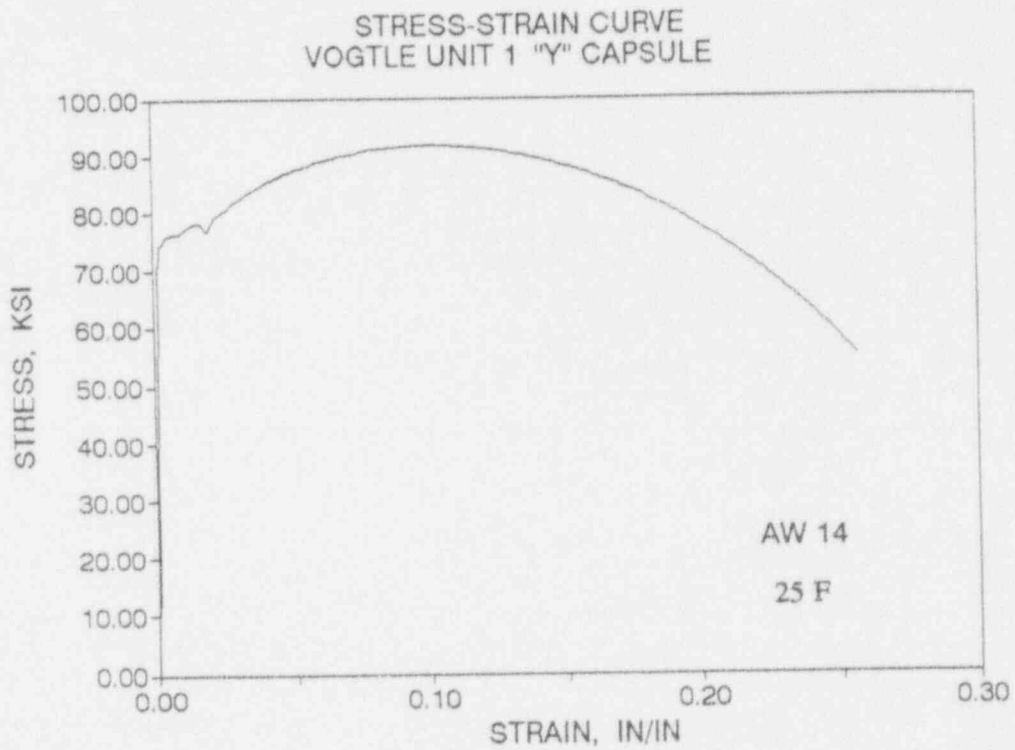
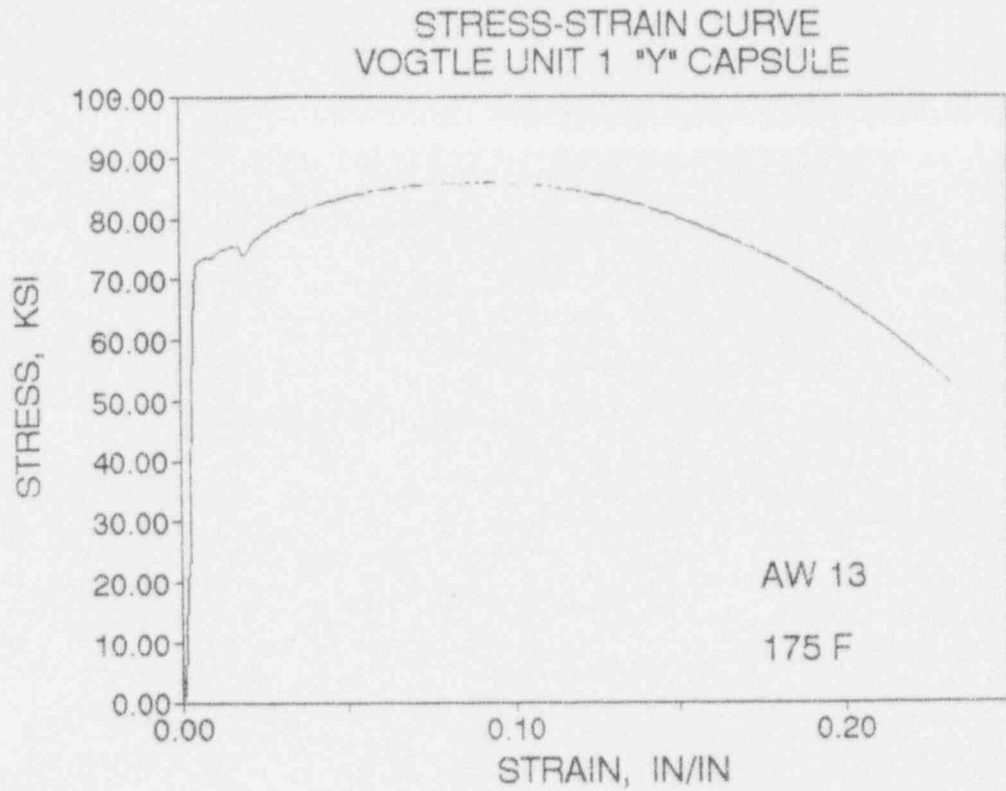


Figure 5-19 Engineering Stress-Strain Curves for Weld Metal Tensile Specimens
AW13 and AW14

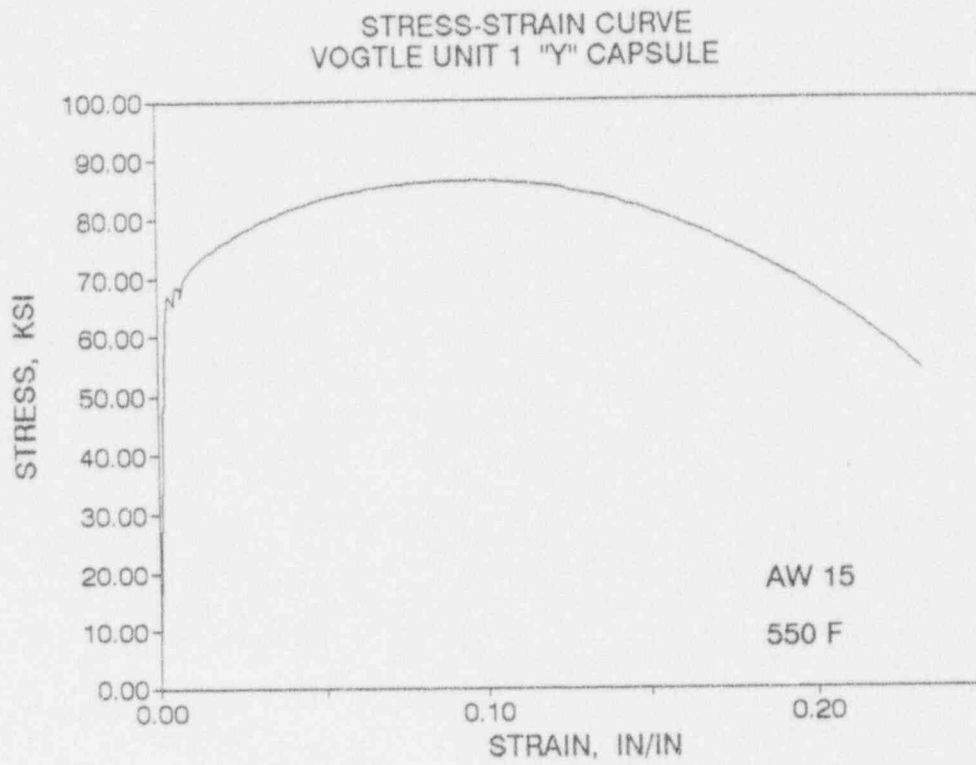


Figure 5-20 Engineering Stress-Strain Curve for Weld Metal Tensile Specimens
AW15

SECTION 6.0
RADIATION ANALYSIS AND NEUTRON DOSIMETRY

6.1 Introduction

Knowledge of the neutron environment within the reactor pressure vessel and surveillance capsule geometry is required as an integral part of LWR reactor pressure vessel surveillance programs for two reasons. First, in order to interpret the neutron radiation induced material property changes observed in the test specimens, the neutron environment (energy spectrum, flux, fluence) to which the test specimens were exposed must be known. Second, in order to relate the changes observed in the test specimens to the present and future condition of the reactor vessel, a relationship must be established between the neutron environment at various positions within the pressure vessel and that experienced by the test specimens. The former requirement is normally met by employing a combination of rigorous analytical techniques and measurements obtained with passive neutron flux monitors contained in each of the surveillance capsules. The latter information is generally derived solely from analysis.

The use of fast neutron fluence ($E > 1.0$ MeV) to correlate measured material property changes to the neutron exposure of the material has traditionally been accepted for development of damage trend curves as well as for the implementation of trend curve data to assess vessel condition. In recent years, however, it has been suggested that an exposure model that accounts for differences in neutron energy spectra between surveillance capsule locations and positions within the vessel wall could lead to an improvement in the uncertainties associated with damage trend curves as well as to a more accurate evaluation of damage gradients through the pressure vessel wall.

Because of this potential shift away from a threshold fluence toward an energy dependent damage function for data correlation, ASTM Standard Practice E853, "Analysis and Interpretation of Light Water Reactor Surveillance Results," recommends reporting displacements per iron atom (dpa) along with fluence ($E > 1.0$ MeV) to provide a data base for future reference. The energy dependent d_{dpa} function to be used for this evaluation is specified in ASTM Standard Practice E693, "Characterizing Neutron Exposures in Ferritic Steels in Terms of Displacements per Atom." The application of the dpa parameter to the assessment of embrittlement gradients through the thickness of the pressure vessel wall has already been promulgated in Revision 2 to Regulatory Guide 1.99, "Radiation Damage to Reactor Vessel Materials."

This section provides the results of the neutron dosimetry evaluations performed in conjunction with the analysis of test specimens contained in surveillance capsule Y, withdrawn at the end of the fourth fuel cycle. Also included is an updated evaluation of the dosimetry contained in capsule U, withdrawn at the conclusion of cycle one. This update is based on current state-of-the-art methodology and nuclear data; and, together with the capsule Y results, provides a consistent up to date data base for use in evaluating the material properties of the Vogtle Unit 1 reactor vessel.

In each of the dosimetry evaluations, fast neutron exposure parameters in terms of neutron fluence ($E > 1.0$ MeV), neutron fluence ($E > 0.1$ MeV), and iron atom displacements (dpa) are established for the capsule irradiation history. The analytical formalism relating the measured capsule exposure to the exposure of the vessel wall is described and used to project the integrated exposure of the vessel wall. Also, uncertainties associated with the derived exposure parameters at the surveillance capsules and with the projected exposure of the pressure vessel are provided.

6.2 Discrete Ordinates Analysis

A plan view of the reactor geometry at the core midplane is shown in Figure 4-1. Six irradiation capsules attached to the thermal shield are included in the reactor design to constitute the reactor vessel surveillance program. The capsules are located at azimuthal angles of 58.5° , 61.0° , 121.5° , 238.5° , 241.0° , and 301.5° relative to the core cardinal axis as shown in Figure 4-1. A plan view of a dual surveillance capsule holder attached to the neutron pad is shown in Figure 6-1. The stainless steel specimen containers are 1.182 by 1-inch and approximately 56 inches in height. The containers are positioned axially such that the test specimens are centered on the core midplane, thus spanning the central 5 feet of the 12 foot high reactor core.

From a neutronic standpoint, the surveillance capsules and associated support structures are significant. The presence of these materials has a marked effect on both the spatial distribution of neutron flux and the neutron energy spectrum in the water annulus between the thermal shield and the reactor vessel. In order to determine the neutron environment at the test specimen location, the capsules themselves must be included in the analytical model.

In performing the fast neutron exposure evaluations for the surveillance capsules and reactor vessel, two distinct sets of transport calculations were carried out. The first, a single computation in the

conventional forward mode, was used primarily to obtain relative neutron energy distributions throughout the reactor geometry as well as to establish relative radial distributions of exposure parameters $\{\phi(E > 1.0 \text{ MeV}), \phi(E > 0.1 \text{ MeV}), \text{ and dpa/sec}\}$ through the vessel wall. The neutron spectral information was required for the interpretation of neutron dosimetry withdrawn from the surveillance capsules as well as for the determination of exposure parameter ratios; i.e., $[\text{dpa/sec}]/[\phi(E > 1.0 \text{ MeV})]$, within the pressure vessel geometry. The relative radial gradient information was required to permit the projection of measured exposure parameters to locations interior to the pressure vessel wall; i.e., the 1/4T, 1/2T, and 3/4T locations.

The second set of calculations consisted of a series of adjoint analyses relating the fast neutron flux, $\phi(E > 1.0 \text{ MeV})$, at surveillance capsule positions and at several azimuthal locations on the pressure vessel inner radius to neutron source distributions within the reactor core. The source importance functions generated from these adjoint analyses provided the basis for all absolute exposure calculations and comparison with measurement. These importance functions, when combined with fuel cycle specific neutron source distributions, yielded absolute predictions of neutron exposure at the locations of interest for each cycle of irradiation. They also established the means to perform similar predictions and dosimetry evaluations for all subsequent fuel cycles. It is important to note that the cycle specific neutron source distributions utilized in these analyses included not only spatial variations of fission rates within the reactor core but also accounted for the effects of varying neutron yield per fission and fission spectrum introduced by the build-up of plutonium as the burnup of individual fuel assemblies increased.

The absolute cycle specific data from the adjoint evaluations together with the relative neutron energy spectra and radial distribution information from the reference forward calculation provided the means to:

- 1 - Evaluate neutron dosimetry obtained from surveillance capsules.
- 2 - Extrapolate dosimetry results to key locations at the inner radius and through the thickness of the pressure vessel wall.
- 3 - Enable a direct comparison of analytical prediction with measurement.
- 4 - Establish a mechanism for projection of pressure vessel exposure as the design of each new fuel cycle evolves.

The forward transport calculation for the reactor model summarized in Figures 4-1 and 6-1 was carried out in R,θ geometry using the DOT two-dimensional discrete ordinates code⁽¹³⁾ and the SAILOR cross-section library⁽¹⁴⁾. The SAILOR library is a 47 energy group ENDF/B-IV based data set produced specifically for light water reactor applications. In these analyses anisotropic scattering was treated with a P_3 expansion of the scattering cross-sections and the angular discretization was modeled with an S_8 order of angular quadrature.

The core power distribution utilized in the reference forward transport calculation was derived from statistical studies of long-term operation of Westinghouse 3-loop plants. Inherent in the development of this reference core power distribution is the use of an out-in fuel management strategy; i.e., fresh fuel on the core periphery. Furthermore, for the peripheral fuel assemblies, the neutron source was increased by a 2σ margin derived from the statistical evaluation of plant to plant and cycle to cycle variations in peripheral power. Since it is unlikely that any single reactor would exhibit power levels on the core periphery at the nominal $+2\sigma$ value for a large number of fuel cycles, the use of this reference distribution is expected to yield somewhat conservative results.

All adjoint calculations were also carried out using an S_8 order of angular quadrature and the P_3 cross-section approximation from the SAILOR library. Adjoint source locations were chosen at several azimuthal locations along the pressure vessel inner radius as well as at the geometric center of each surveillance capsule. Again, these calculations were run in R,θ geometry to provide neutron source distribution importance functions for the exposure parameter of interest, in this case $\phi(E > 1.0 \text{ MeV})$.

Having the importance functions and appropriate core source distributions, the response of interest could be calculated as:

$$R(r,\theta) = \int_r \int_\theta \int_E I(r,\theta,E) S(r,\theta,E) r dr d\theta dE$$

where: $R(r,\theta) = \phi(E > 1.0 \text{ MeV})$ at radius r and azimuthal angle θ .

$I(r,\theta,E) =$ Adjoint source importance function at radius r , azimuthal angle θ , and neutron source energy E .

$S(r,\theta,E) =$ Neutron source strength at core location r,θ and energy E .

Although the adjoint importance functions used in this analysis were based on a response function defined by the threshold neutron flux $\phi(E > 1.0 \text{ MeV})$, prior calculations⁽¹⁵⁾ have shown that, while the

implementation of low leakage loading patterns significantly impacts both the magnitude and spatial distribution of the neutron field, changes in the relative neutron energy spectrum are of second order. Thus, for a given location the ratio of $[dpa/sec]/[\phi(E > 1.0 \text{ MeV})]$ is insensitive to changing core source distributions. In the application of these adjoint importance functions to the Vogtle Unit 1 reactor, therefore, the iron atom displacement rates (dpa/sec) and the neutron flux $\phi(E > 0.1 \text{ MeV})$ were computed on a cycle specific basis by using $[dpa/sec]/[\phi(E > 1.0 \text{ MeV})]$ and $[\phi(E > 0.1 \text{ MeV})]/[\phi(E > 1.0 \text{ MeV})]$ ratios from the forward analysis in conjunction with the cycle specific $\phi(E > 1.0 \text{ MeV})$ solutions from the individual adjoint evaluations.

The reactor core power distributions used in the plant specific adjoint calculations were taken from the fuel cycle design reports for the first four operating cycles of Vogtle Unit 1 [16 through 20].

Selected results from the neutron transport analyses are provided in Tables 6-1 through 6-5. The data listed in these tables establish the means for absolute comparisons of analysis and measurement for the capsule irradiation periods and provide the means to correlate dosimetry results with the corresponding exposure of the pressure vessel wall.

In Table 6-1, the calculated exposure parameters [$\phi(E > 1.0 \text{ MeV})$, $\phi(E > 0.1 \text{ MeV})$, and dpa/sec] are given at the geometric center of the two surveillance capsule positions for both the reference and the plant specific core power distributions. The plant specific data, based on the adjoint transport analysis, are meant to establish the absolute comparison of measurement with analysis. The reference data derived from the forward calculation are provided as a conservative exposure evaluation against which plant specific fluence calculations can be compared. Similar data are given in Table 6-2 for the pressure vessel inner radius. Again, the three pertinent exposure parameters are listed for the reference and the cycle one through four plant specific power distributions. It is important to note that the data for the vessel inner radius were taken at the clad/base metal interface; and, thus, represent the maximum predicted exposure levels of the vessel wall itself.

Radial gradient information applicable to $\phi(E > 1.0 \text{ MeV})$, $\phi(E > 0.1 \text{ MeV})$, and dpa/sec is given in Tables 6-3, 6-4, and 6-5, respectively. The data, obtained from the reference forward neutron transport calculation, are presented on a relative basis for each exposure parameter at several azimuthal locations. Exposure distributions through the vessel wall may be obtained by normalizing the calculated or projected exposure at the vessel inner radius to the gradient data listed in Tables 6-3 through 6-5.

For example, the neutron flux $\phi(E > 1.0 \text{ MeV})$ at the 1/4T depth in the pressure vessel wall along the 45° azimuth is given by:

$$\phi_{1/4T}(45^\circ) = \phi(220.27, 45^\circ) F(225.75, 45^\circ)$$

where: $\phi_{1/4T}(45^\circ)$ = Projected neutron flux at the 1/4T position on the 45° azimuth.
 $\phi(220.27, 45^\circ)$ = Projected or calculated neutron flux at the vessel inner radius on the 45° azimuth.
 $F(225.75, 45^\circ)$ = Ratio of the neutron flux at the 1/4T position to the flux at the vessel inner radius for the 45° azimuth. This data is obtained from Table 6-3.

Similar expressions apply for exposure parameters expressed in terms of $\phi(E > 0.1 \text{ MeV})$ and dpa/sec where the attenuation function F is obtained from Tables 6-4 and 6-5, respectively.

6.3 Neutron Dosimetry

The passive neutron sensors included in the Vogtle Unit 1 surveillance program are listed in Table 6-6. Also given in Table 6-6 are the primary nuclear reactions and associated nuclear constants that were used in the evaluation of the neutron energy spectrum within the surveillance capsules and in the subsequent determination of the various exposure parameters of interest [$\phi(E > 1.0 \text{ MeV})$, $\phi(E > 0.1 \text{ MeV})$, dpa/sec]. The relative locations of the neutron sensors within the capsules are shown in Figure 4-2. The iron, nickel, copper, and cobalt-aluminum monitors, in wire form, were placed in holes drilled in spacers at several axial levels within the capsules. The cadmium shielded uranium and neptunium fission monitors were accommodated within the dosimeter block located near the center of the capsule.

The use of passive monitors such as those listed in Table 6-6 does not yield a direct measure of the energy dependent neutron flux at the point of interest. Rather, the activation or fission process is a measure of the integrated effect that the time and energy dependent neutron flux has on the target material over the course of the irradiation period. An accurate assessment of the average neutron flux level incident on the various monitors may be derived from the activation measurements only if the irradiation parameters are well known. In particular, the following variables are of interest:

- The measured specific activity of each monitor.

- The physical characteristics of each monitor.
- The operating history of the reactor.
- The energy response of each monitor.
- The neutron energy spectrum at the monitor location.

The specific activity of each of the neutron monitors was determined using established ASTM procedures^[24 through 34]. Following sample preparation and weighing, the activity of each monitor was determined by means of a lithium-drifted germanium, Ge(Li), gamma spectrometer. The irradiation history of the Vogtle Unit 1 reactor during cycles one through four was supplied by NUREG-0020, "Licensed Operating Reactors Status Summary Report," for the applicable period. The irradiation history applicable to capsules Y and U is given in Table 6-7. Note that the Vogtle Unit 1 uprating / T-hot reduction has increased the full power design reactor power rating from 3411 to 3565 MWt. The analysis performed for capsule Y used the new power rating for all calculations.

Having the measured specific activities, the physical characteristics of the sensors, and the operating history of the reactor, reaction rates referenced to full power operation were determined from the following equation:

$$R = \frac{A}{N_0 F Y \sum \frac{P_j}{P_{ref}} C_j [1 - e^{-\lambda t_j}] [e^{-\lambda t_d}]}$$

where:

- R = Reaction rate averaged over the irradiation period and referenced to operation at a core power level of P_{ref} (r./s./nucleus).
- A = Measured specific activity (dps/gm).
- N_0 = Number of target element atoms per gram of sensor.
- F = Weight fraction of the target isotope in the sensor material.
- Y = Number of product atoms produced per reaction.
- P_j = Average core power level during irradiation period j (MW).
- P_{ref} = Maximum or reference power level of the reactor (MW).
- C_j = Calculated ratio of $\phi(E > 1.0 \text{ MeV})$ during irradiation period j to the time weighted average $\phi(E > 1.0 \text{ MeV})$ over the entire irradiation period.
- λ = Decay constant of the product isotope (1/sec).
- t_j = Length of irradiation period j (sec).
- t_d = Decay time following irradiation period j (sec).

and the summation is carried out over the total number of monthly intervals comprising the irradiation period.

In the equation describing the reaction rate calculation, the ratio $[P_j]/[P_{ref}]$ accounts for month by month variation of reactor core power level within any given fuel cycle as well as over multiple fuel cycles. The ratio C_j , which can be calculated for each fuel cycle using the adjoint transport technology discussed in Section 6.2, accounts for the change in sensor reaction rates caused by variations in flux level induced by changes in core spatial power distributions from fuel cycle to fuel cycle. For a single cycle irradiation C_j is normally taken to be 1.0. However, for multiple cycle irradiations, particularly those employing low leakage fuel management, the additional C_j term should be employed. The impact of changing flux levels for constant power operation can be quite significant for sensor sets that have been irradiated for many cycles in a reactor that has transitioned from non-low leakage to low leakage fuel management or for sensor sets contained in surveillance capsules that have been moved from one capsule location to another.

For the irradiation history of capsules Y, the flux level term in the reaction rate calculations was developed from the plant specific analysis provided in Table 6-1. Measured and saturated reaction product specific activities as well as the derived full power reaction rates are listed in Table 6-8.

Values of key fast neutron exposure parameters were derived from the measured reaction rates using the FERRET least squares adjustment code^[35]. The FERRET approach used the measured reaction rate data, sensor reaction cross-sections, and a calculated trial spectrum as input and proceeded to adjust the group fluxes from the trial spectrum to produce a best fit (in a least squares sense) to the measured reaction rate data. The "measured" exposure parameters along with the associated uncertainties were then obtained from the adjusted spectrum.

In the FERRET evaluations, a log-normal least squares algorithm weights both the a priori values and the measured data in accordance with the assigned uncertainties and correlations. In general, the measured values f are linearly related to the flux ϕ by some response matrix A:

$$f_i^{(s,r)} = \sum_g A_{ig}^{(s)} \phi_g^{(\alpha)}$$

where i indexes the measured values belonging to a single data set s , g designates the energy group, and α delineates spectra that may be simultaneously adjusted. For example,

$$R_i = \sum_g \sigma_{ig} \phi_g$$

relates a set of measured reaction rates R_i to a single spectrum ϕ_g by the multigroup reaction cross-section σ_{ig} . The log-normal approach automatically accounts for the physical constraint of positive fluxes, even with large assigned uncertainties.

In the least squares adjustment, the continuous quantities (i.e., neutron spectra and cross-sections) were approximated in a multi-group format consisting of 53 energy groups. The trial input spectrum was converted to the FERRET 53 group structure using the SAND-II code^[36]. This procedure was carried out by first expanding the 47 group calculated spectrum into the SAND-II 620 group structure using a SPLINE interpolation procedure in regions where group boundaries do not coincide. The 620 point spectrum was then re-collapsed into the group structure used in FERRET.

The sensor set reaction cross-sections, obtained from the ENDF/B-V dosimetry file, were also collapsed into the 53 energy group structure using the SAND-II code. In this instance, the trial spectrum, as expanded to 620 groups, was employed as a weighting function in the cross-section collapsing procedure. Reaction cross-section uncertainties in the form of a 53 x 53 covariance matrix for each sensor reaction were also constructed from the information contained on the ENDF/B-V data files. These matrices included energy group to energy group uncertainty correlations for each of the individual reactions. However, correlations between cross-sections for different sensor reactions were not included. The omission of this additional uncertainty information does not significantly impact the results of the adjustment.

Due to the importance of providing a trial spectrum that exhibits a relative energy distribution close to the actual spectrum at the sensor set locations, the neutron spectrum input to the FERRET evaluation was taken from the center of the surveillance capsule modeled in the reference forward transport calculation. While the 53 x 53 group covariance matrices applicable to the sensor reaction cross-sections were developed from the ENDF/B-V data files, the covariance matrix for the input trial spectrum was constructed from the following relation:

$$M_{gg'} = R_n^2 + R_g R_{g'} P_{gg'}$$

where R_g specifies an overall fractional normalization uncertainty (i.e., complete correlation) for the set of values. The fractional uncertainties R_g specify additional random uncertainties for group g that are correlated with a correlation matrix given by:

$$P_{gg'} = [1 - \theta] \delta_{gg'} + \theta e^{-H}$$

where:

$$H = \frac{(g - g')^2}{2 \gamma^2}$$

The first term in the correlation matrix equation specifies purely random uncertainties, while the second term describes short range correlations over a group range γ (θ specifies the strength of the latter term). The value of δ is 1 when $g = g'$ and 0 otherwise. For the trial spectrum used in the current evaluations, a short range correlation of $\gamma = 6$ groups was used. This choice implies that neighboring groups are strongly correlated when θ is close to 1. Strong long range correlations (or anti-correlations) were justified based on information presented by R. E. Maerker^[37]. Maerker's results are closely duplicated when $\gamma = 6$.

The uncertainties associated with the measured reaction rates included both statistical (counting) and systematic components. The systematic component of the overall uncertainty accounts for counter efficiency, counter calibrations, irradiation history corrections, and corrections for competing reactions in the individual sensors.

Results of the FERRET evaluations of the capsule Y and U dosimetry are given in Table 6-12. The data summarized in this table include fast neutron exposure evaluations in terms of $\Phi(E > 1.0 \text{ MeV})$, $\Phi(E > 0.1 \text{ MeV})$, and dpa. In general good results were achieved in the fits of the adjusted spectra to the individual measured reaction rates. The adjusted spectra from the least squares evaluations are given in Tables 6-11 in the FERRET 53 energy group structure. The results for capsule Y are consistent with results obtained from similar evaluations of dosimetry from other Westinghouse reactors.

6.4 Projections of Pressure Vessel Exposure

Neutron exposure projections at key locations on the pressure vessel inner radius are given in Table 6-13. Along with the current (4.64 EFPY) exposure, projections are also provided for exposure periods of 16 EFPY and 32 EFPY. In computing these vessel exposures, the calculated values from Table 6-2

were scaled by the average measurement/calculation ratios (M/C) observed from the evaluations of dosimetry from capsules Y and U for each fast neutron exposure parameter. This procedure resulted in bias factors of 1.08, 1.04, and 1.02 being applied to the calculated values of $\Phi(E > 1.0 \text{ MeV})$, $\Phi(E > 0.1 \text{ MeV})$, and dpa, respectively. Projections for future operation were based on the assumption that the average exposure rates characteristic of the cycle one through four irradiation would continue to be applicable throughout plant life.

The overall uncertainty associated with the best estimate exposure projections at the pressure vessel wall depends on the individual uncertainties in the measurement process, the uncertainty in the dosimetry location, and on the uncertainty in the extrapolation of results from the measurement points to the point of interest in the vessel wall. For Vogtle Unit 1, the uncertainty in each individual capsule derived fluence is estimated to consist of a 6% random component and a 5% systematic component, and the extrapolation uncertainty is estimated to be 5%. A statistical combination of these uncertainties for the two capsules produces an overall uncertainty estimate in the exposure of the pressure vessel wall in the beltline region of 8% (1σ) for $\Phi(E > 1.0 \text{ MeV})$.

In the calculation of exposure gradients for use in the development of heatup and cooldown curves for the Vogtle Unit 1 reactor coolant system, exposure projections to 16 EFPY and 32 EFPY were also employed. Data based on both a $\Phi(E > 1.0 \text{ MeV})$ slope and a plant specific dpa slope through the vessel wall are provided in Table 6-14.

In order to define RT_{NDT} from existing correlation curves vs fluence ($E > 1.0 \text{ MeV}$), dpa equivalent fast neutron fluence levels for the 1/4T and 3/4T positions were defined by the relations:

$$\phi(1/4T) = \phi(0T) \frac{dpa(1/4T)}{dpa(0T)}$$

and

$$\phi(3/4T) = \phi(0T) \frac{dpa(3/4T)}{dpa(0T)}$$

Using this approach results in the dpa equivalent fluence values listed in Table 6-14. In Table 6-15 updated lead factors are listed for each of the Vogtle Unit 1 surveillance capsules. Lead factor data based on the accumulated fluence through cycle four are provided for each remaining capsule.

FIGURE 6-1

Plan View of a Dual Reactor Vessel Surveillance Capsule

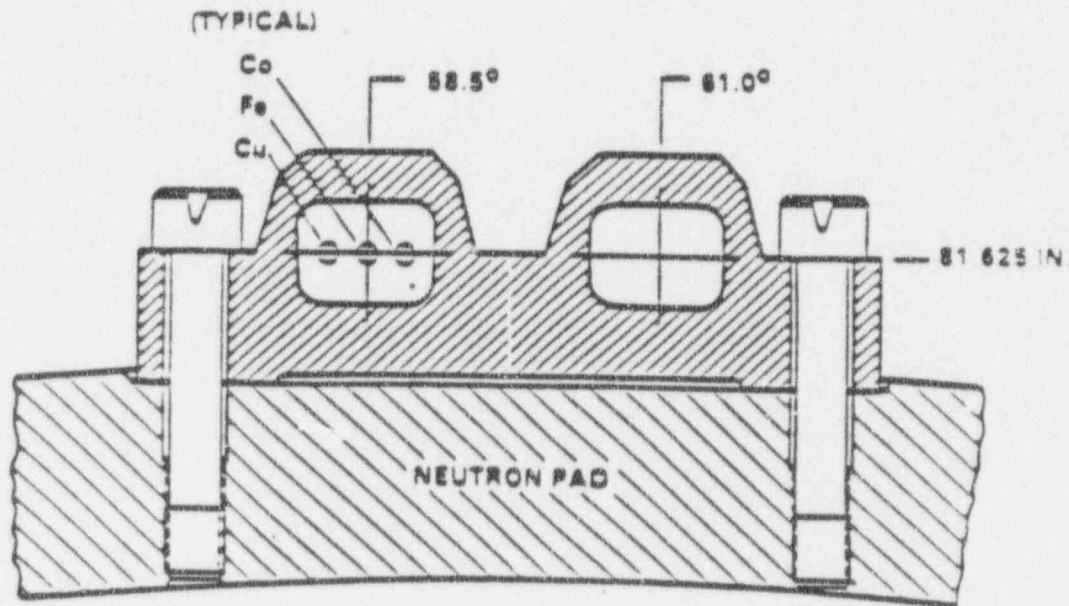


FIGURE 6-2

Axial Distribution of Neutron Fluence ($E > 1.0$ MEV) Along the 45 Degree Azimuth

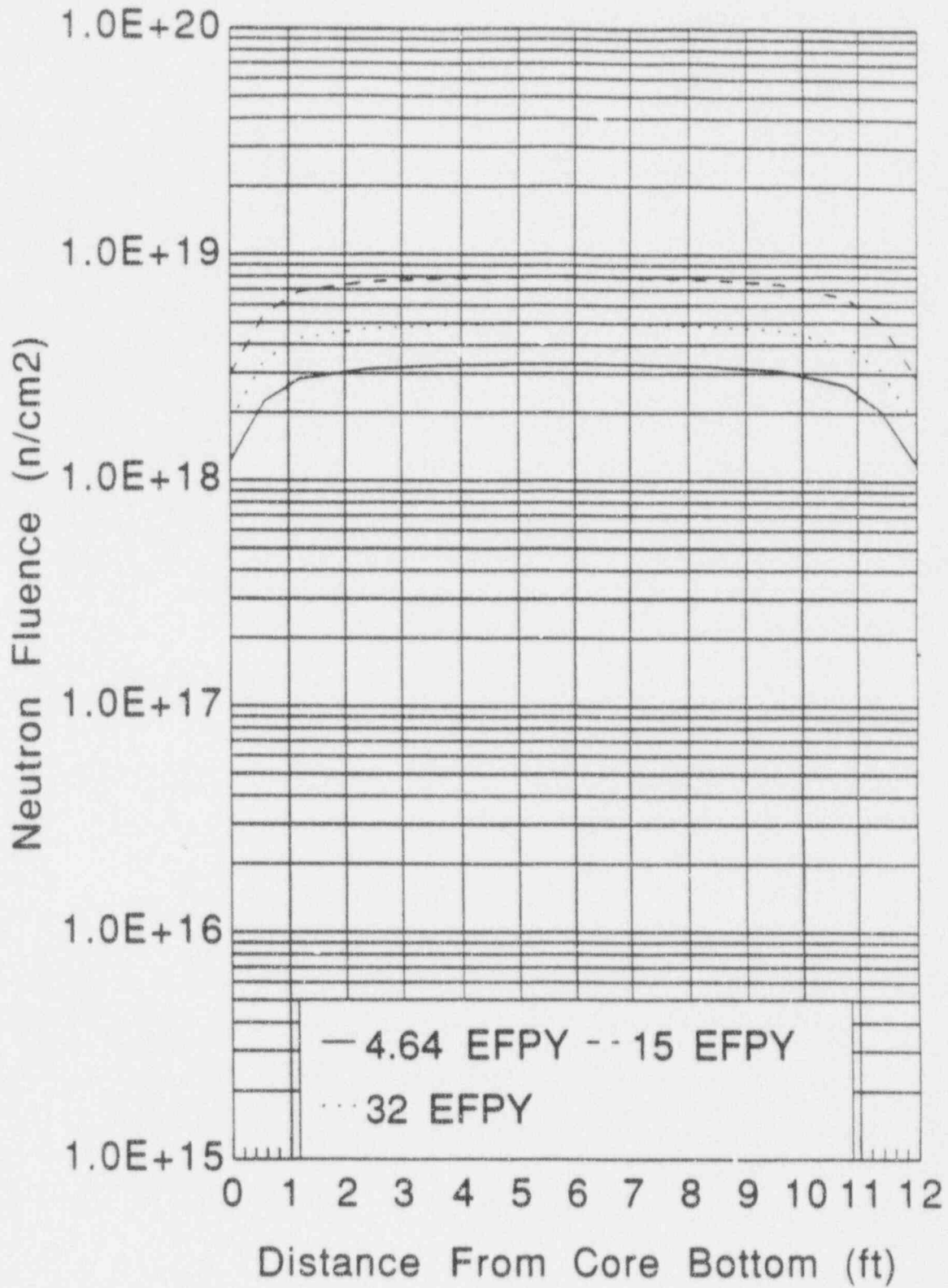


TABLE 6-1

Calculated Fast Neutron Exposure Rates at the Surveillance Capsule Center

CALCULATED FLUX ϕ ($E > 1.0$ MeV [n/cm^2 -sec]) AT THE SURVEILLANCE CAPSULES

	CAPSULE LOCATION	
	<u>29.0°</u>	<u>31.5°</u>
CYCLE 1	8.946E+10	9.537E+10
CYCLE 2	7.634E+10	8.131E+10
CYCLE 3	7.806E+10	8.570E+10
CYCLE 4	6.359E+10	6.857E+10
CRSD Data	1.130E+11	1.210E+11

CALCULATED FLUX ϕ ($E > 0.1$ MeV [n/cm^2 -sec]) AT THE SURVEILLANCE CAPSULES

	<u>29.0°</u>	<u>31.5°</u>
	CYCLE 1	3.869E+11
CYCLE 2	3.302E+11	3.486E+11
CYCLE 3	3.376E+11	3.674E+11
CYCLE 4	2.750E+11	2.940E+11
CRSD Data	4.887E+11	5.187E+11

CALCULATED Iron Displacement Rate [dpa/sec] AT THE SURVEILLANCE CAPSULES

	<u>29.0°</u>	<u>31.5°</u>
	CYCLE 1	1.753E-10
CYCLE 2	1.496E-10	1.586E-10
CYCLE 3	1.530E-10	1.671E-10
CYCLE 4	1.246E-10	1.337E-10
CRSD Data	2.215E-10	2.360E-10

TABLE 6-2

Calculated Azimuthal Variation of Fast Neutron Exposure Rates
at the Pressure Vessel Clad/Base Metal Interface

	<u>$\phi(E > 1.0\text{MeV})$ [n/cm²-sec]</u>				
	<u>0 °</u>	<u>15 °</u>	<u>25 °</u>	<u>35 °</u>	<u>45 °</u>
CYCLE 1	1.407E+10	2.077E+10	2.378E+10	1.933E+10	2.209E+10
CYCLE 2	1.094E+10	1.708E+10	2.011E+10	1.616E+10	1.762E+10
CYCLE 3	9.943E+09	1.550E+10	1.964E+10	1.719E+10	1.903E+10
CYCLE 4	1.110E+10	1.508E+10	1.693E+10	1.406E+10	1.614E+10
CRSD Data	1.780E+10	2.660E+10	3.010E+10	2.450E+10	2.810E+10

	<u>$\phi(E > 0.1\text{MeV})$ [n/cm²-sec]</u>				
	<u>0 °</u>	<u>15 °</u>	<u>25 °</u>	<u>35 °</u>	<u>45 °</u>
CYCLE 1	2.925E+10	4.373E+10	6.494E+10	5.491E+10	5.534E+10
CYCLE 2	2.274E+10	3.596E+10	5.492E+10	4.591E+10	4.414E+10
CYCLE 3	2.067E+10	3.263E+10	5.363E+10	4.883E+10	4.768E+10
CYCLE 4	2.307E+10	3.175E+10	4.623E+10	3.994E+10	4.044E+10
CRSD Data	3.700E+10	5.600E+10	8.220E+10	6.960E+10	7.040E+10

	<u>Iron Atom Displacement Rate [dpa/sec]</u>				
	<u>0 °</u>	<u>15 °</u>	<u>25 °</u>	<u>35 °</u>	<u>45 °</u>
CYCLE 1	2.190E-11	3.217E-11	3.982E-11	3.274E-11	3.522E-11
CYCLE 2	1.702E-11	2.645E-11	3.367E-11	2.737E-11	2.809E-11
CYCLE 3	1.547E-11	2.401E-11	3.289E-11	2.912E-11	3.034E-11
CYCLE 4	1.727E-11	2.336E-11	2.835E-11	2.382E-11	2.573E-11
CRSD Data	2.770E-11	4.120E-11	5.040E-11	4.150E-11	4.480E-11

TABLE 6-3

Relative Radial Distribution of $\phi(E > 1.0 \text{ MeV})$ within the Pressure Vessel Wall

Radius (cm)	<u>0.0°</u>	<u>15.0°</u>	<u>25.0°</u>	<u>35.0°</u>	<u>45.0°</u>
220.27 ⁽¹⁾	1.00	1.00	1.00	1.00	1.00
220.64	0.976	0.979	0.980	0.977	0.979
221.66	0.888	0.891	0.893	0.891	0.889
222.99	0.768	0.770	0.772	0.770	0.766
224.31	0.653	0.653	0.657	0.655	0.648
225.63	0.551	0.550	0.554	0.552	0.543
226.95	0.462	0.460	0.465	0.463	0.452
228.28	0.386	0.384	0.388	0.386	0.375
229.60	0.321	0.319	0.324	0.321	0.311
230.92	0.267	0.263	0.275	0.267	0.257
232.25	0.221	0.219	0.225	0.221	0.211
233.57	0.183	0.181	0.185	0.183	0.174
234.89	0.151	0.149	0.153	0.151	0.142
236.22	0.124	0.122	0.126	0.124	0.116
237.54	0.102	0.100	0.104	0.102	0.0945
238.86	0.0828	0.0817	0.0846	.0835	0.0762
240.19	0.0671	0.0660	0.0689	.0679	0.0608
241.51	0.0538	0.0522	0.0550	0.0545	0.0471
242.17 ⁽²⁾	0.0506	0.0488	0.0518	0.0521	0.0438

NOTES: 1) Base Metal Inner Radius
2) Base Metal Outer Radius

TABLE 6-4

Relative Radial Distribution of $\phi(E > 0.1 \text{ MeV})$ within the Pressure Vessel Wall

Radius (cm)	<u>0.0°</u>	<u>15.0°</u>	<u>25.0°</u>	<u>35.0°</u>	<u>45.0°</u>
220.27 ⁽¹⁾	1.00	1.00	1.00	1.00	1.00
220.64	1.00	1.00	1.00	1.00	1.00
221.66	1.00	1.00	1.00	0.999	0.995
222.99	0.974	0.969	0.974	0.959	0.956
224.31	0.927	0.920	0.927	0.907	0.901
225.63	0.874	0.865	0.874	0.850	0.842
226.95	0.818	0.808	0.818	0.792	0.782
228.28	0.761	0.750	0.716	0.734	0.721
229.60	0.705	0.693	0.704	0.677	0.662
230.92	0.649	0.637	0.649	0.621	0.605
232.25	0.594	0.582	0.594	0.567	0.549
233.57	0.540	0.529	0.542	0.515	0.495
234.89	0.487	0.478	0.490	0.465	0.443
236.22	0.436	0.428	0.440	0.416	0.392
237.54	0.386	0.380	0.392	0.369	0.343
238.86	0.337	0.333	0.344	0.324	0.295
240.19	0.289	0.287	0.298	0.279	0.248
241.51	0.244	0.238	0.249	0.233	0.201
242.17 ⁽²⁾	0.233	0.226	.237	0.223	0.188

NOTES: 1) Base Metal Inner Radius
2) Base Metal Outer Radius

TABLE 6-5

Relative Radial Distribution of dpa/sec within the Pressure Vessel Wall

Radius (cm)	<u>0.0°</u>	<u>15.0°</u>	<u>25.0°</u>	<u>35.0°</u>	<u>45.0°</u>
220.27 ⁽¹⁾	1.00	1.00	1.00	1.00	1.00
220.64	0.984	0.981	0.984	0.983	0.984
221.66	0.912	0.909	0.917	0.921	0.915
222.99	0.815	0.812	0.826	0.833	0.821
224.31	0.722	0.719	0.737	0.747	0.730
225.63	0.638	0.634	0.656	0.668	0.647
226.95	0.563	0.559	0.584	0.597	0.572
228.28	0.497	0.493	0.519	0.533	0.506
229.60	0.439	0.435	0.462	0.475	0.447
230.92	0.387	0.383	0.410	0.423	0.394
232.25	0.341	0.338	0.364	0.376	0.347
233.57	0.300	0.297	0.322	0.334	0.305
234.89	0.263	0.261	0.285	0.295	0.266
236.22	0.230	0.228	0.250	0.260	0.231
237.54	0.199	0.198	0.218	0.227	0.199
238.86	0.171	0.170	0.189	0.196	0.169
240.19	0.145	0.144	0.161	0.167	0.140
241.51	0.121	0.119	0.135	0.139	0.113
242.17 ⁽²⁾	0.116	0.113	0.128	0.134	0.106

NOTES: 1) Base Metal Inner Radius
2) Base Metal Outer Radius

TABLE 6-6

Nuclear Parameters Used In the Evaluation of Neutron Sensors

<u>Monitor Material</u>	<u>Reaction of Interest</u>	<u>Target Weight Fraction</u>	<u>Response Range</u>	<u>Product Half-Life</u>	<u>Fission Yield (%)</u>
Copper	$\text{Cu}^{63}(\text{n},\alpha)\text{Co}^{60}$	0.6917	$E > 4.7 \text{ MeV}$	5.271 yrs	
Iron	$\text{Fe}^{54}(\text{n},\text{p})\text{Mn}^{54}$	0.0580	$E > 1.0 \text{ MeV}$	312.5 days	
Nickel	$\text{Ni}^{58}(\text{n},\text{p})\text{Co}^{58}$	0.6827	$E > 1.0 \text{ MeV}$	70.78 days	
Uranium-238*	$\text{U}^{238}(\text{n},\text{f})\text{Cs}^{137}$	1.0	$E > 0.4 \text{ MeV}$	30.12 yrs	6.00
Neptunium-237*	$\text{Np}^{237}(\text{n},\text{f})\text{Cs}^{137}$	1.0	$E > 0.08 \text{ MeV}$	30.12 yrs	6.27
Cobalt-Aluminum*	$\text{Co}^{59}(\text{n},\gamma)\text{Co}^{60}$	0.0015	$0.4\text{ev} > E > 0.015 \text{ MeV}$	5.271 yrs	
Cobalt-Aluminum	$\text{Co}^{59}(\text{n},\gamma)\text{Co}^{60}$	0.0015	$E > 0.015 \text{ MeV}$	5.271 yrs	

*Denotes that monitor is cadmium shielded.

TABLE 6-7

Monthly Thermal Generation During the First Four Fuel Cycles of the Vogtle Unit 1 Reactor

Thermal Generation			Thermal Generation		
<u>Year</u>	<u>Month</u>	<u>(MW-hr)</u>	<u>Year</u>	<u>Month</u>	<u>(MW-hr)</u>
1987	3	68,766	1991	1	2,534,837
	4	797,491		2	2,260,779
	5	1,044,332		3	2,495,386
	6	759,746		4	2,449,552
	7	1,835,718		5	2,533,685
	8	2,509,822		6	2,449,889
	9	2,452,829		7	2,534,501
	10	707,673		8	2,483,204
	11	1,927,388		9	969,976
	12	2,467,702		10	0
1988	1	1,365,280		1	215,953
	2	1,387,377		2	2,466,013
	3	2,456,340	1992	1	2,534,684
	4	1,907,244		2	2,371,364
	5	2,531,355		3	2,528,590
	6	2,444,967		4	2,239,948
	7	2,220,349		5	1,866,712
	8	2,415,264		6	2,452,840
	9	2,370,737		7	2,534,681
	10	483,956		8	2,535,008
	11	52,233		9	2,188,889
	12	2,135,007		10	2,538,900
1989	1	1,771,903		11	2,454,211
	2	1,905,573		12	2,536,190
	3	2,533,004	1993	1	2,536,730
	4	2,380,073		2	2,273,143
	5	2,264,902		3	849,752
	6	2,452,382			
	7	2,443,387			
	8	2,286,024			
	9	2,450,229			
	10	2,142,954			
	11	2,391,716			
	12	2,535,607			
1990	1	2,374,089			
	2	1,811,171			
	3	0			
	4	591,136			
	5	2,311,713			
	6	2,299,026			
	7	2,196,834			
	8	2,512,580			
	9	2,452,206			
	10	2,534,258			
	11	2,428,733			
	12	1,692,955			
				Cumulative	1.449E+08

TABLE 6-8

Measured Sensor Activities and Reaction Rates
 Surveillance Capsule Y
 Saturated Activities and Derived Fast Neutron Flux

<u>MONITOR AND AXIAL LOCATION</u>	<u>MEASURED ACTIVITY (dis/sec-gm)</u>	<u>SATURATED ACTIVITY (dis/sec-gm)</u>	<u>REACTION RATE (rps/nucleus)</u>
<u>Cu-63 (n,α) Co-60</u>			
93-3522 TOP	1.380E+05	3.684E+05	
93-3527 MID	1.210E+05	3.230E+05	
93-3532 BOT	1.230E+05	3.284E+05	
AVERAGES	1.273E+05	3.400E+05	5.186E-17
<u>Fe-54 (n,p) Mn-54</u>			
93-3524 TOP	1.630E+06	3.222E+06	
93-3529 MID	1.470E+06	2.906E+06	
93-3534 BOT	1.480E+06	2.925E+06	
AVERAGES	1.527E+06	3.018E+06	4.825E-15
<u>Ni-58 (n,p) Co-58</u>			
93-3523 TOP	8.430E+06	5.031E+07	
93-3528 MID	7.750E+06	4.625E+07	
93-3533 BOT	7.630E+06	4.553E+07	
AVERAGES	7.937E+06	4.736E+07	6.763E-15
<u>Co-59 (n,γ) Co-60</u>			
93-3520 TOP	2.340E+07	6.247E+07	
93-3525 MID	2.350E+07	6.274E+07	
93-3530 BOT	2.340E+07	6.247E+07	
AVERAGES	2.343E+07	6.256E+07	4.082E-12
<u>Co-59 (n,γ) Co-60</u>			
93-3521 TOP	1.200E+07	3.204E+07	
93-3526 MID	1.290E+07	3.444E+07	
93-3531 BOT	1.290E+07	3.444E+07	
AVERAGES	1.260E+07	3.364E+07	2.195E-12
<u>U-238 (n,f) Cs-137</u>			
93-3518 MID	5.070E+05	5.473E+06	3.607E-14
<u>Np-237 (n,f) Cs-137</u>			
93-3519 MID	3.380E+06	3.649E+07	2.291E-13

TABLE 6-9

Summary of Neutron Dosimetry Results
Surveillance Capsules Y and U

Calculation of Measured Fluence for Capsule Y	Flux	Time	Fluence	Uncertainty
Meas Fluence < 0.414 ev = (Meas Flux < 0.414) * (EFPS)	7.696E+10	1.464E+08	1.127E+19	±22%
Meas Fluence > 0.1 Mev = (Meas Flux > .1) * (EFPS)	3.415E+11	1.464E+08	5.000E+19	±15%
Meas Fluence > 1.0 Mev = (Meas Flux > 1) * (EFPS)	8.484E+10	1.464E+08	1.242E+19	±8%
dpa	1.542E-10	1.464E+08	2.258E-02	±11%
Calculation of Measured Fluence for Capsule U	Flux	Time	Fluence	Uncertainty
Meas Fluence < 0.414 ev = (Meas Flux < 0.414) * (EFPS)	1.035E+11	3.449E+07	3.569E+18	±21%
Meas Fluence > 0.1 Mev = (Meas Flux > .1) * (EFPS)	4.296E+11	3.449E+07	1.481E+19	±15%
Meas Fluence > 1.0 Mev = (Meas Flux > 1) * (EFPS)	9.967E+10	3.449E+07	3.437E+18	±8%
dpa	1.882E-10	3.449E+07	6.490E-03	±11%

TABLE 6-10

Comparison of Measured and FERRET Calculated Reaction Rates at the Surveillance Capsule Center
Surveillance Capsule Y

<u>REACTION</u>	<u>MEASURED</u>	<u>ADJUSTED CALCULATION</u>	<u>C/M</u>
Cu-63 (n, α) Co-60	5.19E-17	5.26E-17	1.01
Fe-54 (n,p) Mn-54	4.83E-15	4.87E-15	1.01
Ni-58 (n,p) Co-58	6.76E-15	6.71E-15	0.99
U-238 (n,f) Cs-137 (Cd)	3.01E-14	2.71E- 4	0.90
NP237(N,F)CS137	2.29E-13	2.49E-13	1.09
Co-59 (n, γ) Co-60	4.08E-12	4.05E-12	0.99
Co-59 (n, γ) Co-60 (Cd)	2.20E-12	2.21E-12	1.0

TABLE 6-11

Adjusted Neutron Energy Spectrum at the Center of Surveillance Capsule Y

<u>GROUP</u>	<u>ENERGY</u> (MeV)	<u>ADJUSTED FLUX</u> (n/cm ² -sec)	<u>GROUP</u>	<u>ENERGY</u> (MeV)	<u>ADJUSTED FLUX</u> (n/cm ² -sec)
1	1.733E+01	7.406E+06	27	1.503E-02	1.289E+10
2	1.492E+01	1.678E+07	28	9.119E-03	1.604E+10
3	1.350E+01	6.479E+07	29	5.531E-03	1.910E+10
4	1.162E+01	1.444E+08	30	3.355E-03	6.083E+09
5	1.000E+01	3.189E+08	31	2.839E-03	5.914E+09
6	8.607E+00	5.427E+08	32	2.404E-03	5.821E+09
7	7.408E+00	1.241E+09	33	2.035E-03	1.721E+10
8	6.065E+00	1.757E+09	34	1.234E-03	1.660E+10
9	4.966E+00	3.635E+09	35	7.485E-04	1.481E+10
10	3.679E+00	4.731E+09	36	4.540E-04	1.286E+10
11	2.865E+00	9.785E+09	37	2.754E-04	1.491E+10
12	2.231E+00	1.322E+10	38	1.670E-04	1.653E+10
13	1.738E+00	1.799E+10	39	1.013E-04	1.638E+10
14	1.353E+00	1.941E+10	40	6.144E-05	1.617E+10
15	1.108E+00	3.506E+10	41	3.727E-05	1.592E+10
16	8.208E-01	3.806E+10	42	2.260E-05	1.546E+10
17	6.393E-01	4.026E+10	43	1.371E-05	1.492E+10
18	4.979E-01	2.742E+10	44	8.315E-06	1.422E+10
19	3.877E-01	3.932E+10	45	5.043E-06	1.328E+10
20	3.020E-01	4.218E+10	46	3.059E-06	1.237E+10
21	1.832E-01	3.987E+10	47	1.855E-06	1.118E+10
22	1.111E-01	3.061E+10	48	1.125E-06	8.577E+09
23	6.738E-02	2.430E+10	49	6.826E-07	1.068E+10
24	4.087E-02	1.233E+10	50	4.140E-07	1.337E+10
25	2.554E-02	1.700E+10	51	2.511E-07	1.327E+10
26	1.989E-02	8.614E+09	52	1.523E-07	1.253E+10
			53	9.237E-08	3.779E+10

Note: Tabulated energy levels represent the upper energy in each group.

TABLE 6-12

Comparison of Calculated and Measured Neutron Exposure Levels for
Vogtle Unit 1 Surveillance Capsules Y and U

Comparison of Calculated and Measured INTEGRATED Neutron EXPOSURE Rate for Capsule Y

	Calculated	Measured	C / M	M / C
Fluence (E > 1.0 Mev) [n/cm ² -sec]	1.122E+19	1.242E+19	0.903	1.107
Fluence (E > 0.1 Mev) [n/cm ² -sec]	4.853E+19	5.000E+19	0.970	1.030
dpa	2.199E-02	2.258E-02	0.974	1.027

Comparison of Calculated and Measured INTEGRATED Neutron EXPOSURE Rate for Capsule U

	Calculated	Measured	C / M	M / C
Fluence (E > 1.0 Mev) [n/cm ² -sec]	3.289E+18	3.437E+18	0.957	1.045
Fluence (E > 0.1 Mev) [n/cm ² -sec]	1.410E+19	1.481E+19	0.952	1.051
dpa	6.414E-03	6.490E-03	0.988	1.012

TABLE 6-13

Neutron Exposure Projections at Key Locations on the Pressure Vessel Clad/Base Metal Interface

BEST ESTIMATE EXPOSURE (4.64 EFPY) AT THE PRESSURE VESSEL INNER RADIUS

	<u>0°</u>	<u>15°</u>	<u>25°</u>	<u>30°</u>	<u>35°</u>	<u>45°</u>
E > 1.0	1.802E+18	2.678E+18	3.155E+18	2.000E+18	2.622E+18	2.942E+18
E > 0.1	3.623E+18	5.453E+18	8.332E+18		7.204E+18	7.127E+18
dpa	2.657E-03	3.930E-03	5.004E-03		4.208E-03	4.443E-03

BEST ESTIMATE EXTRAPOLATION FLUX AT THE PRESSURE VESSEL INNER RADIUS

	<u>0°</u>	<u>15°</u>	<u>25°</u>	<u>30°</u>	<u>35°</u>	<u>45°</u>
E > 1.0	1.231E+10	1.829E+10	2.155E+10	1.366E+10	1.791E+10	2.009E+10
E > 0.1	2.474E+10	3.724E+10	5.690E+10		4.920E+10	4.868E+10
dpa	1.815E-11	2.684E-11	3.418E-11		2.874E-11	3.034E-11

BEST ESTIMATE EXPOSURE (16.0 EFPY) AT THE PRESSURE VESSEL INNER RADIUS

	<u>0°</u>	<u>15°</u>	<u>25°</u>	<u>30°</u>	<u>35°</u>	<u>45°</u>
E > 1.0	6.216E+18	9.236E+18	1.088E+19	6.897E+18	9.043E+18	1.015E+19
E > 0.1	1.249E+19	1.880E+19	2.873E+19		2.484E+19	2.458E+19
dpa	9.162E-03	1.355E-02	1.726E-02		1.451E-02	1.532E-02

BEST ESTIMATE EXPOSURE (32.0 EFPY) AT THE PRESSURE VESSEL INNER RADIUS

	<u>0°</u>	<u>15°</u>	<u>25°</u>	<u>30°</u>	<u>35°</u>	<u>45°</u>
E > 1.0	1.243E+19	1.847E+19	2.176E+19	1.379E+19	1.809E+19	2.029E+19
E > 0.1	2.499E+19	3.761E+19	5.746E+19		4.968E+19	4.916E+19
dpa	1.832E-02	2.710E-02	3.451E-02		2.902E-02	3.064E-02

TABLE 6-14

Neutron Exposure Values at the 1/4T and 3/4T Locations of the Reactor Vessel Base Metal

FLUENCE BASED ON E > 1.0 MeV SLOPE

	<u>0°</u>	<u>15°</u>	<u>25°</u>	<u>30°</u>	<u>35°</u>	<u>45°</u>
16 EFPY FLUENCE						
SURFACE	6.216E+18	9.236E+18	1.088E+19	6.897E+18	9.043E+18	1.015E+19
1/4T	3.375E+18	4.997E+18	5.941E+18		4.938E+18	5.407E+18
3/4T	7.210E+17	1.053E+18	1.284E+18		1.058E+18	1.096E+18
32 EFPY FLUENCE						
SURFACE	1.243E+19	1.847E+19	2.176E+19	1.379E+19	1.809E+19	2.029E+19
1/4T	6.750E+18	9.994E+18	1.188E+19		9.875E+18	1.081E+19
3/4T	1.442E+18	2.106E+18	2.568E+18		2.116E+18	2.191E+18

FLUENCE BASED ON dpa SLOPE

	<u>0°</u>	<u>15°</u>	<u>25°</u>	<u>30°</u>	<u>35°</u>	<u>45°</u>
16 EFPY FLUENCE						
SURFACE	6.216E+18	9.236E+18	1.088E+19	6.897E+18	9.043E+18	1.015E+19
1/4T	3.922E+18	5.782E+18	7.072E+18		6.005E+18	6.473E+18
3/4T	1.361E+18	2.004E+18	2.600E+18		2.252E+18	2.212E+18
32 EFPY FLUENCE						
SURFACE	1.243E+19	1.847E+19	2.176E+19	1.379E+19	1.809E+19	2.029E+19
1/4T	7.844E+18	1.156E+19	1.414E+19		1.201E+19	1.295E+19
3/4T	2.722E+18	4.009E+18	5.201E+18		4.504E+18	4.423E+18

TABLE 6-15

Updated Lead Factors For Vogtle Unit 1 Surveillance Capsules

<u>CAPSULE</u>	<u>LEAD FACTOR</u>
U	WITHDRAWN EOC 1
V	3.83
X	4.12
W	4.12
Y	3.83*
Z	4.12

* WITHDRAWN EOC 4, BASIS FOR THIS ANALYSIS

SECTION 7.0
SURVEILLANCE CAPSULE REMOVAL SCHEDULE

The surveillance capsule withdrawal schedule of Table 7-1 meets the requirements of ASTM E185-82 and is recommended for removal of future capsules from the Vogtle Unit 1 reactor vessel.

<u>TABLE 7-1</u>				
Vogtle Unit 1 Reactor Vessel Surveillance Capsule Withdrawal Schedule				
Capsule	Location	Lead Factor	Removal Time (EFPY) ^(a)	Fluence (n/cm ² , E>1.0 MeV)
U	58.5°	4.01	1.14	3.44 x 10 ¹⁸ ^(b)
Y	241.0°	3.83	4.64	1.24 x 10 ¹⁹ ^(b)
V	61.0°	3.83	8.37	2.18 x 10 ¹⁹ ^(c)
X	238.5°	4.12	11.64	3.26 x 10 ¹⁹
W	121.5°	4.12	Stand-by	- -
Z	301.5°	4.12	Stand-By	- -

- (a) Effective Full Power Years (EFPY) from plant startup.
- (b) Actual measured neutron fluence
- (c) Approximate EOL (32 EFPY) peak vessel inner surface fluence.

SECTION 8.0
REFERENCES

1. Regulatory Guide 1.99, Revision 2, *Radiation Embrittlement of Reactor Vessel Materials*, U.S. Nuclear Regulatory Commission, May, 1988.
2. Singer, L.R., *Georgia Power Company Alvin W. Vogtle Unit No. 1 Reactor Vessel Radiation Surveillance Program*, WCAP-11011, February 1986.
3. ASTM E185-82, *Standard Practice for Conducting Surveillance Tests for Light-Water Cooled Nuclear Power Reactor Vessels, E706 (IF)*, in ASTM Standards, Section 3, American Society for Testing and Materials, Philadelphia, PA, 1993.
4. Section III of the ASME Boiler and Pressure Vessel Code, Appendix G, *Protection Against Nonductile Failure*.
5. ASTM E208, *Standard Test Method for Conducting Drop-Weight Test to Determine Nil-Ductility Transition Temperature of Ferritic Steels*, in ASTM Standards, Section 3, American Society for Testing and Materials, Philadelphia, PA.
6. S.E. Yanichko, S.L. Anderson, L. Albertin, N.K. Ray, *Analysis of Capsule U from the Georgia Power Company Vogtle Unit 1 Reactor Vessel Radiation Surveillance Program*, WCAP-12256, May 1989.
7. Code of Federal Regulations, 10CFR50, Appendix G, *Fracture Toughness Requirements*, and Appendix H, *Reactor Vessel Material Surveillance Program Requirements*, U.S. Nuclear Regulatory Commission, Washington, D.C.
8. ASTM E23-92, *Standard Test Methods for Notched Bar Impact Testing of Metallic Materials*, in ASTM Standards, Section 3, American Society for Testing and Materials, Philadelphia, PA, 1992.

9. ASTM A370-92, *Standard Test Methods and Definitions for Mechanical Testing of Steel Products*, in ASTM Standards, Section 3, American Society for Testing and Materials, Philadelphia, PA, 1993.
10. ASTM E8-91, *Standard Test Methods of Tension Testing of Metallic Materials*, in ASTM Standards, Section 3, American Society for Testing and Materials, Philadelphia, PA, 1992.
11. ASTM E21-79(1988), *Standard Practice for Elevated Temperature Tension Tests of Metallic Materials*, in ASTM Standards, Section 3, American Society for Testing and Materials, Philadelphia, PA, 1992.
12. ASTM E83-92, *Standard Practice for Verification and Classification of Extensometers*, in ASTM Standards, Section 3, American Society for Testing and Materials, Philadelphia, PA, 1993.
13. R. G. Soltesz, R. K. Disney, J. Jedruch, and S. L. Ziegler, *Nuclear Rocket Shielding Methods, Modification, Updating and Input Data Preparation. Vol. 5--Two-Dimensional Discrete Ordinates Transport Technique*, WANL-TR(LL)-034, Vol. 5, August 1970.
14. ORNL RSCI Data Library Collection DLC-76 SAILOR Coupled Self-Shielded, 47 Neutron, 20 Gamma-Ray, P3, Cross Section Library for Light Water Reactors.
15. R. E. Maerker, et al, *Accounting for Changing Source Distributions in Light Water Reactor Surveillance Dosimetry Analysis*, Nuclear Science and Engineering, Volume 94, Pages 291-308, 1986.
16. S. T. Lesho, W. R. Perry, et al., *The Nuclear Design and Core Physics Characteristics of the Alvin W. Vogtle Unit 1 Nuclear Power Plant Cycle 1*, Westinghouse WCAP-11338, November, 1986.
17. K. A. Potter, K. W. Bonadio, *The Nuclear Design and Core Physics Characteristics of the Alvin W. Vogtle Unit 1 Nuclear Power Plant Cycle 2*, Westinghouse WCAP-11980, October, 1988.

18. K. A. Potter, K. W. Bonadio, et al., *The Nuclear Design Report for the Vogtle Electric Generating Plant, Unit 1, Cycle 3*, Westinghouse WCAP-12480, February, 1990.
19. K. A. Potter, K. W. Bonadio, et al., *The Nuclear Design Report for the Vogtle Electric Generating Plant, Unit 1, Cycle 4*, Westinghouse WCAP-13023, September, 1991.
20. K. A. Potter, K. W. Bonadio, et al., *The Nuclear Design Report for the Vogtle Electric Generating Plant, Unit 1, Cycle 5*, Westinghouse WCAP-13607, February, 1993.
21. ASTM Designation E482-89, *Standard Guide for Application of Neutron Transport Methods for Reactor Vessel Surveillance*, in ASTM Standards, Section 12, American Society for Testing and Materials, Philadelphia, PA, 1991.
22. ASTM Designation E560-84, *Standard Recommended Practice for Extrapolating Reactor Vessel Surveillance Dosimetry Results*, in ASTM Standards, Section 12, American Society for Testing and Materials, Philadelphia, PA, 1991.
23. ASTM Designation E693-79, *Standard Practice for Characterizing Neutron Exposures in Ferritic Steels in Terms of Displacements per Atom (dpa)*, in ASTM Standards, Section 12, American Society for Testing and Materials, Philadelphia, PA, 1991.
24. ASTM Designation E706-87, *Standard Master Matrix for Light-Water Reactor Pressure Vessel Surveillance Standard*, in ASTM Standards, Section 12, American Society for Testing and Materials, Philadelphia, PA, 1991.
25. ASTM Designation E853-87, *Standard Practice for Analysis and Interpretation of Light-Water Reactor Surveillance Results*, in ASTM Standards, Section 12, American Society for Testing and Materials, Philadelphia, PA, 1991.
26. ASTM Designation E261-90, *Standard Method for Determining Neutron Flux, Fluence, and Spectra by Radioactivation Techniques*, in ASTM Standards, Section 12, American Society for Testing and Materials, Philadelphia, PA, 1991.

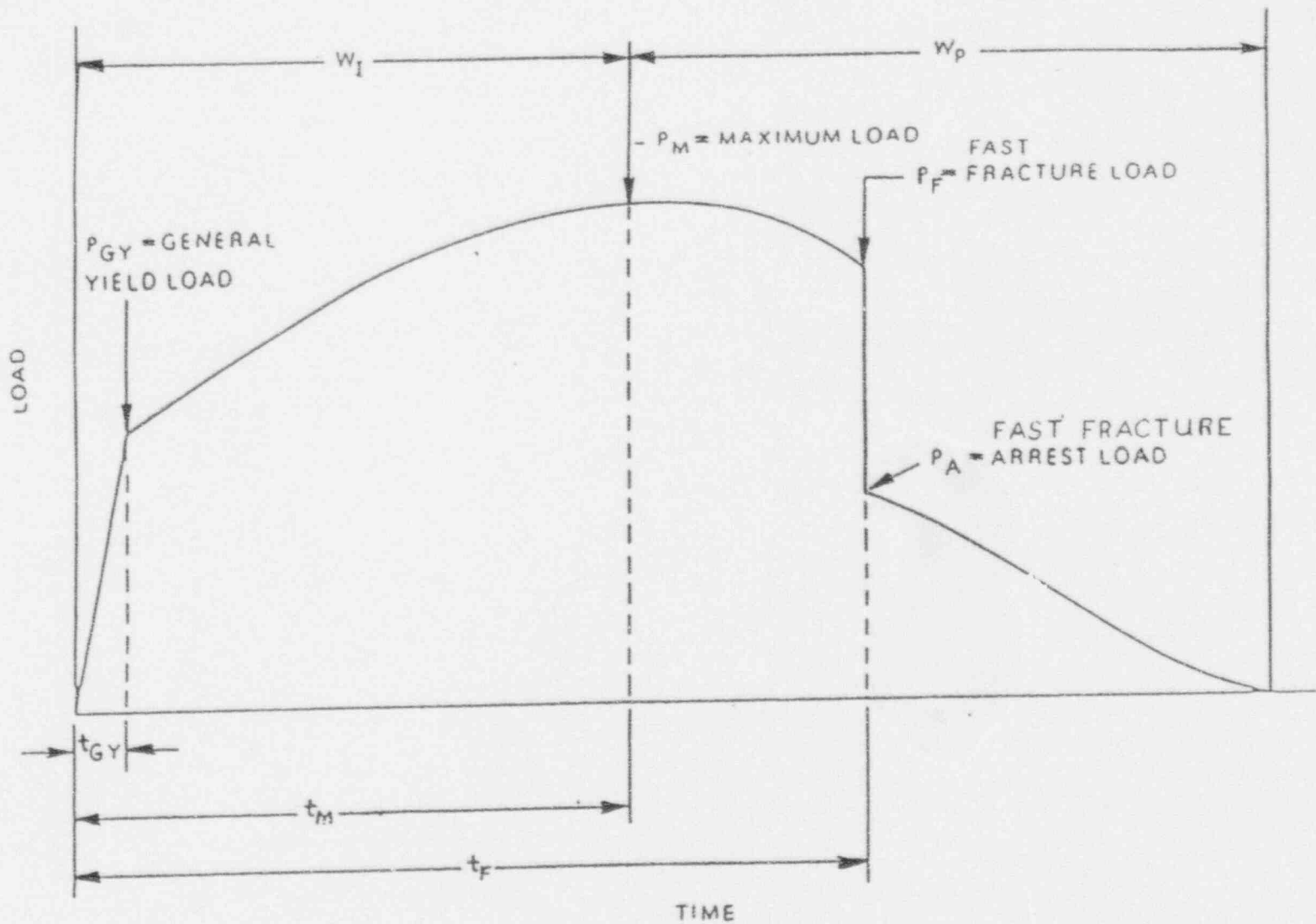
27. ASTM Designation E262-86, *Standard Method for Measuring Thermal Neutron Flux by Radioactivation Techniques*, in ASTM Standards, Section 12, American Society for Testing and Materials, Philadelphia, PA, 1991.
28. ASTM Designation E263-88, *Standard Method for Determining Fast-Neutron Flux Density by Radioactivation of Iron*, in ASTM Standards, Section 12, American Society for Testing and Materials, Philadelphia, PA, 1991.
29. ASTM Designation E264-87, *Standard Method for Determining Fast-Neutron Flux Density by Radioactivation of Nickel*, in ASTM Standards, Section 12, American Society for Testing and Materials, Philadelphia, PA, 1991.
30. ASTM Designation E481-86, *Standard Method for Measuring Neutron-Flux Density by Radioactivation of Cobalt and Silver*, in ASTM Standards, Section 12, American Society for Testing and Materials, Philadelphia, PA, 1991.
31. ASTM Designation E523-87, *Standard Method for Determining Fast-Neutron Flux Density by Radioactivation of Copper*, in ASTM Standards, Section 12, American Society for Testing and Materials, Philadelphia, PA, 1991.
32. ASTM Designation E704-90, *Standard Method for Measuring Reaction Rates by Radioactivation of Uranium-238*, in ASTM Standards, Section 12, American Society for Testing and Materials, Philadelphia, PA, 1991.
33. ASTM Designation E705-90, *Standard Method for Measuring Fast-Neutron Flux Density by Radioactivation of Neptunium-237*, in ASTM Standards, Section 12, American Society for Testing and Materials, Philadelphia, PA, 1991.
34. ASTM Designation E1005-84, *Standard Method for Application and Analysis of Radiometric Monitors for Reactor Vessel Surveillance*, in ASTM Standards, Section 12, American Society for Testing and Materials, Philadelphia, PA, 1991.
35. F. A. Schmittroth, *FERRET Data Analysis Code*, HEDL-TME 79-40, Hanford Engineering Development Laboratory, Richland, WA, September 1979.

36. W. N. McElroy, S. Berg and T. Crocket, *A Computer-Automated Iterative Method of Neutron Flux Spectra Determined by Foil Activation*, AFWL-TR-7-41, Vol. I-IV, Air Force Weapons Laboratory, Kirkland AFB, NM, July 1967.

37. EPRI-NP-2188, *Development and Demonstration of an Advanced Methodology for LWR Dosimetry Applications*, R. E. Maerker, et al., 1981.

APPENDIX A

Load-Time Records for Charpy Specimen Tests



W_I = Fracture initiation region
 W_P = Fracture propagation region

t_{GY} = Time to general yielding
 t_M = Time to maximum load
 t_F = Time to fast (brittle) fracture start

Figure A-1. Idealized load-time record

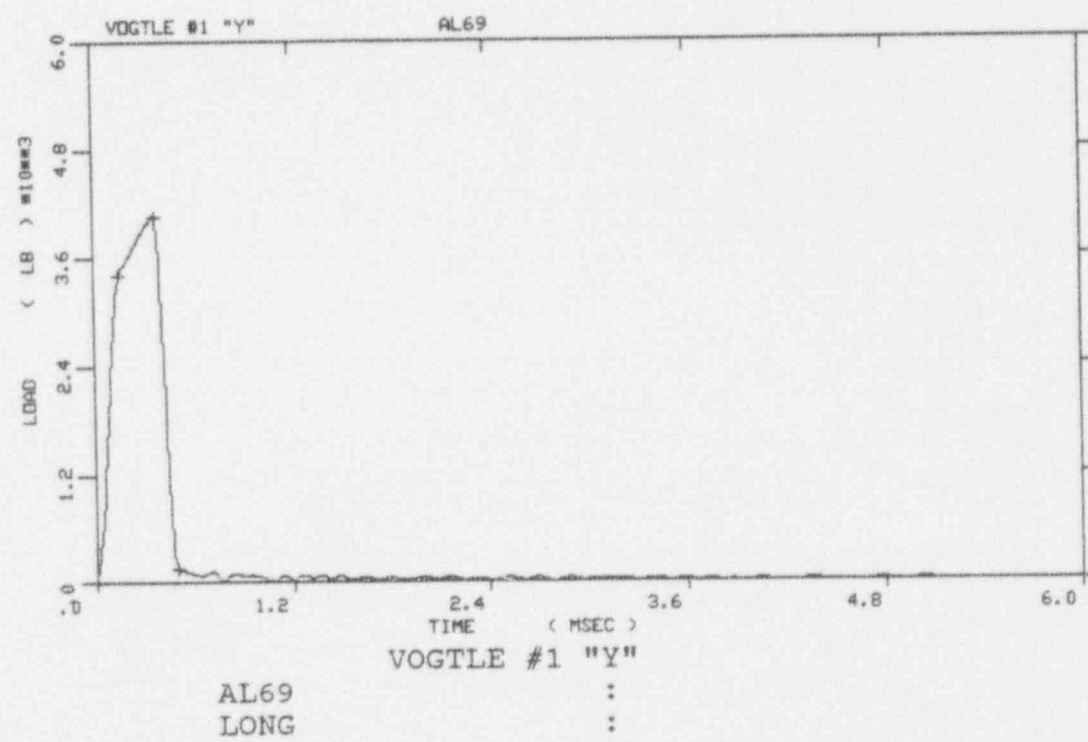
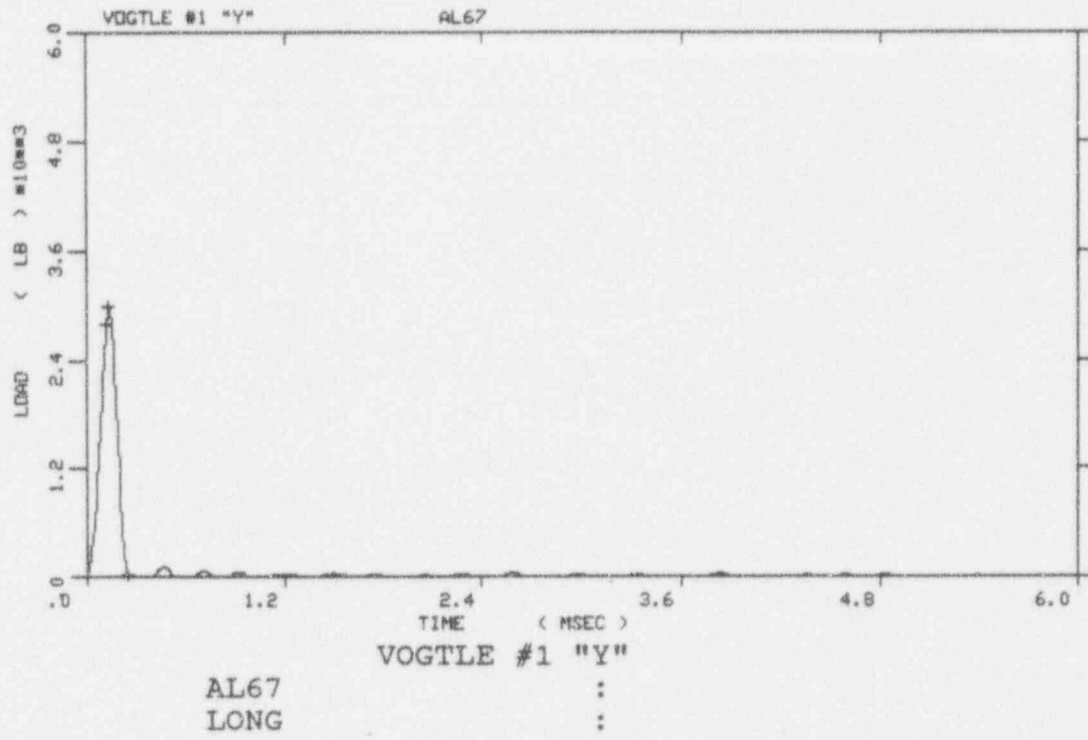


Figure A-2. Load-time records for Specimens AL67 and AL69

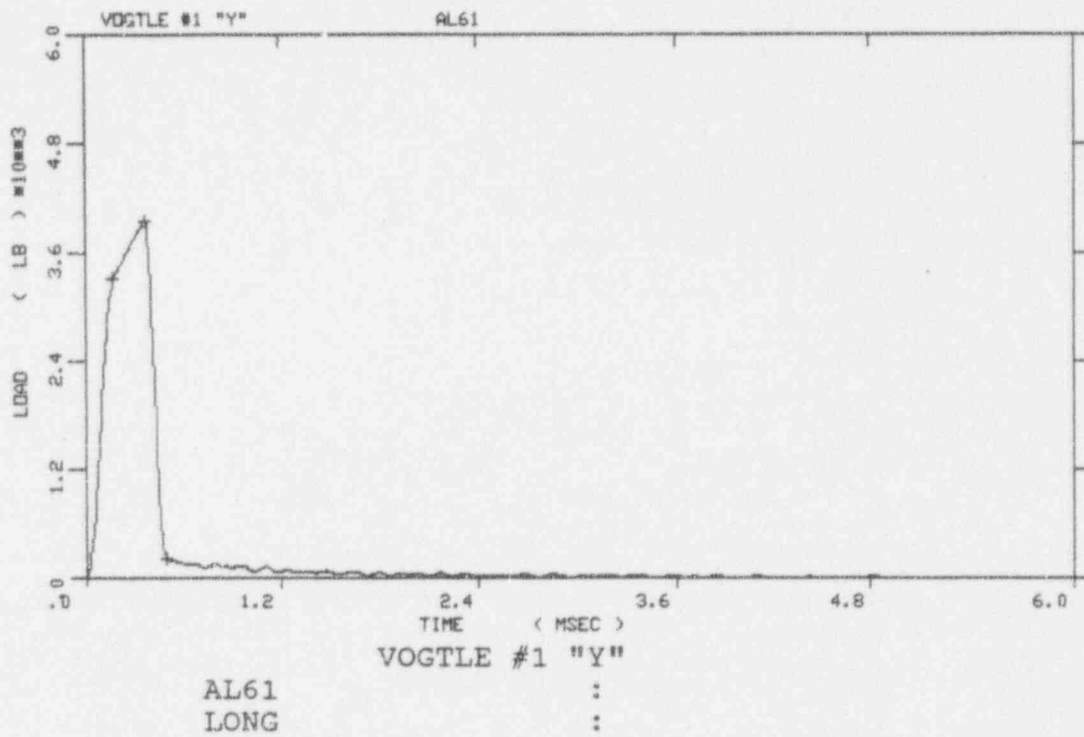
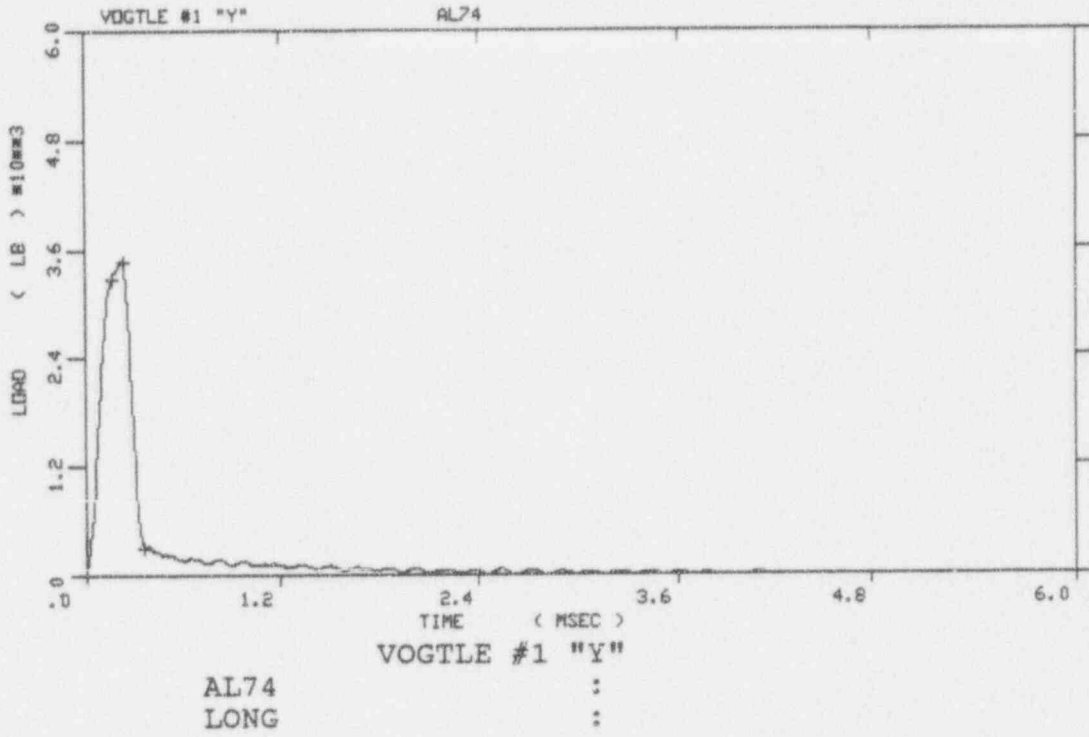


Figure A-3. Load-time records for Specimens AL74 and AL61

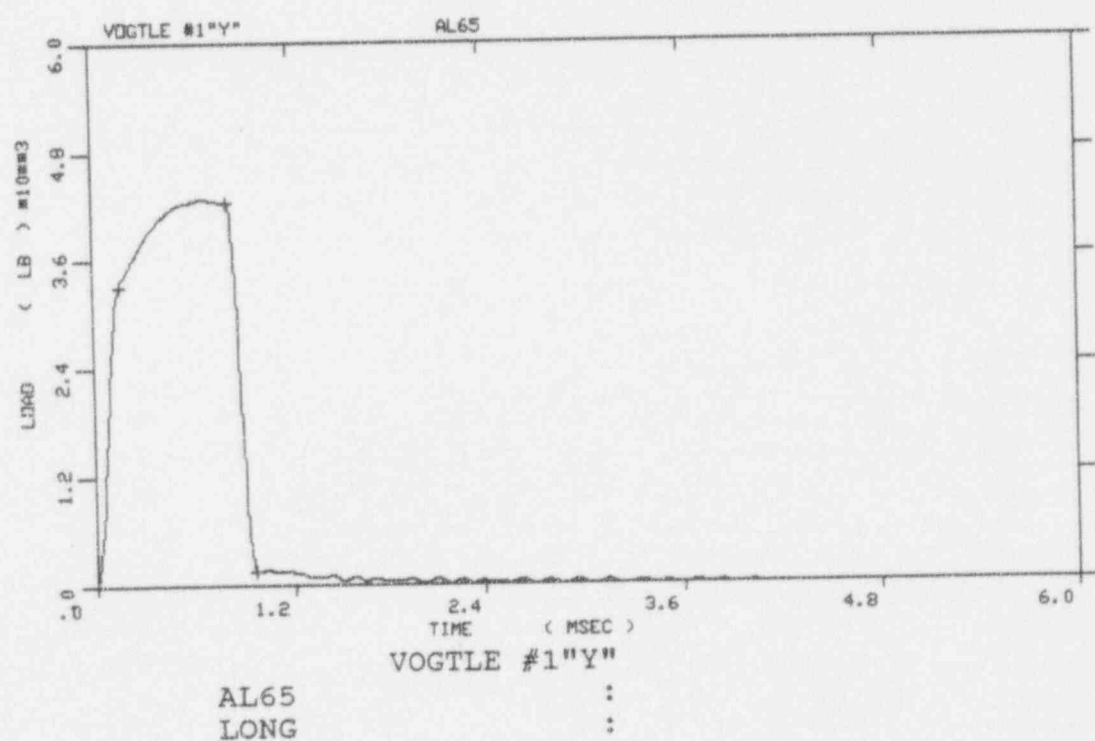
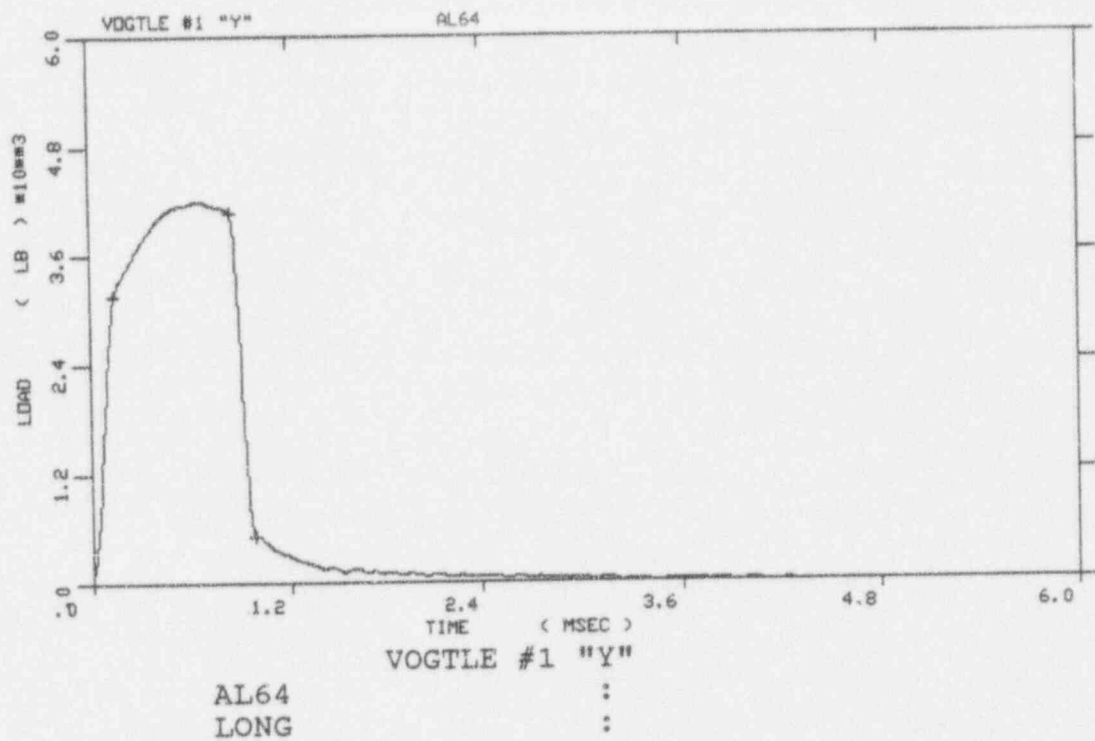


Figure A-4. Load-time records for Specimens AL65 and AL64

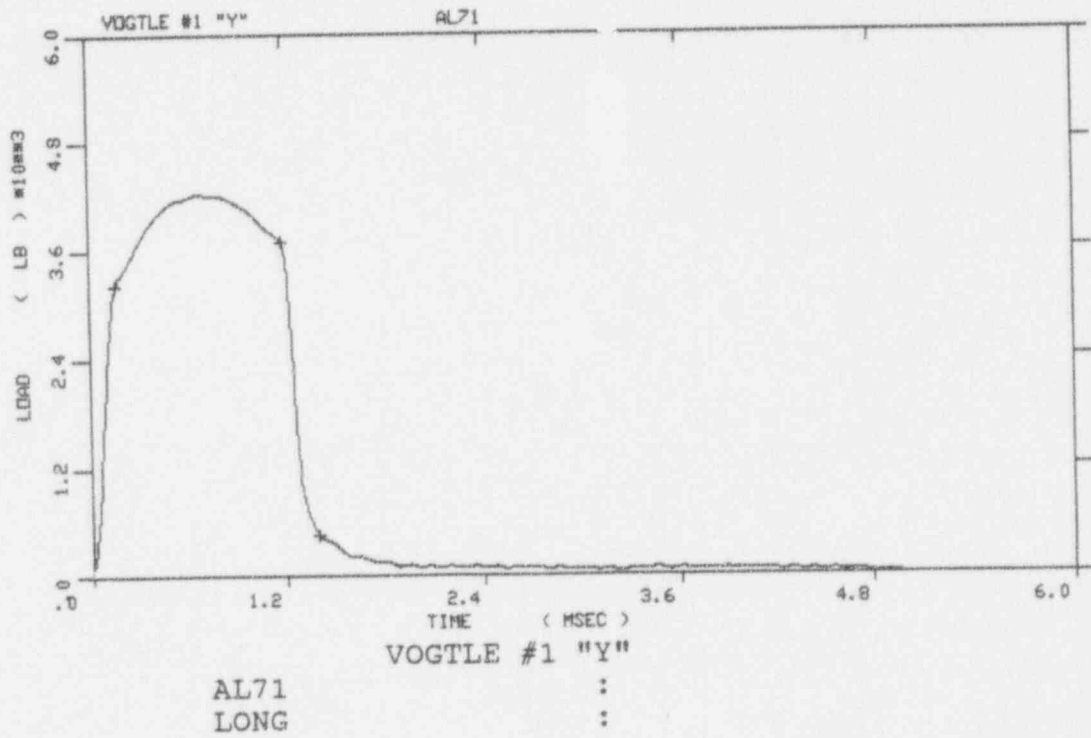
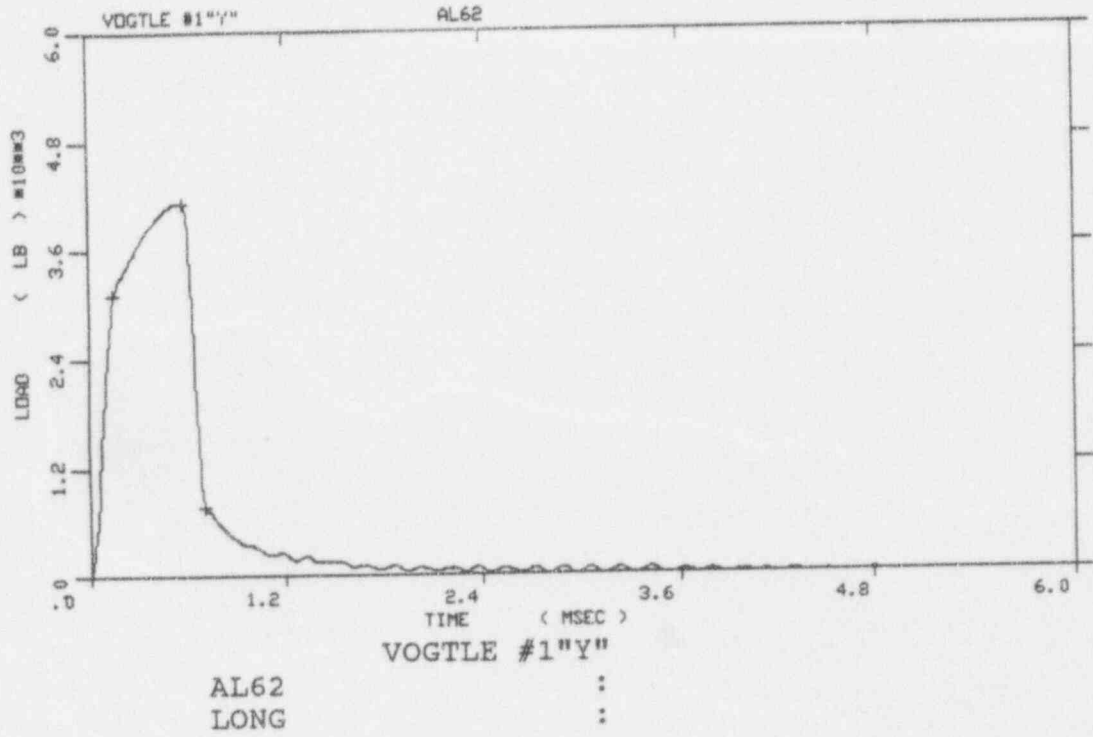


Figure A-5. Load-time records for Specimens AL62 and AL71

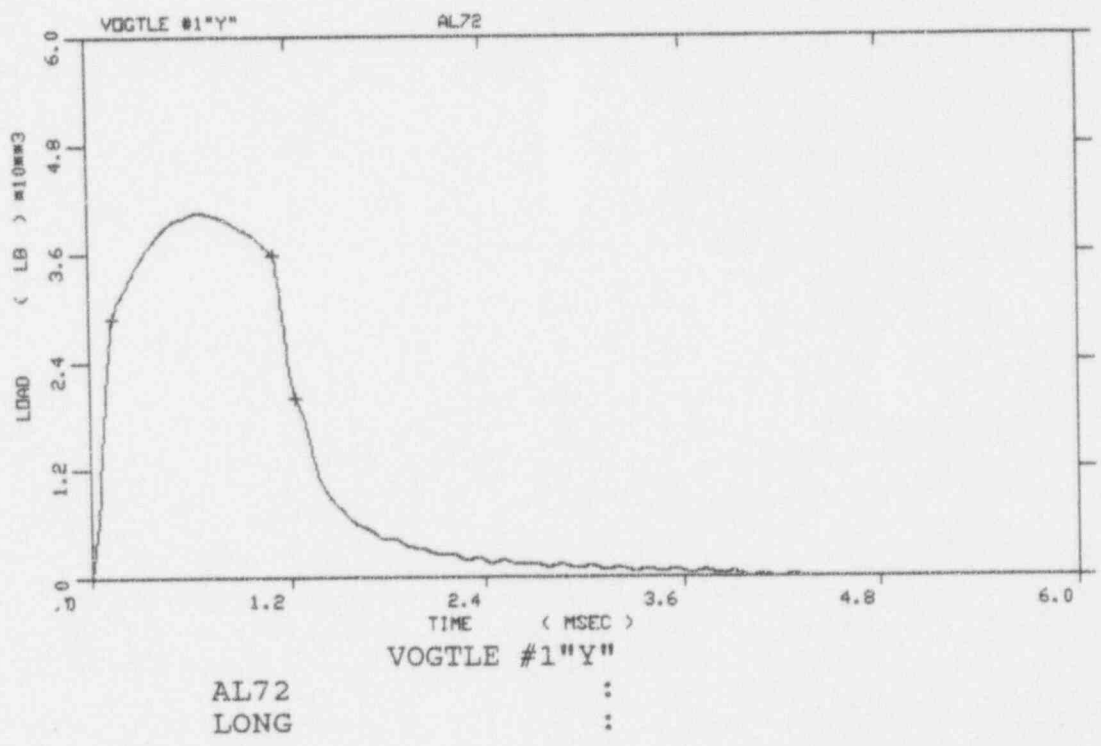
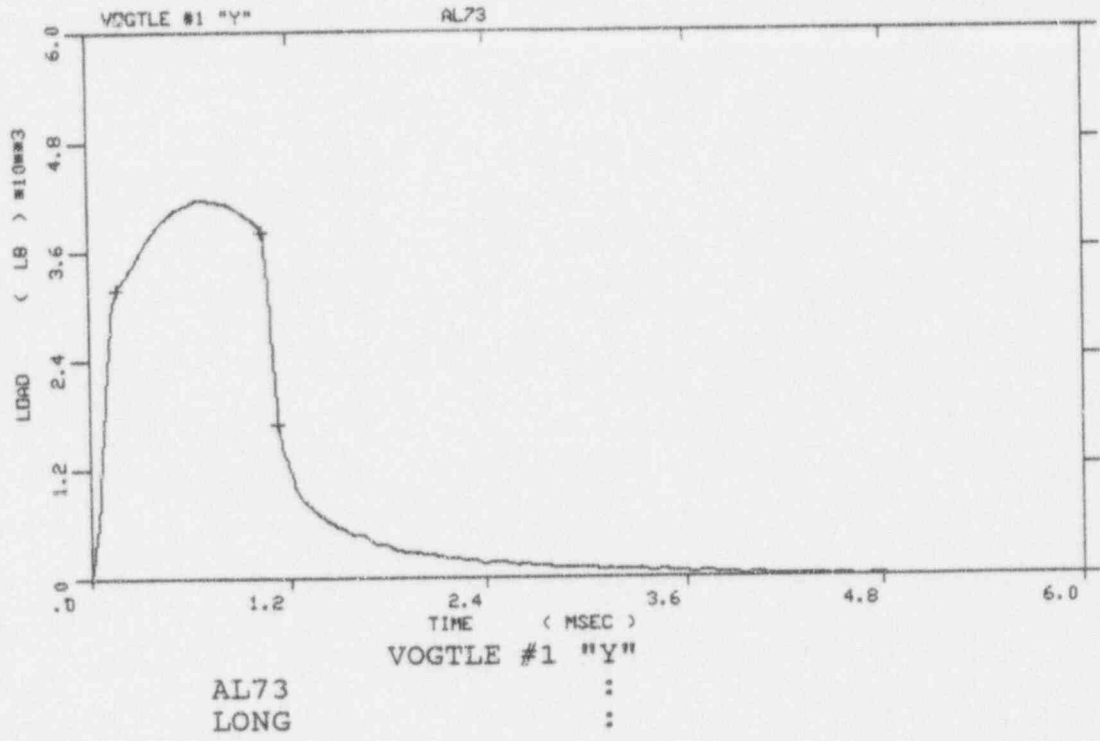


Figure A-6. Load-time records for Specimens AL73 and AL72

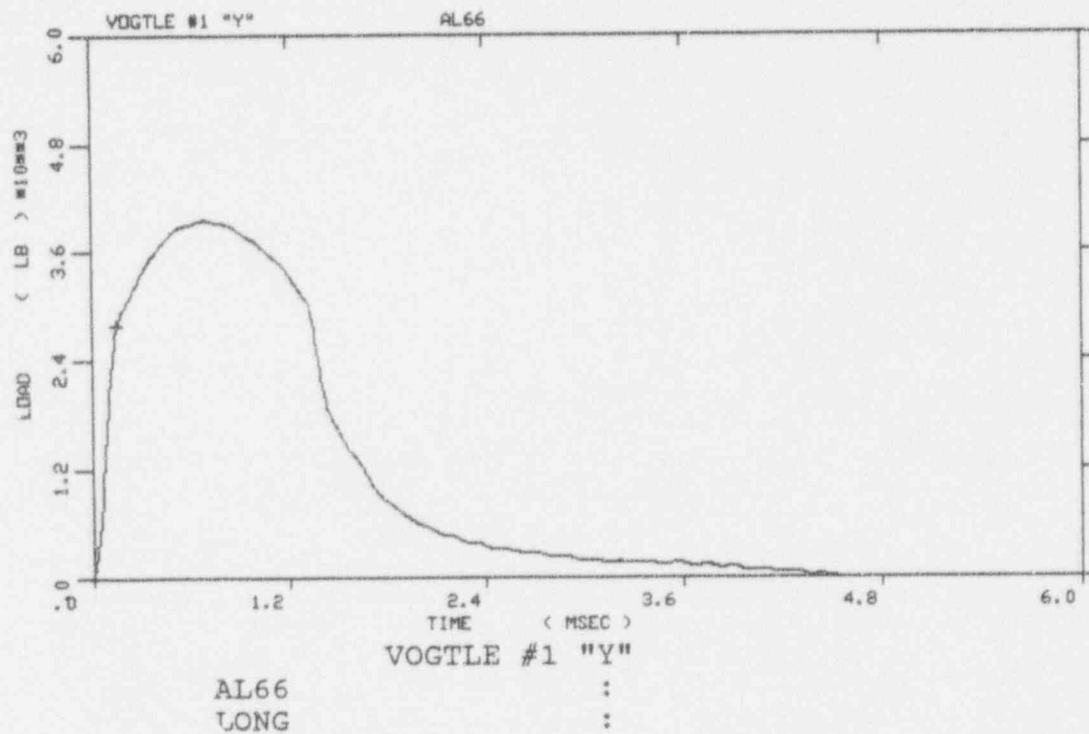
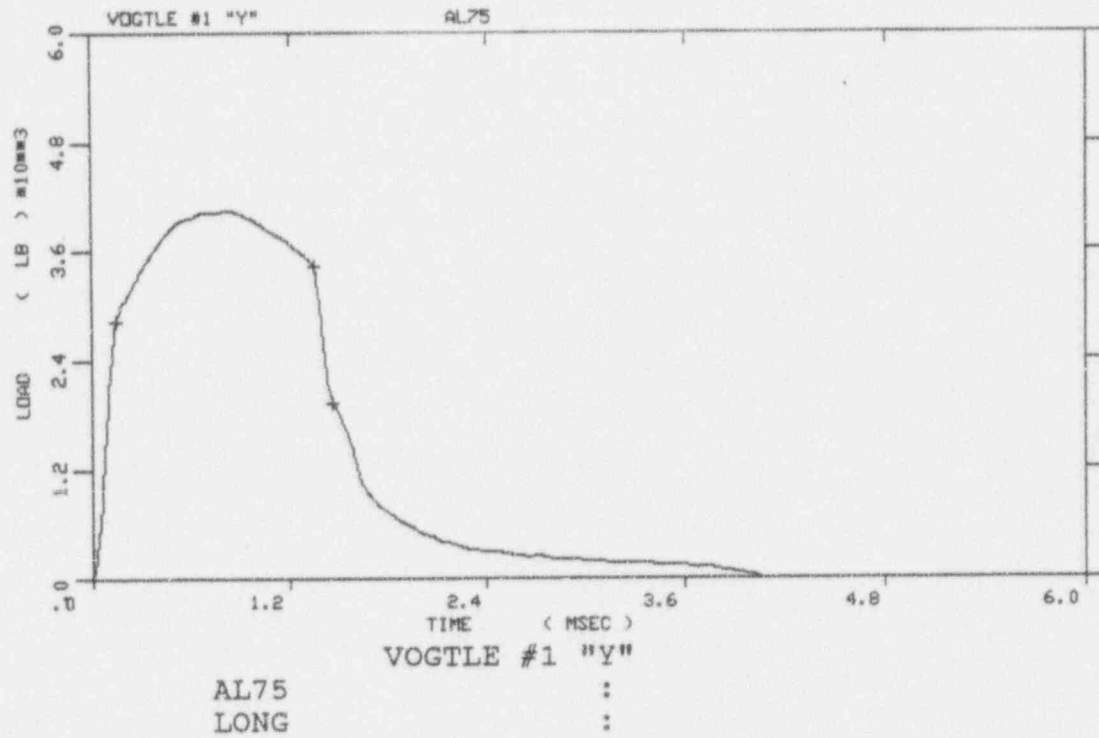


Figure A-7. Load-time records for Specimens AL75 and AL66

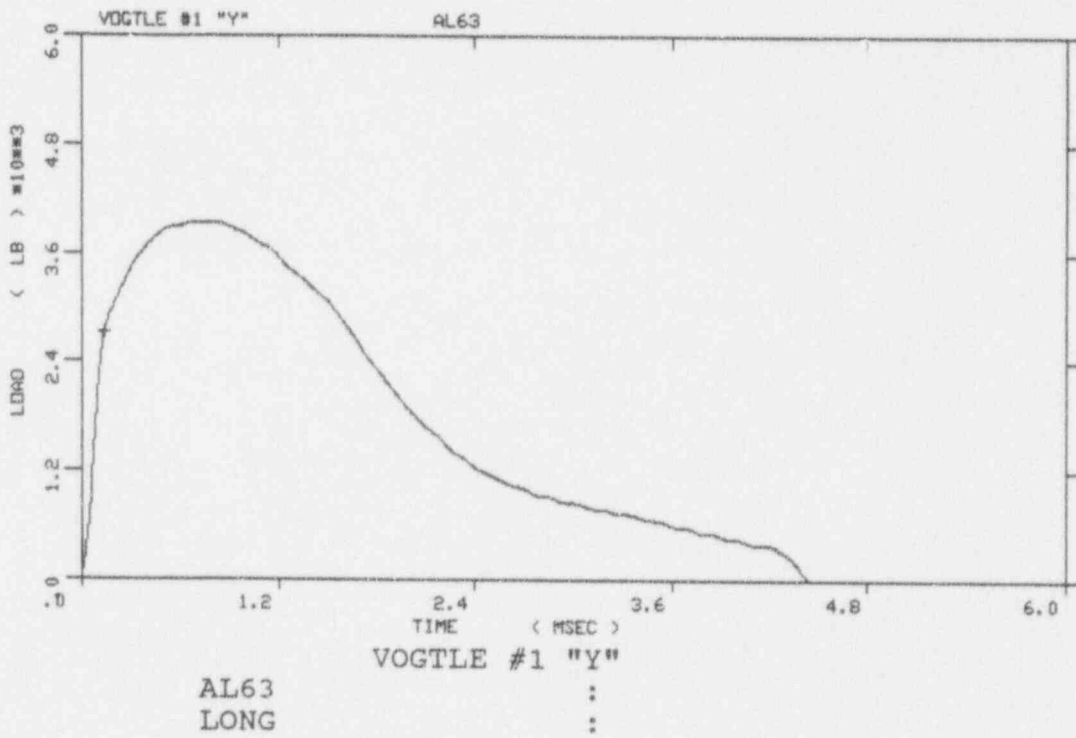
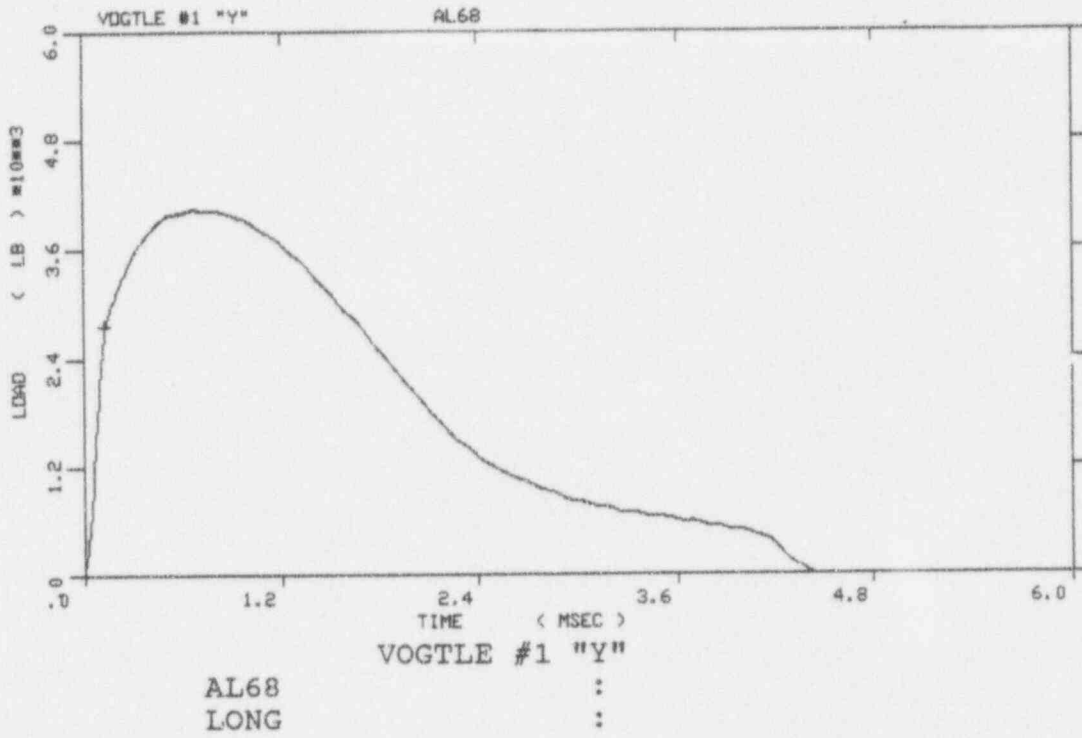


Figure A-8. Load-time records for Specimens AL68 and AL63

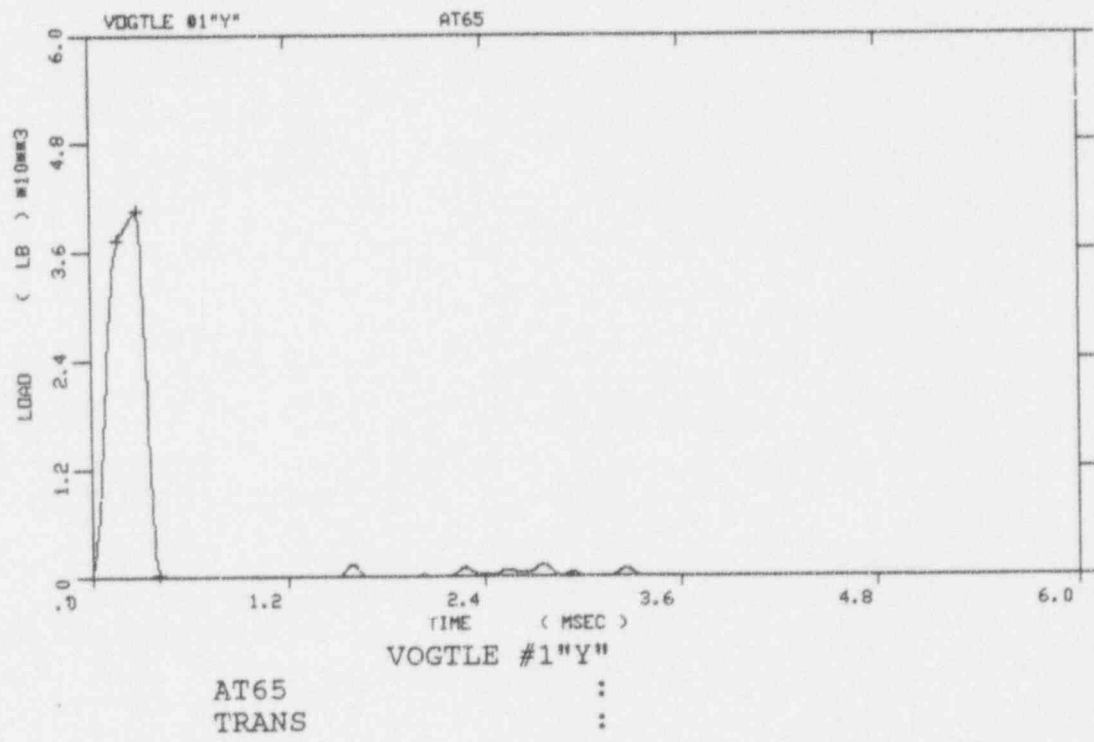
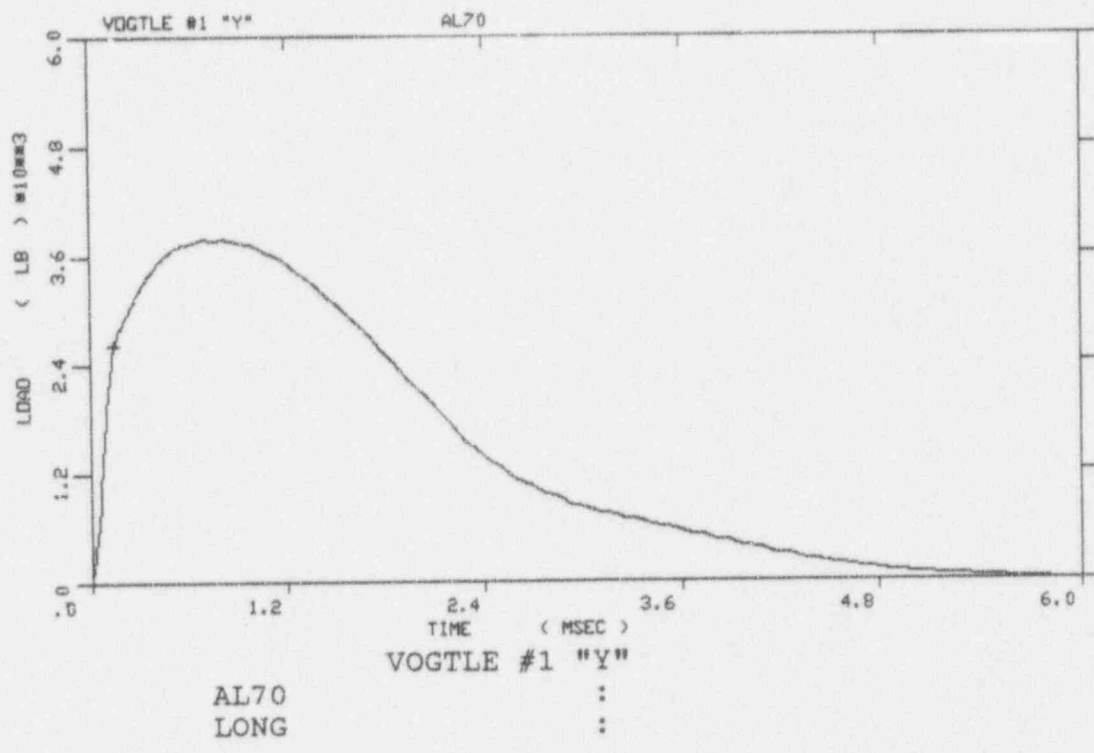


Figure A-9. Load-time records for Specimens AL70 and AT65

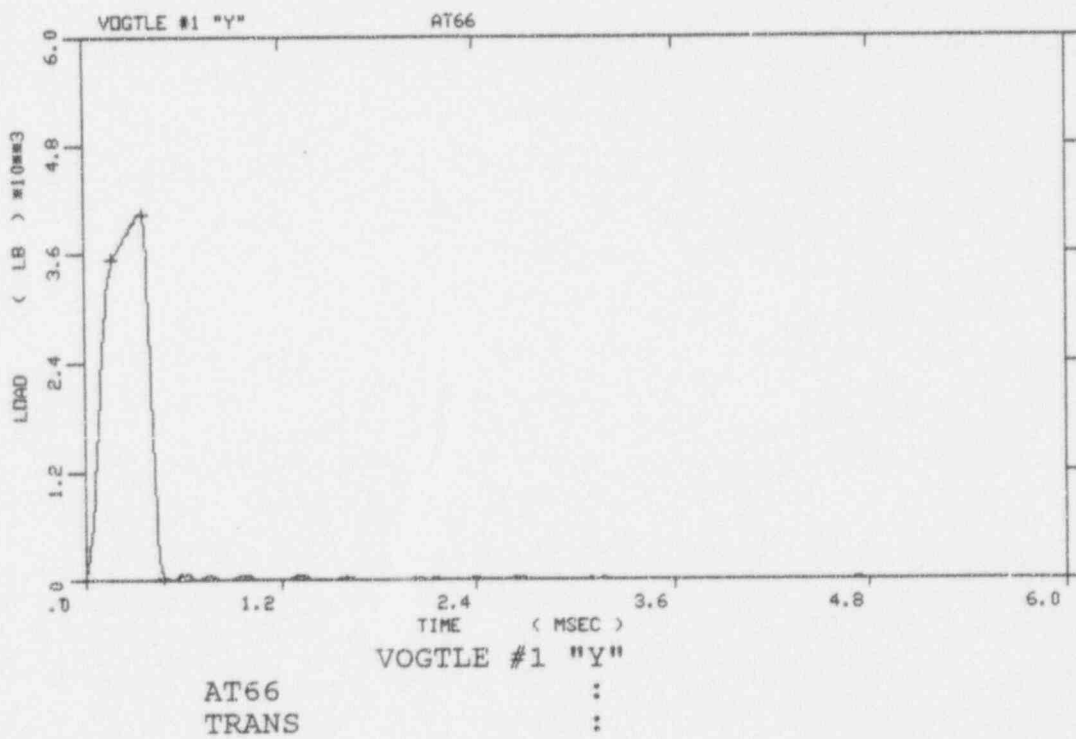
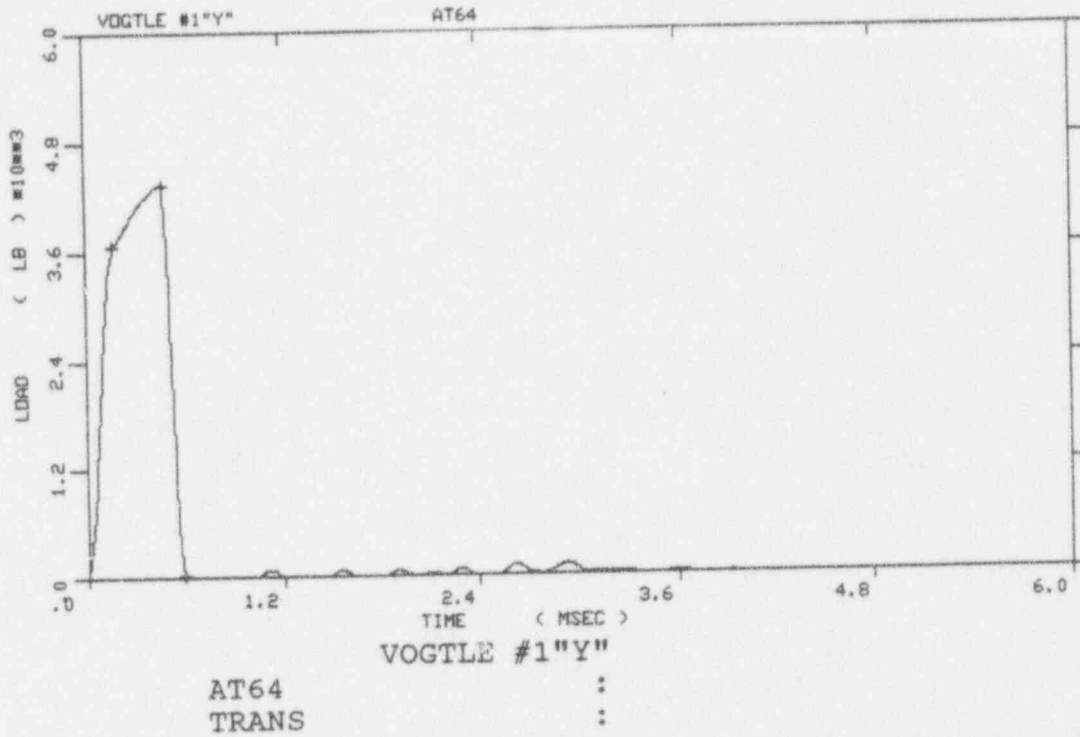


Figure A-10. Load-time records for Specimens AT64 and AT66

AT72 record not available
due to computer malfunction

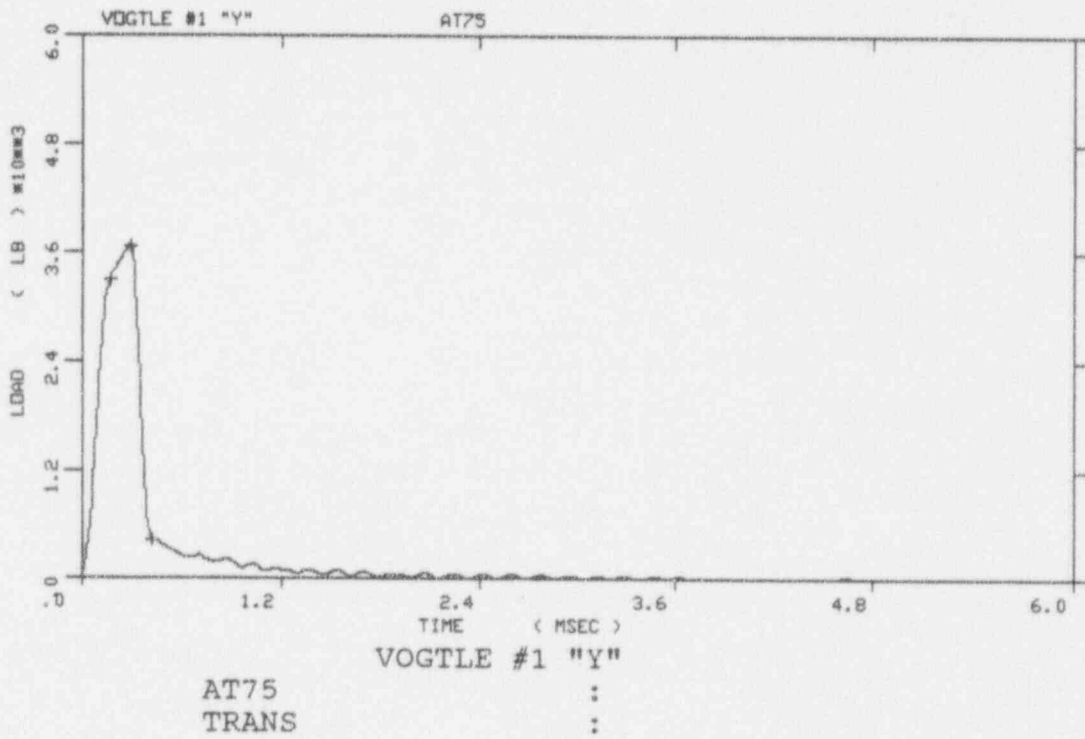


Figure A-11. Load-time records for Specimens AT72 and AT75

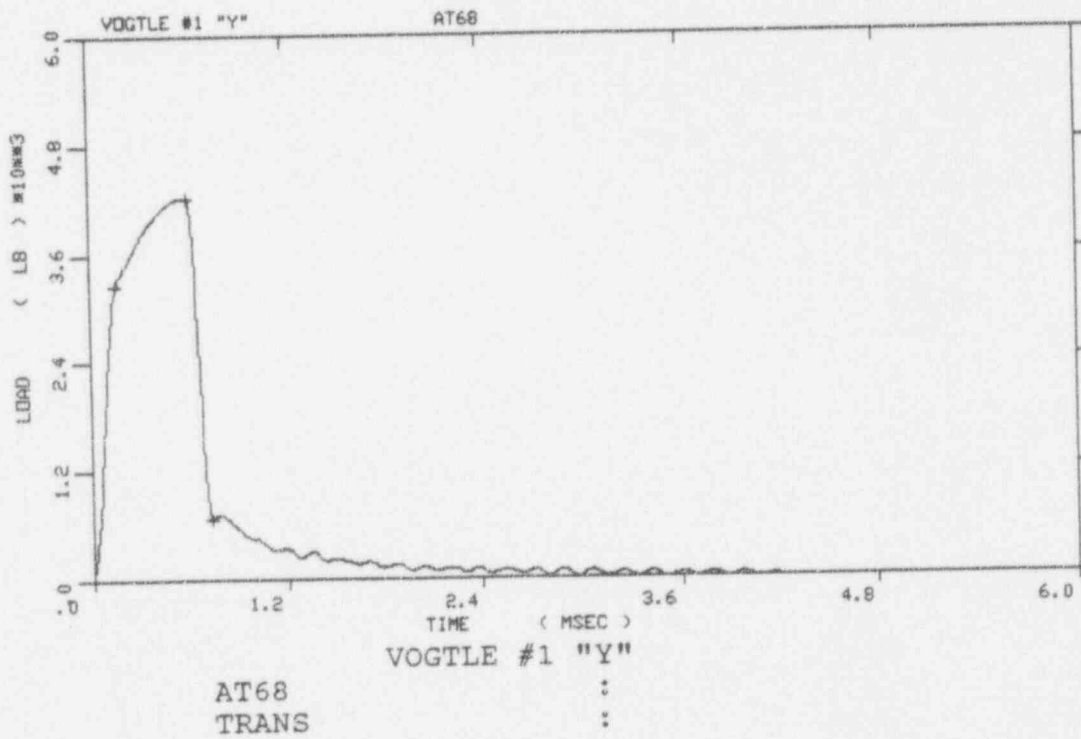
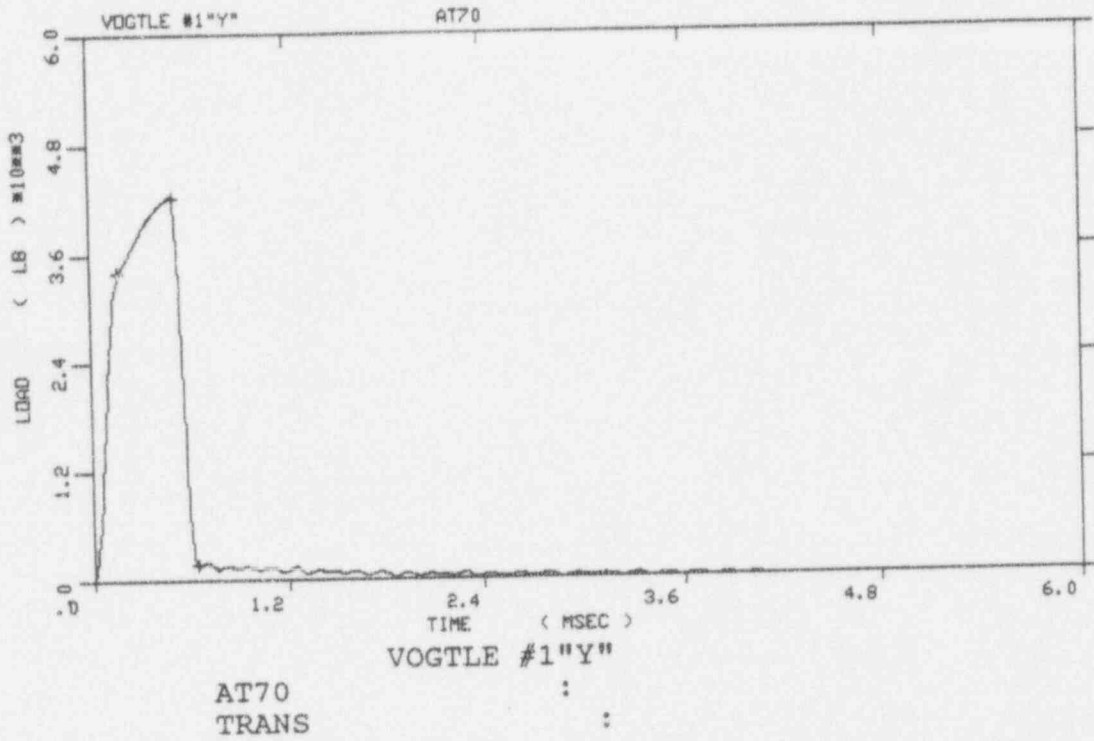


Figure A-12. Load-time records for Specimens AT70 and AT68

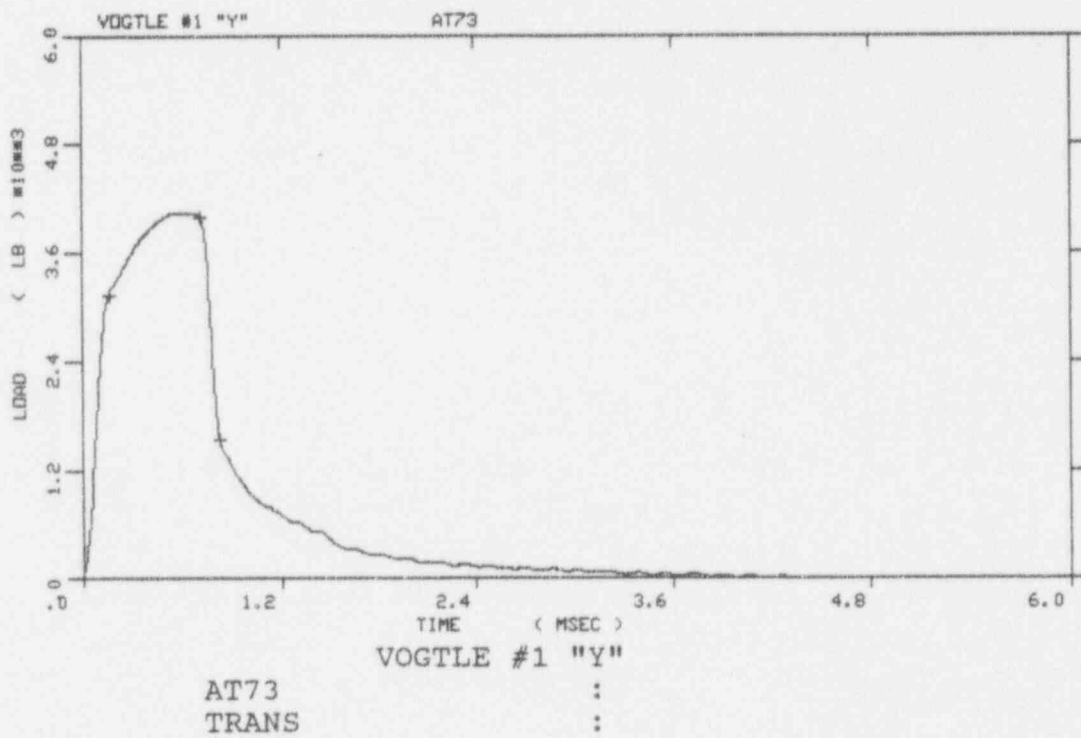
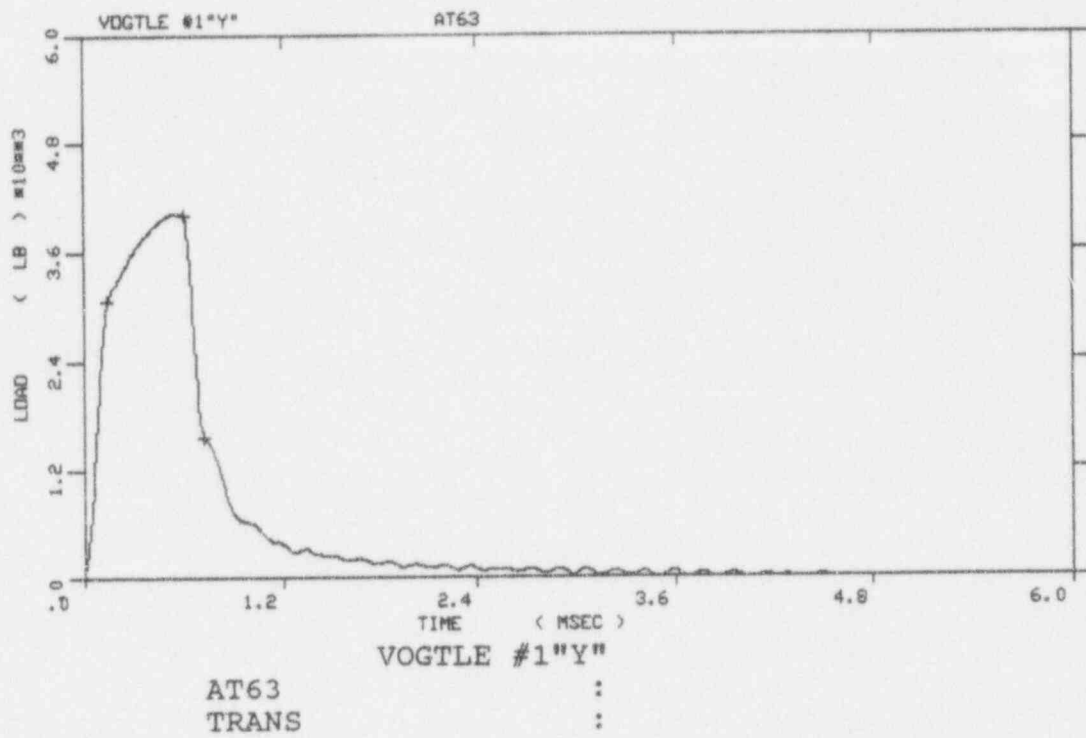


Figure A-13. Load-time records for Specimens AT63 and AT73

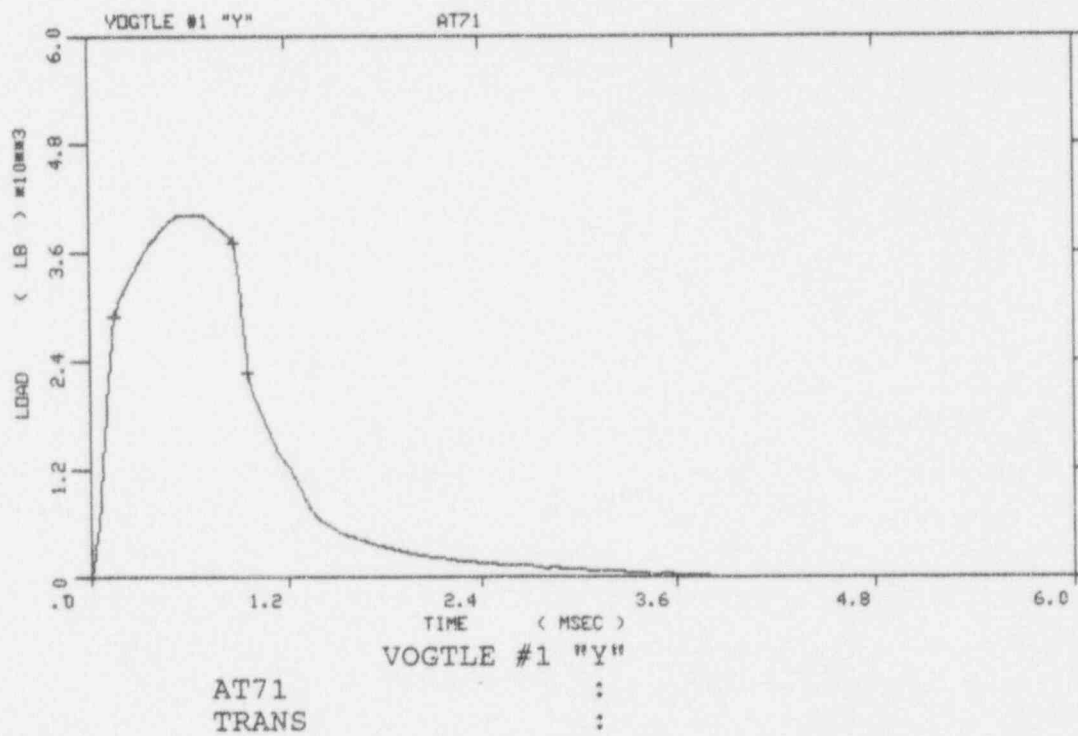
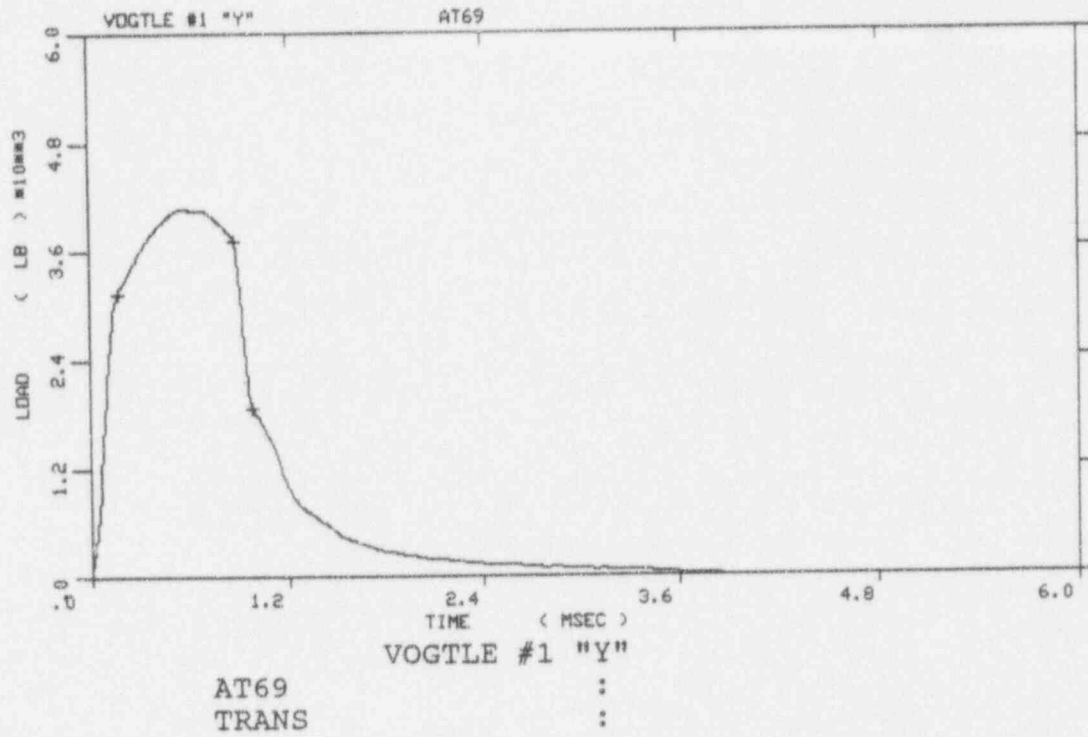


Figure A-14. Load-time records for Specimens AT69 and AT71

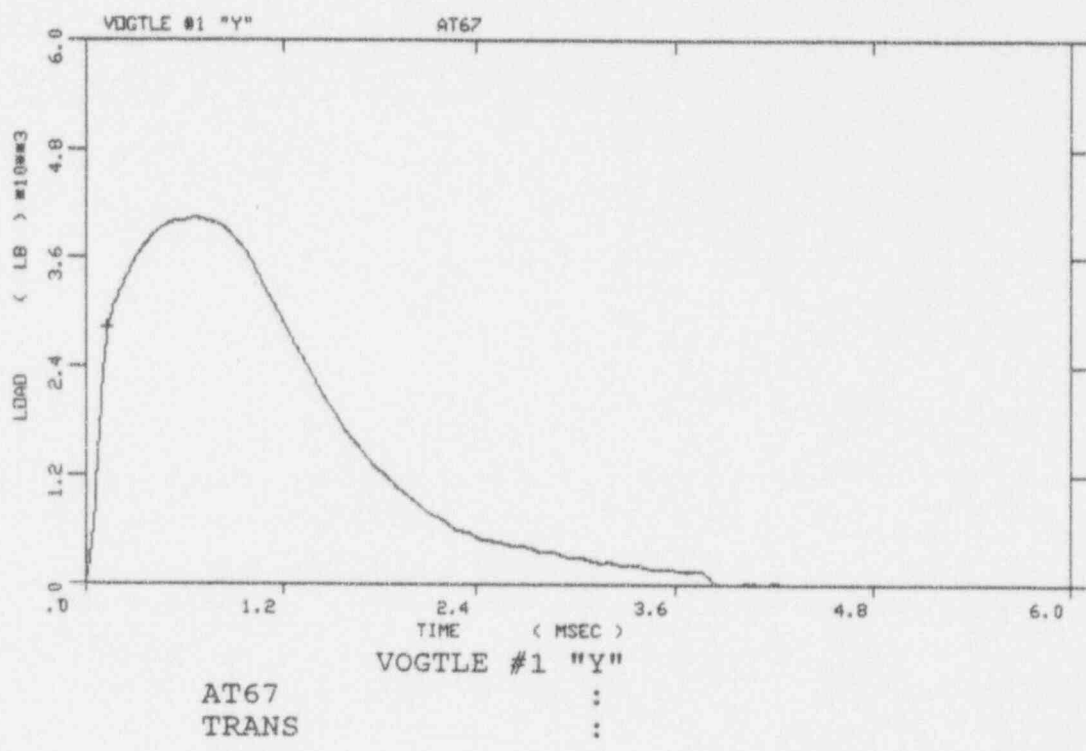
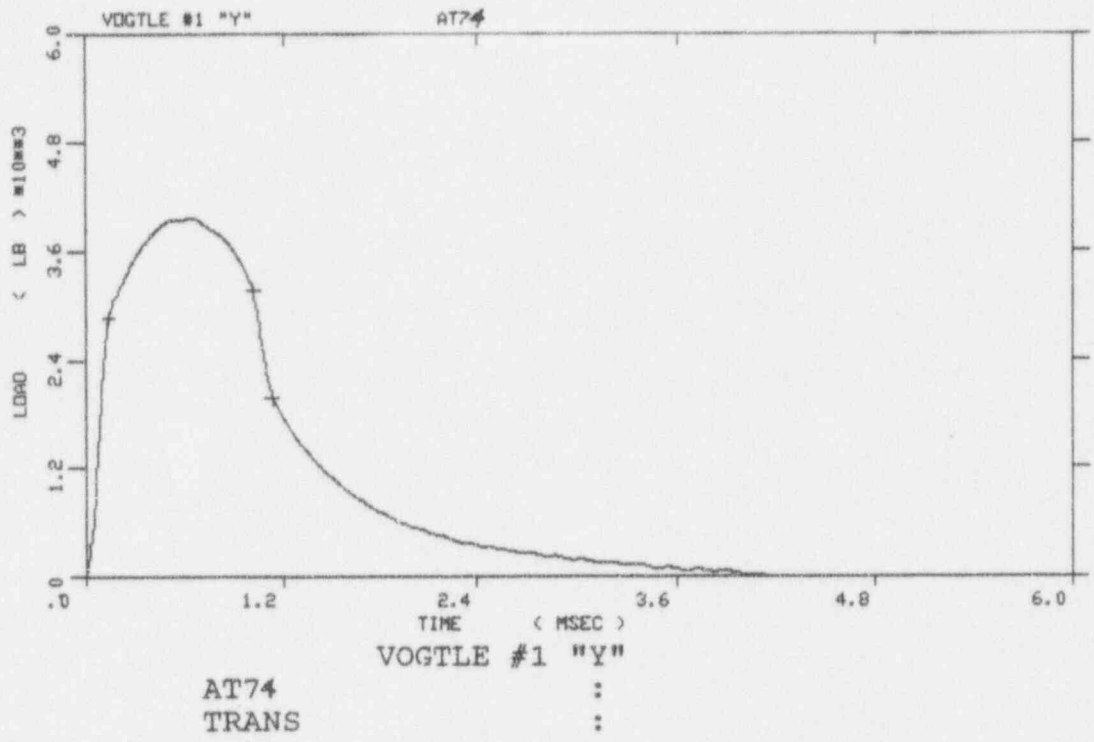


Figure A-15. Load-time records for Specimens AT74 and AT67

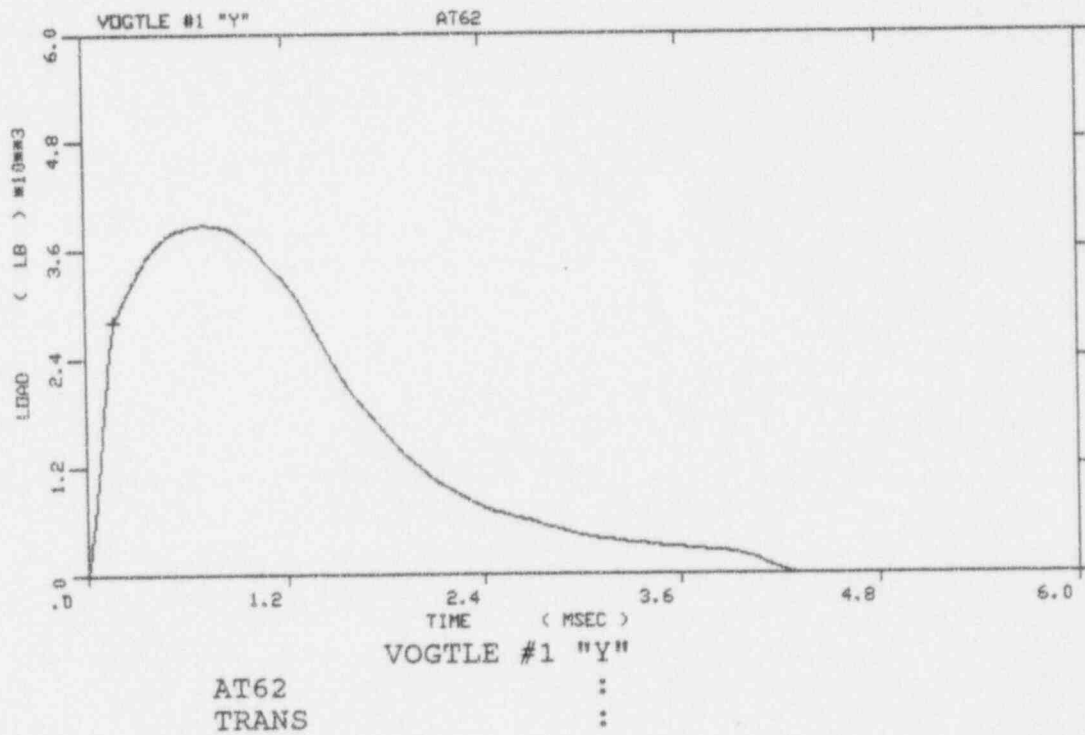
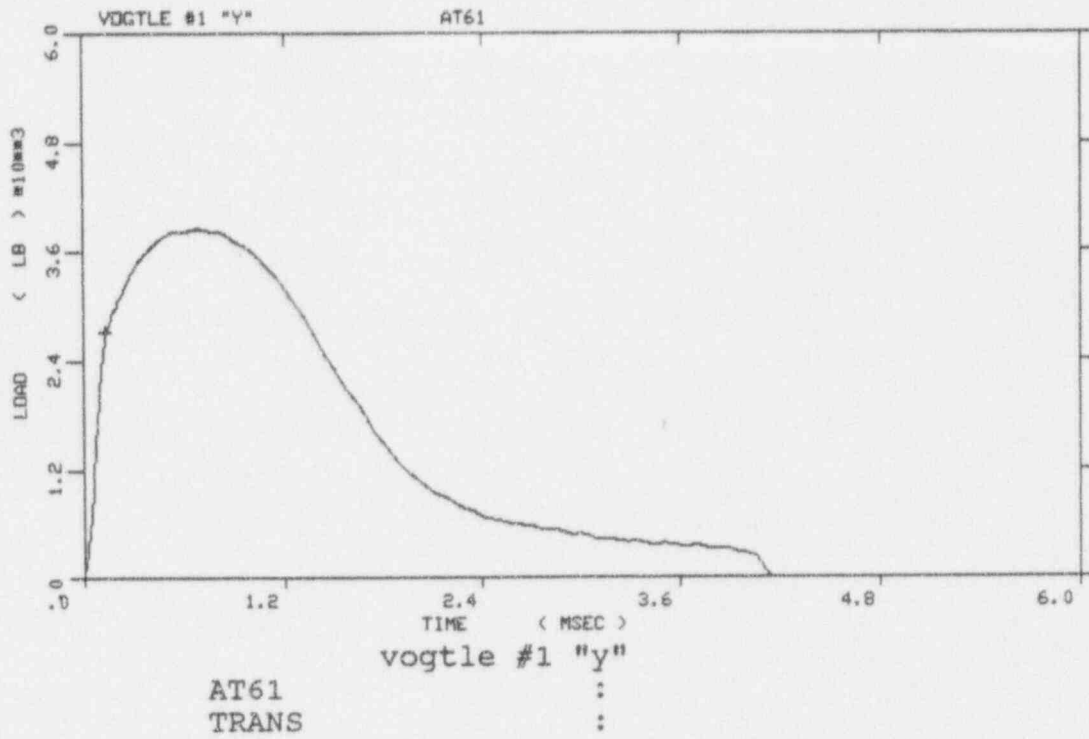


Figure A-16. Load-time records for Specimens AT61 and AT62

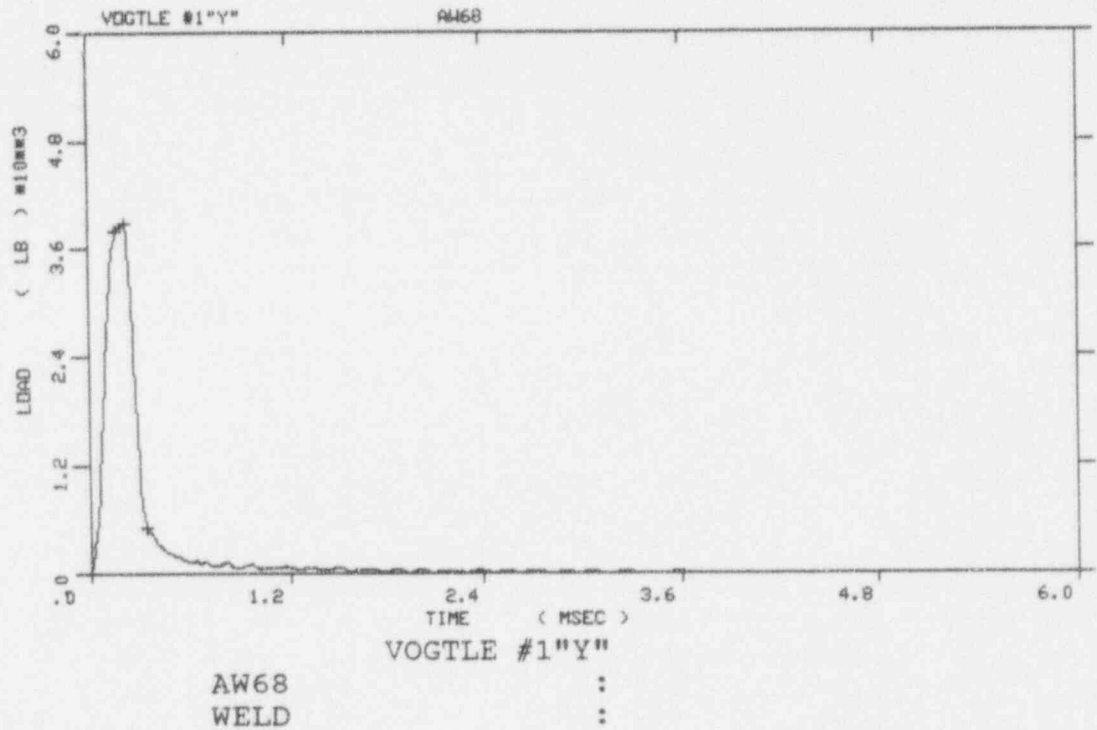
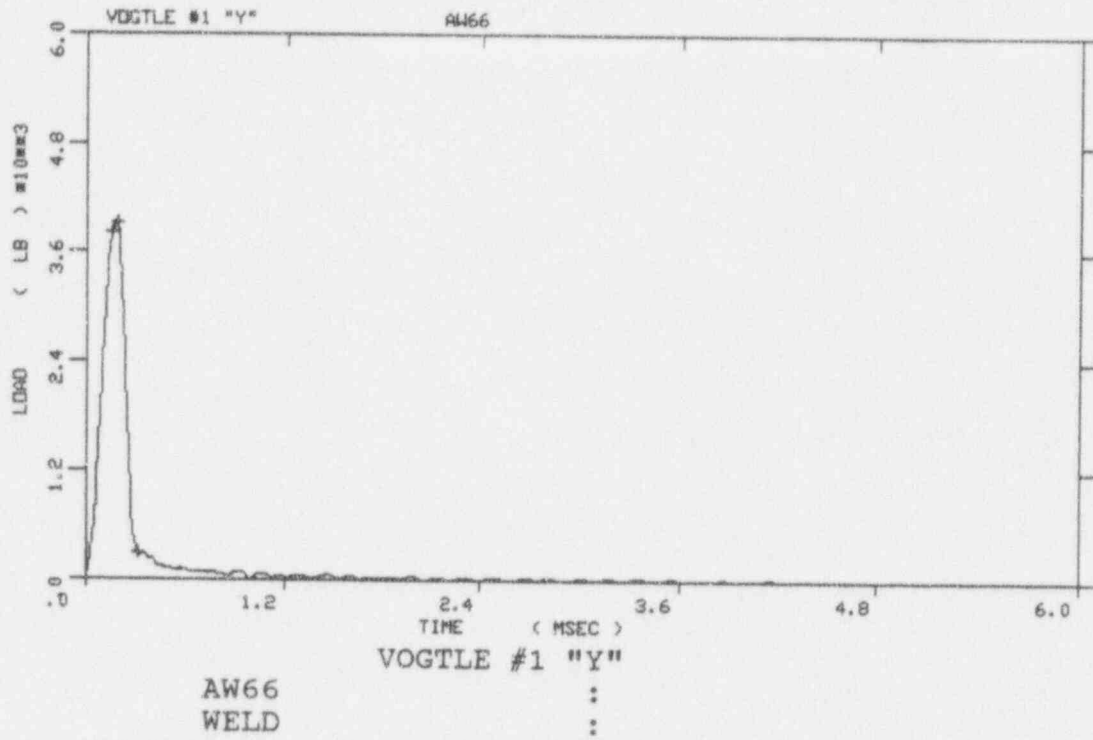


Figure A-17. Load-time records for Specimens AW66 and AW68

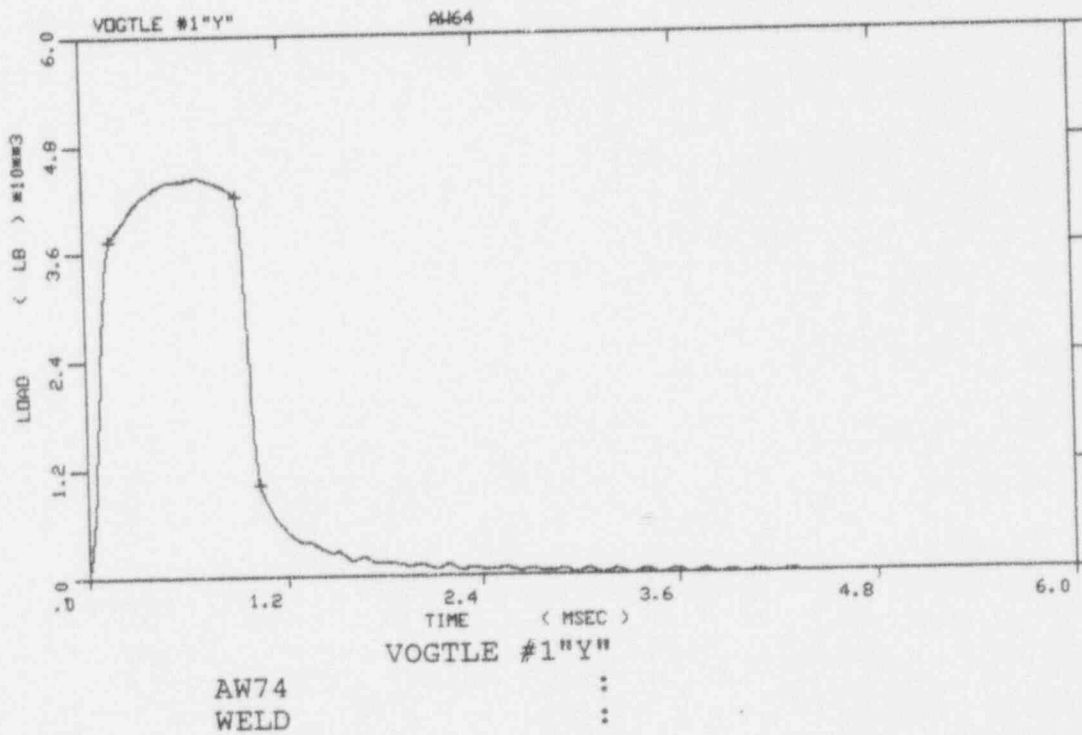
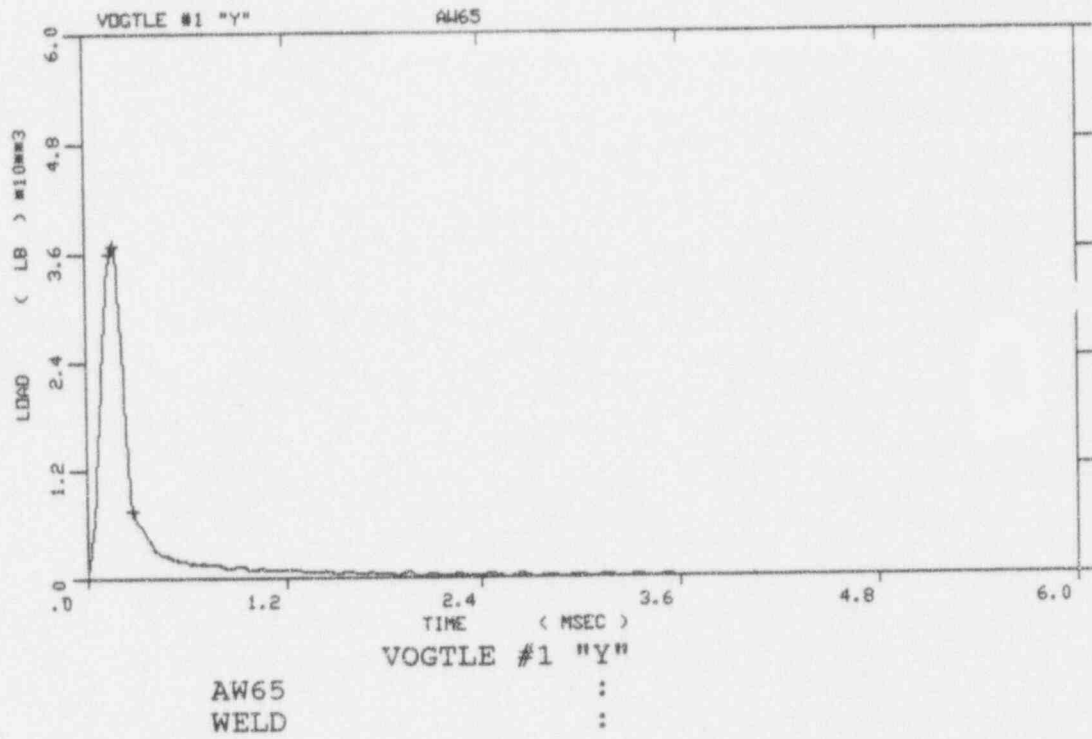


Figure A-18. Load-time records for Specimens AW65 and AW74

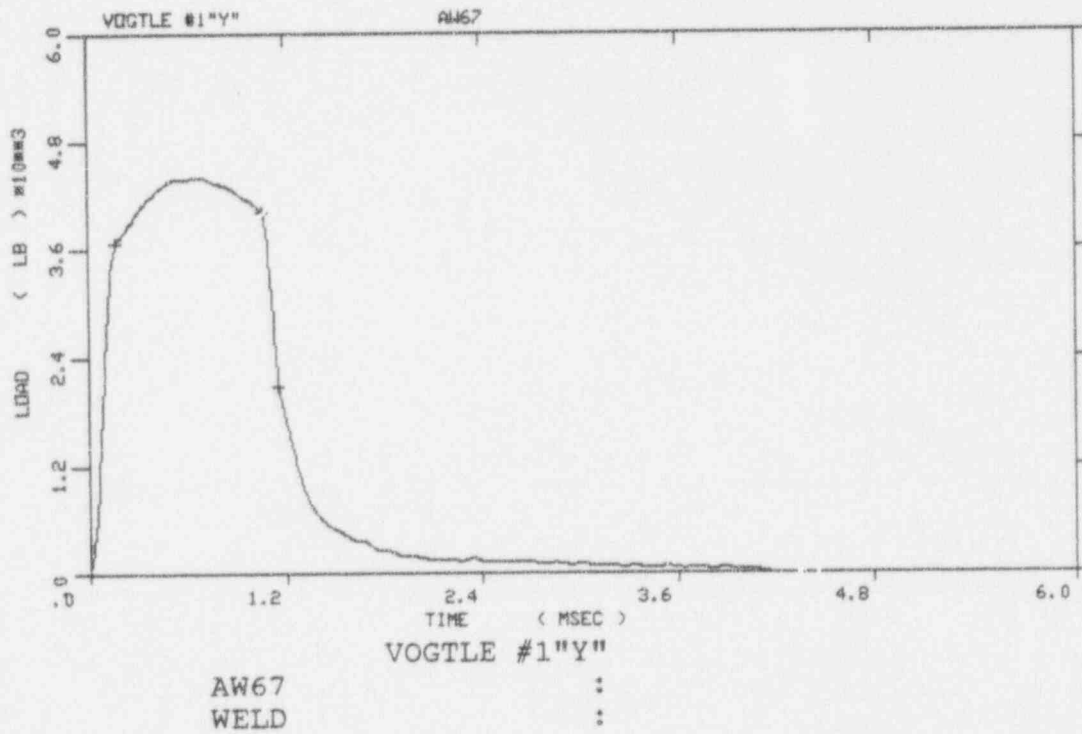
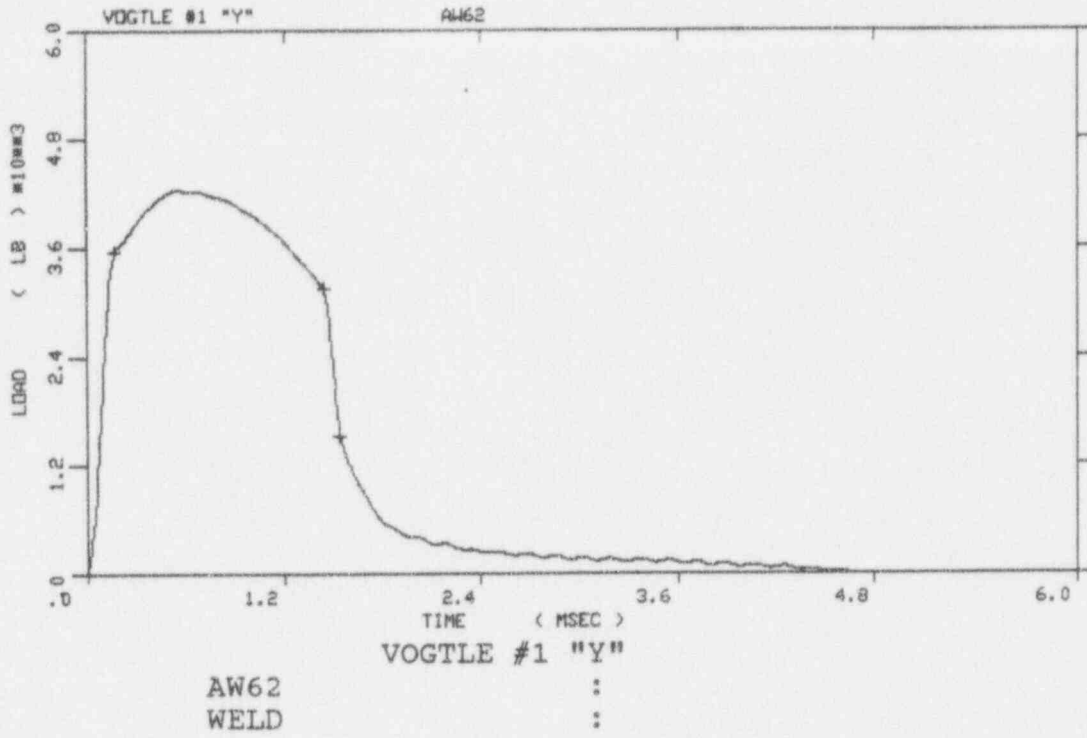


Figure A-19. Load-time records for Specimens AW62 and AW67

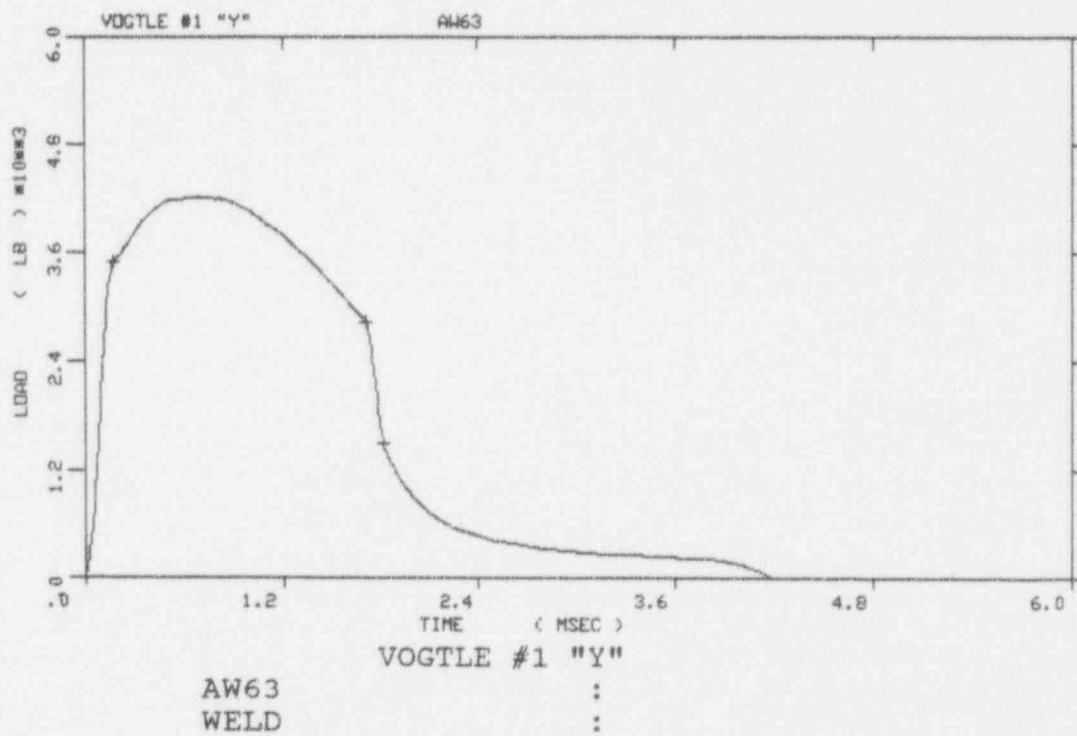
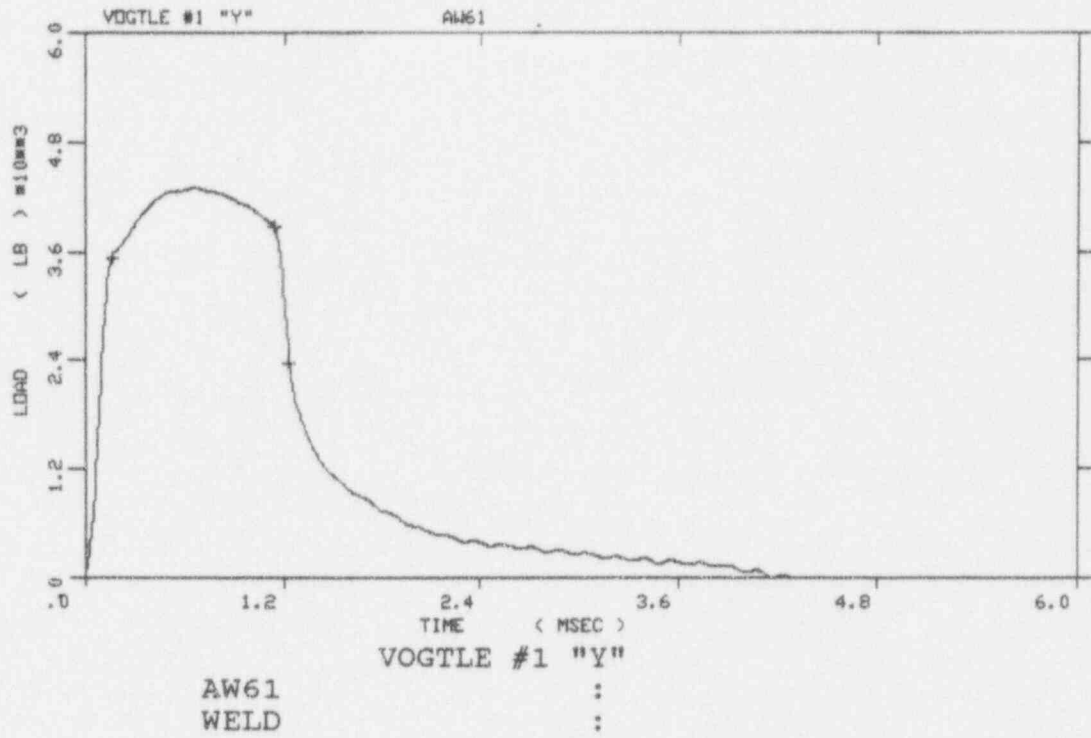


Figure A-20. Load-time records for Specimens AW61 and AW63

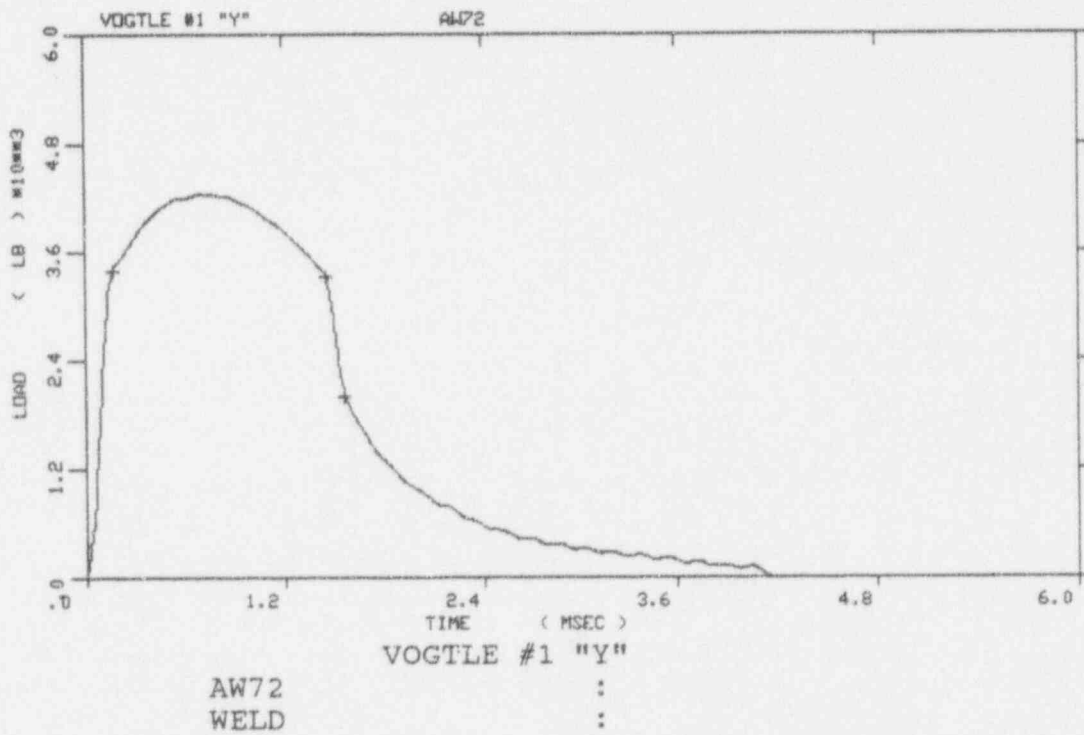
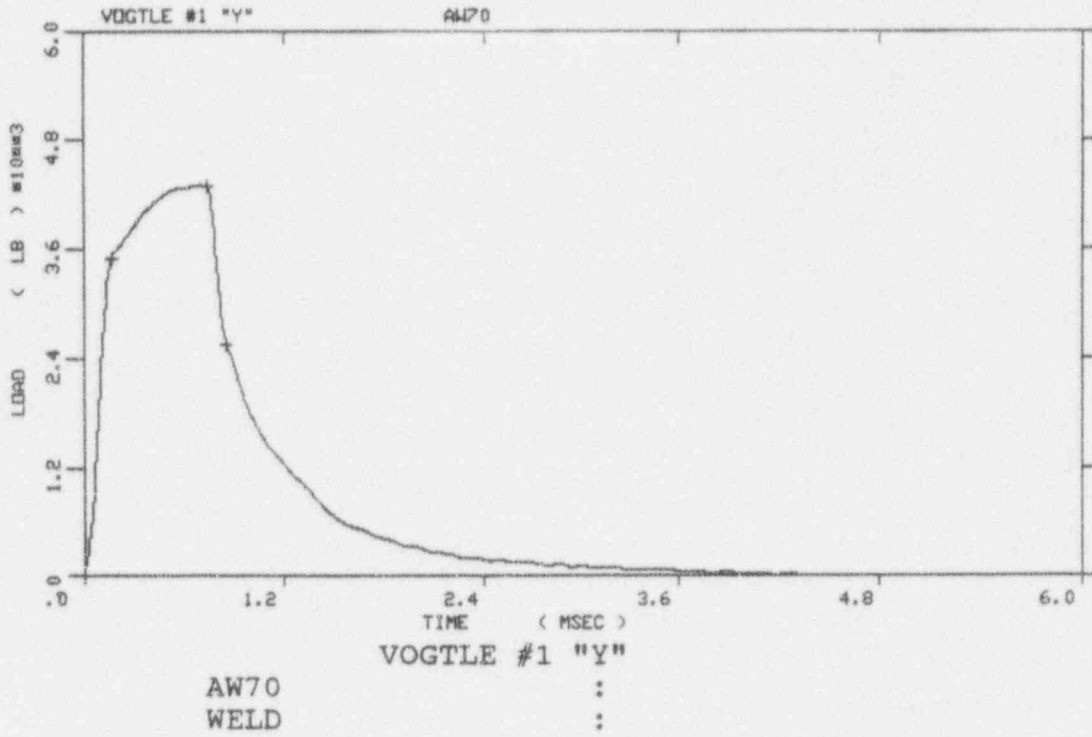


Figure A-21. Load-time records for Specimens AW70 and AW72

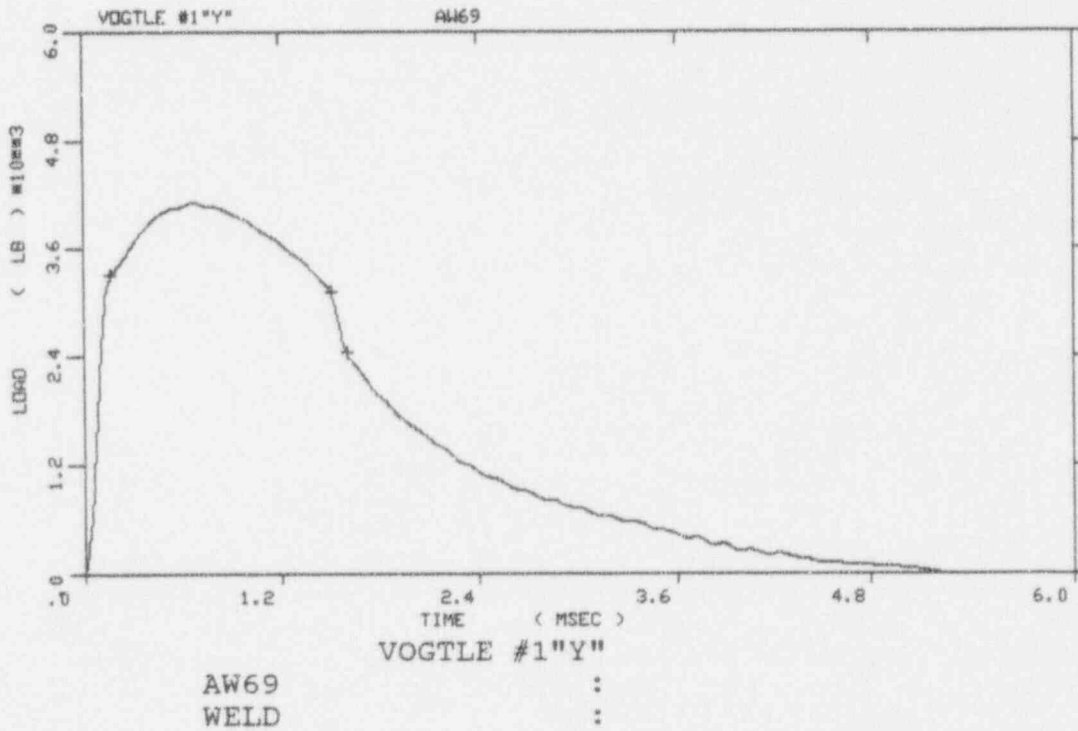
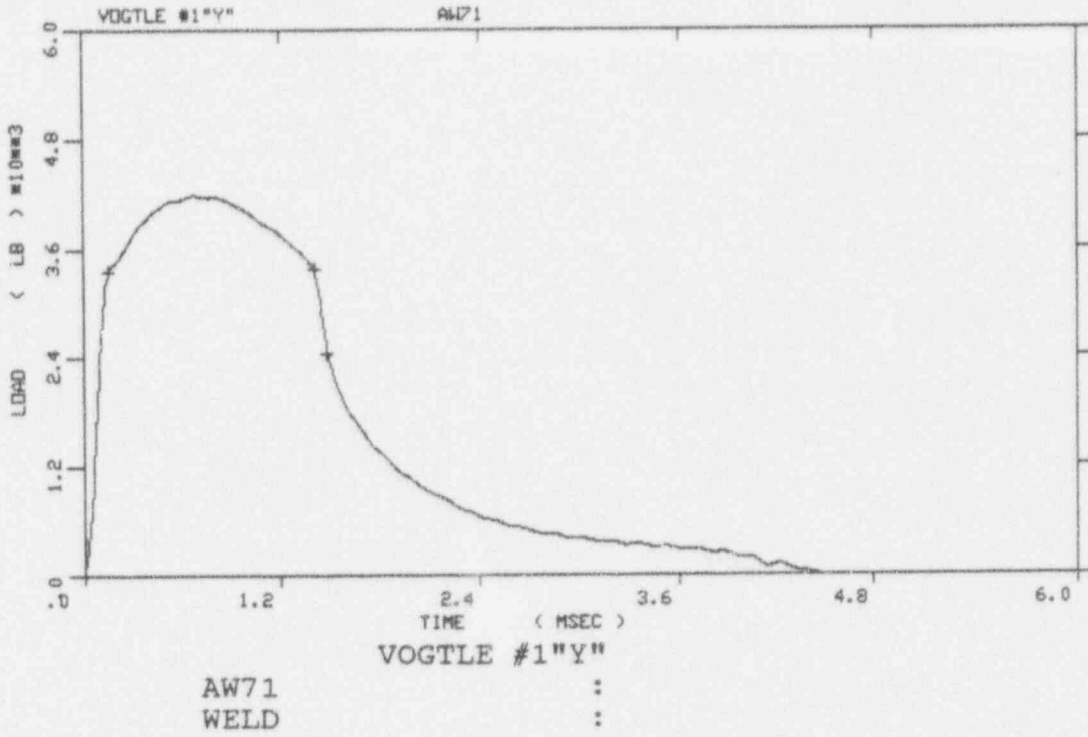


Figure A-22. Load-time records for Specimens AW71 and AW69

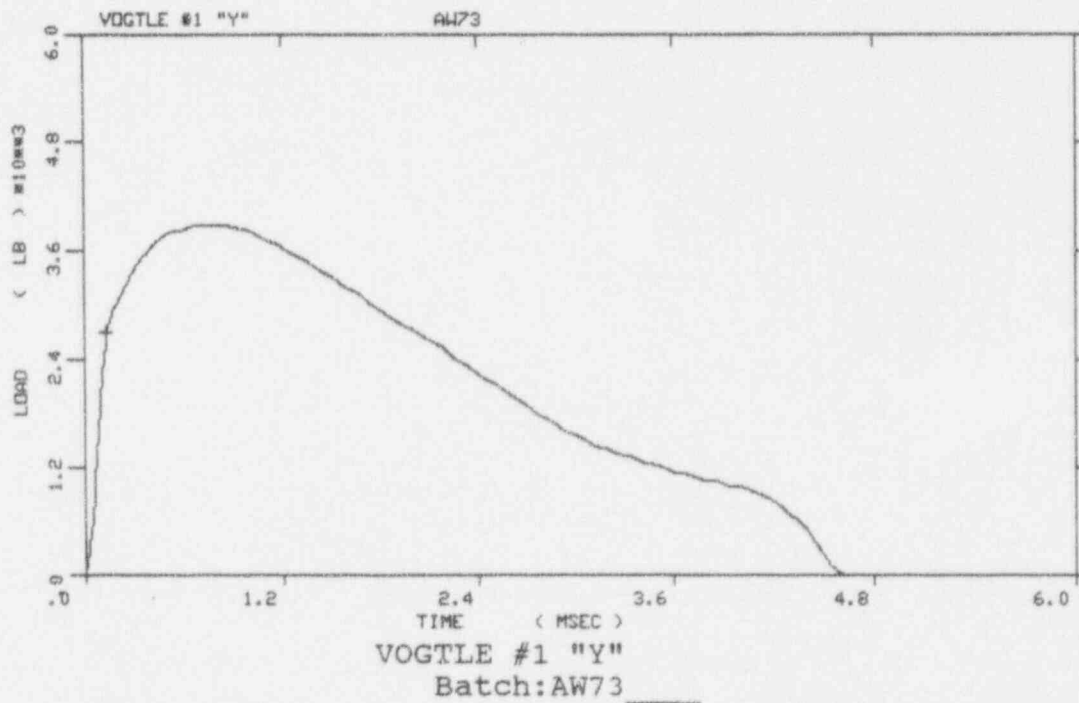
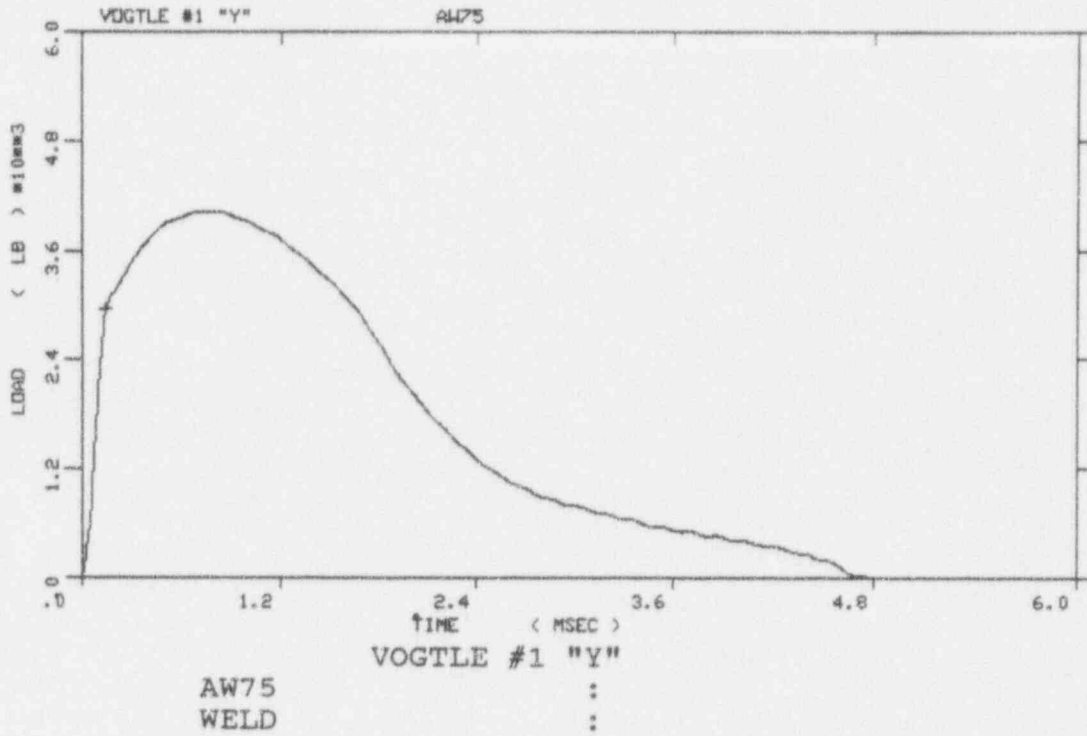


Figure A-23. Load-time records for Specimens AW75 and AW73

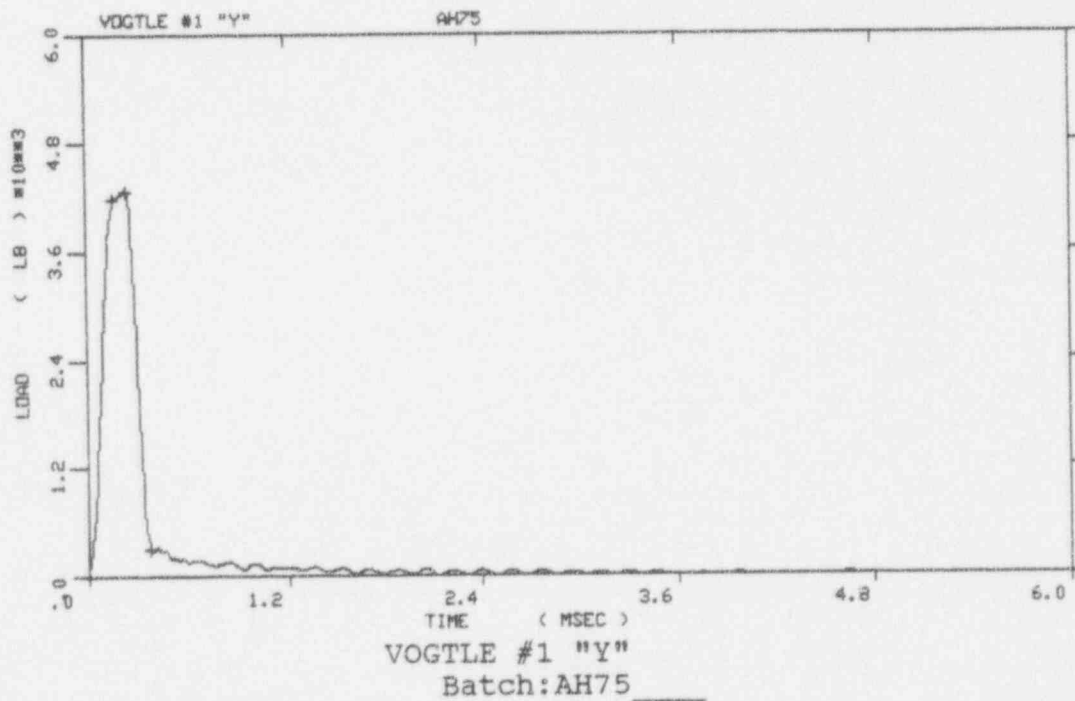
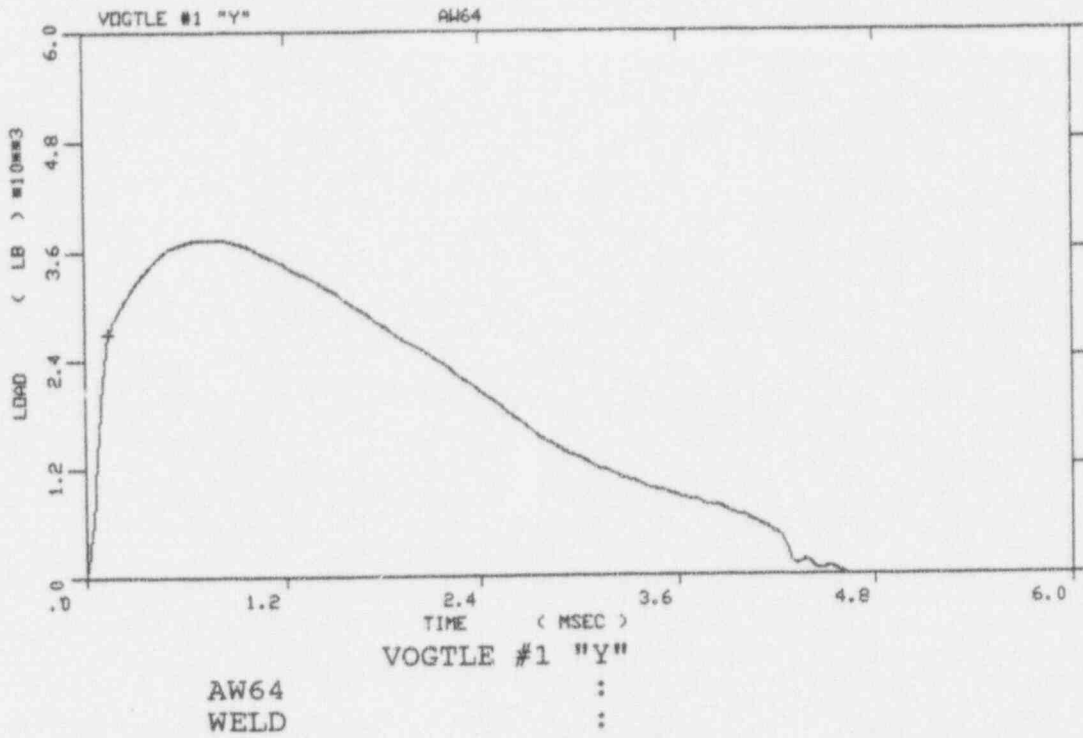


Figure A-24. Load-time records for Specimens AW64 and AH75

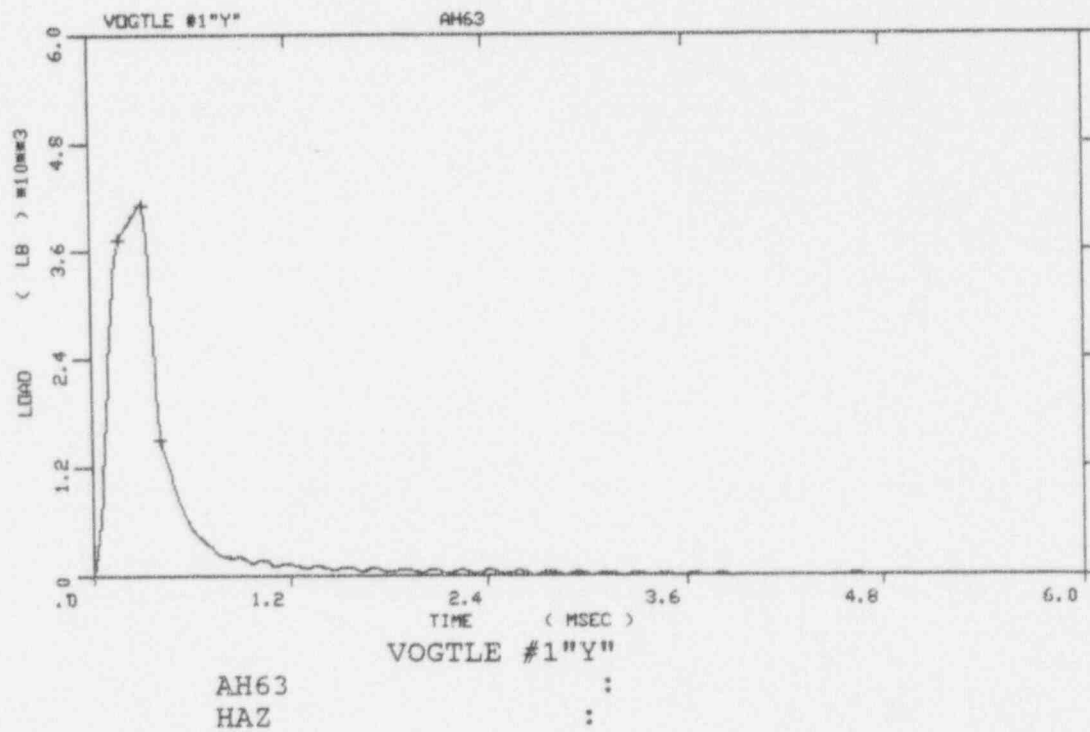
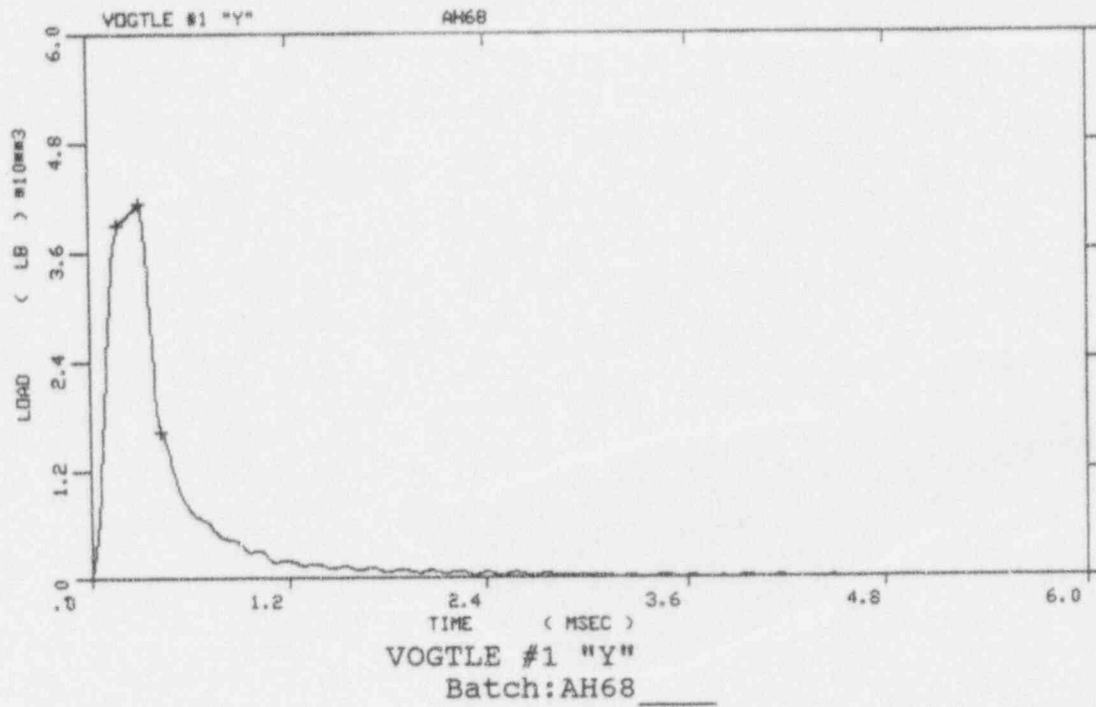


Figure A-25. Load-time records for Specimens AH68 and AH63

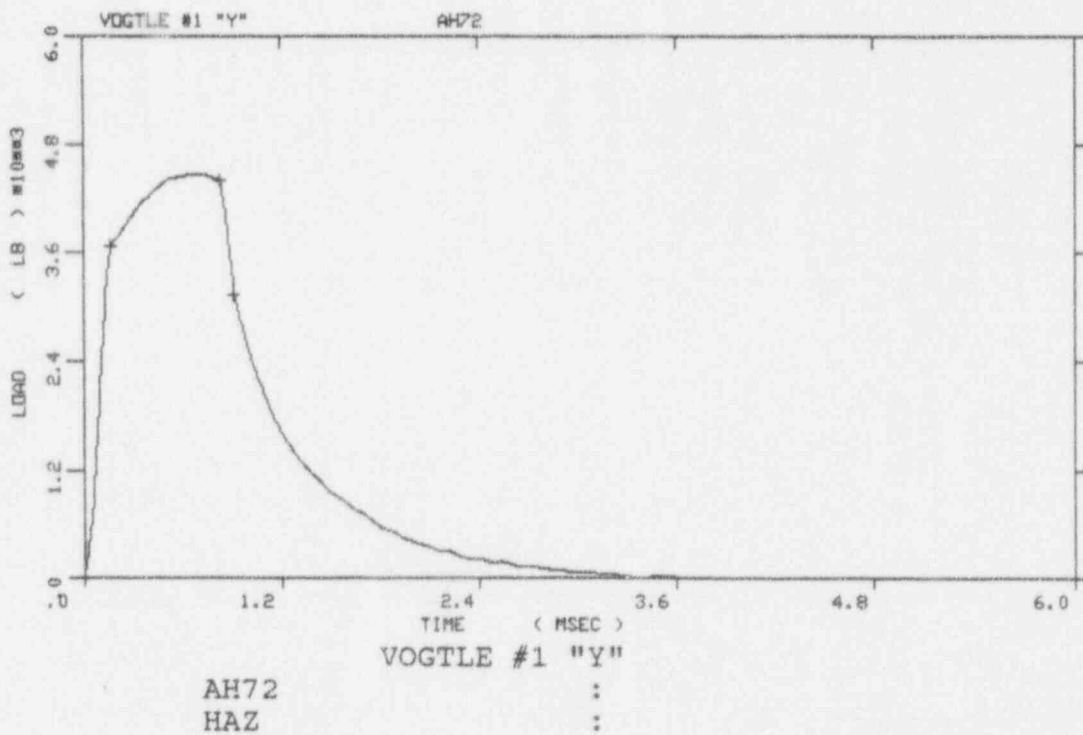
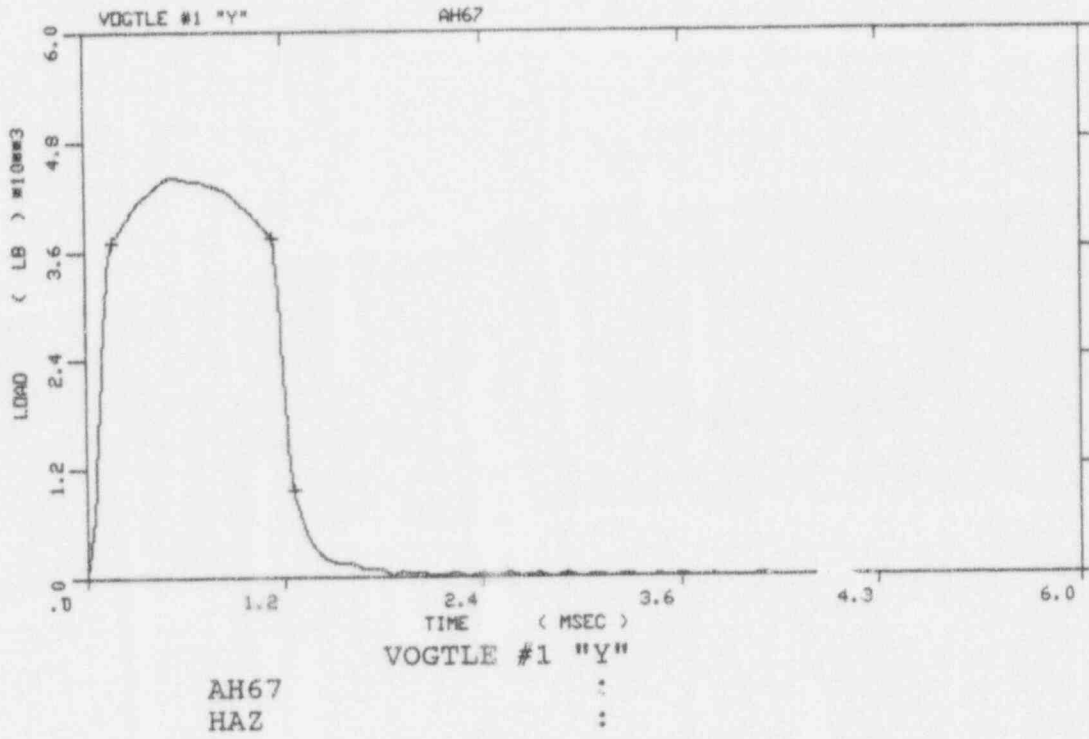


Figure A-26. Load-time records for Specimens AH67 and AH72

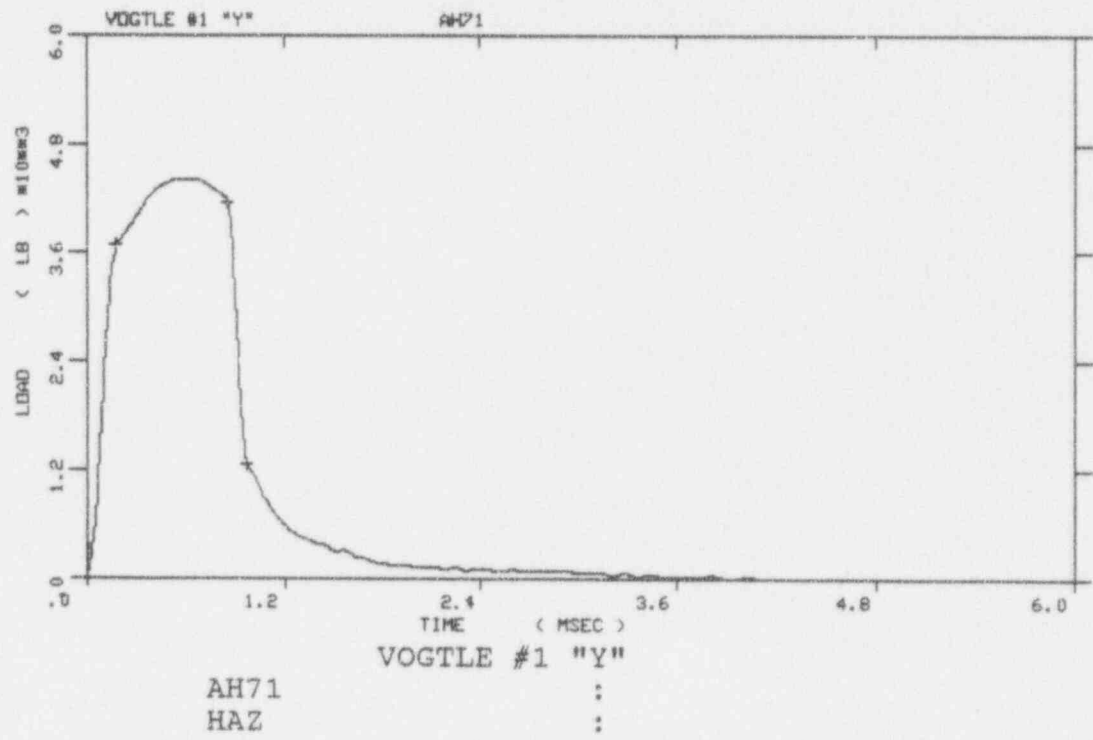
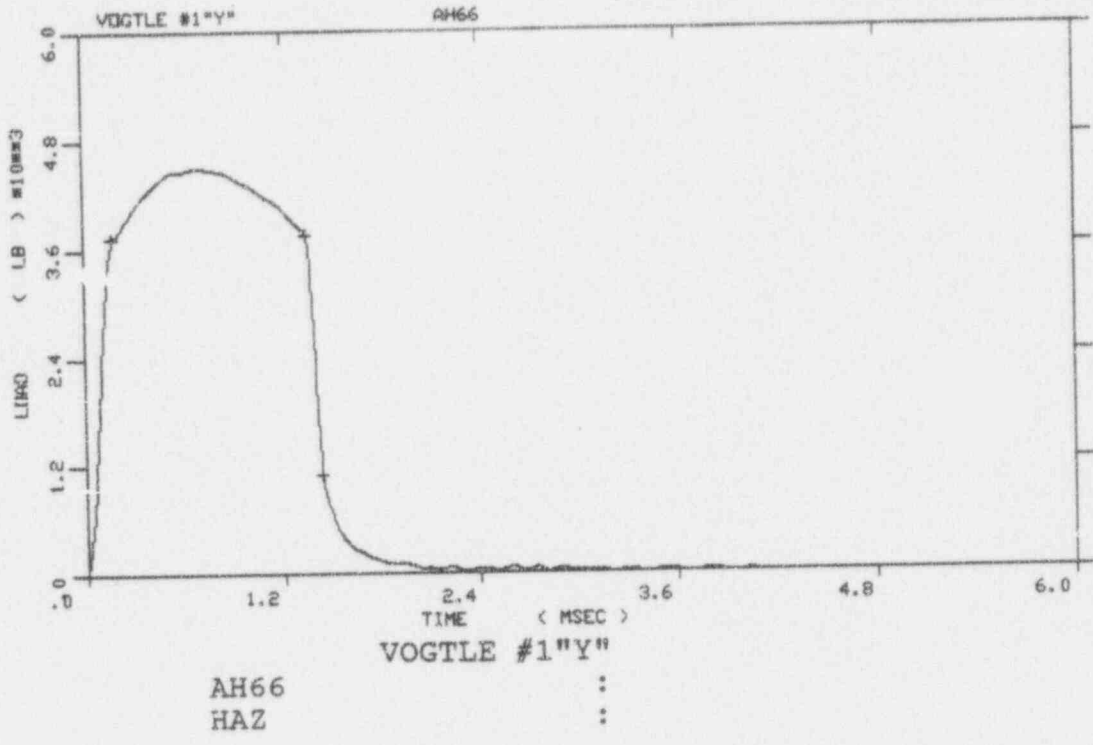


Figure A-27. Load-time records for Specimens AH66 and AH71

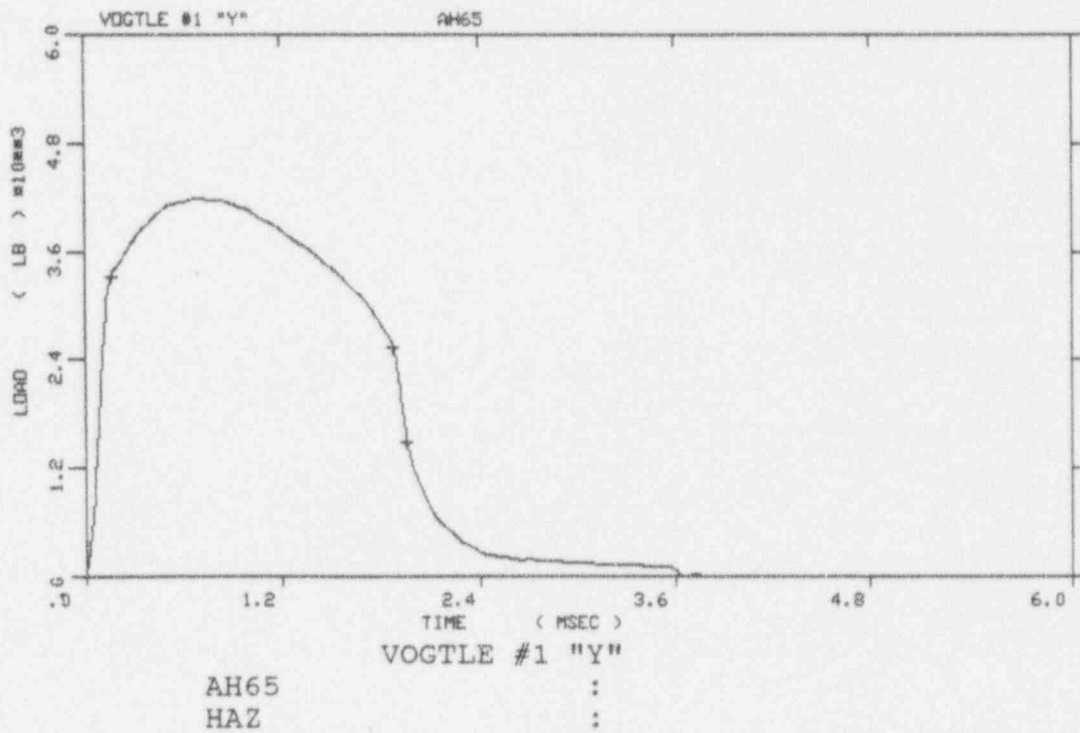
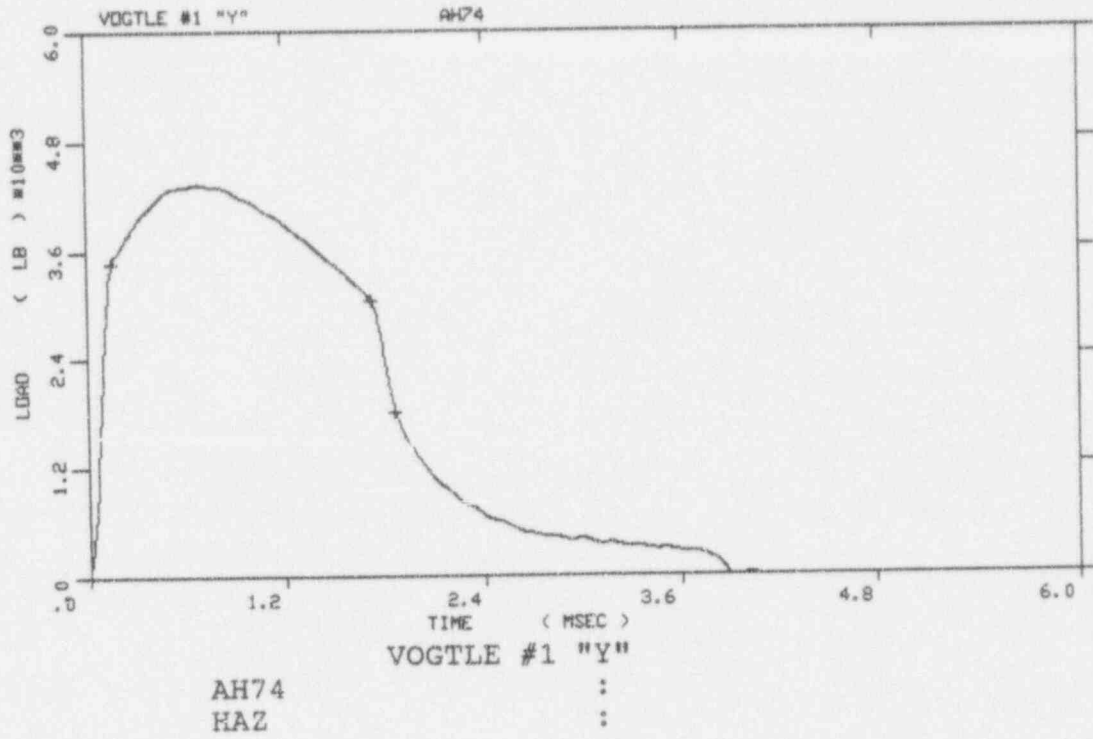


Figure A-28. Load-time records for Specimens AH74 and AH65

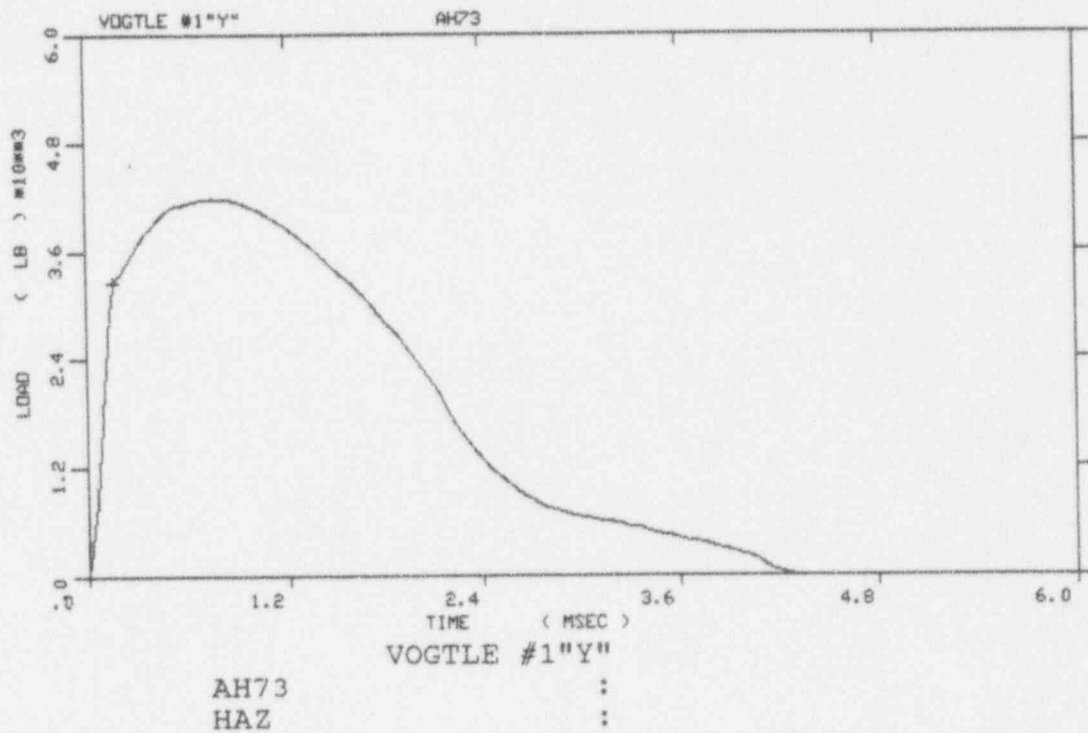
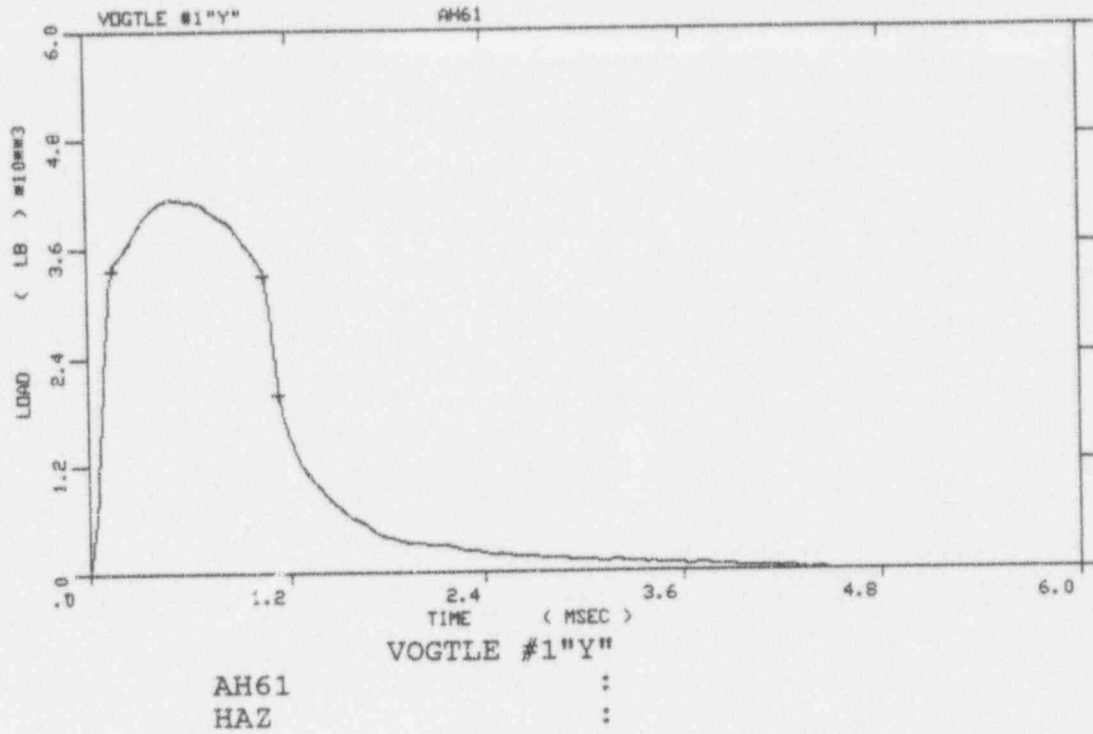


Figure A-29. Load-time records for Specimens AH61 and AH73

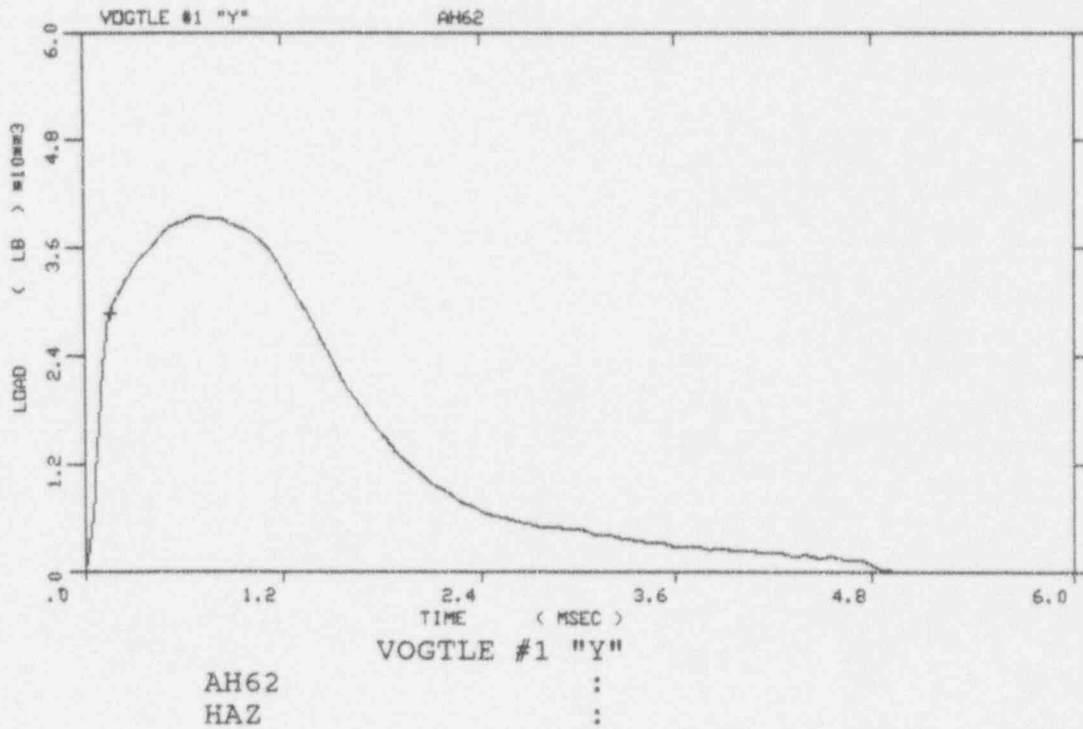
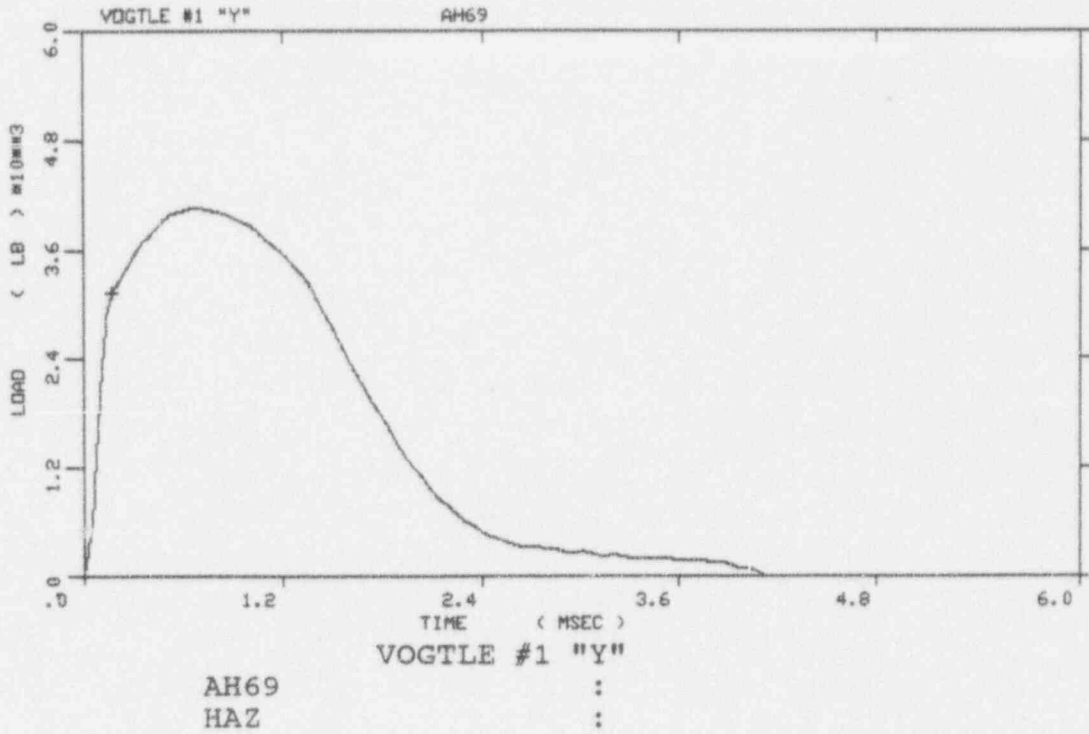


Figure A-30. Load-time records for Specimens AH69 and AH62

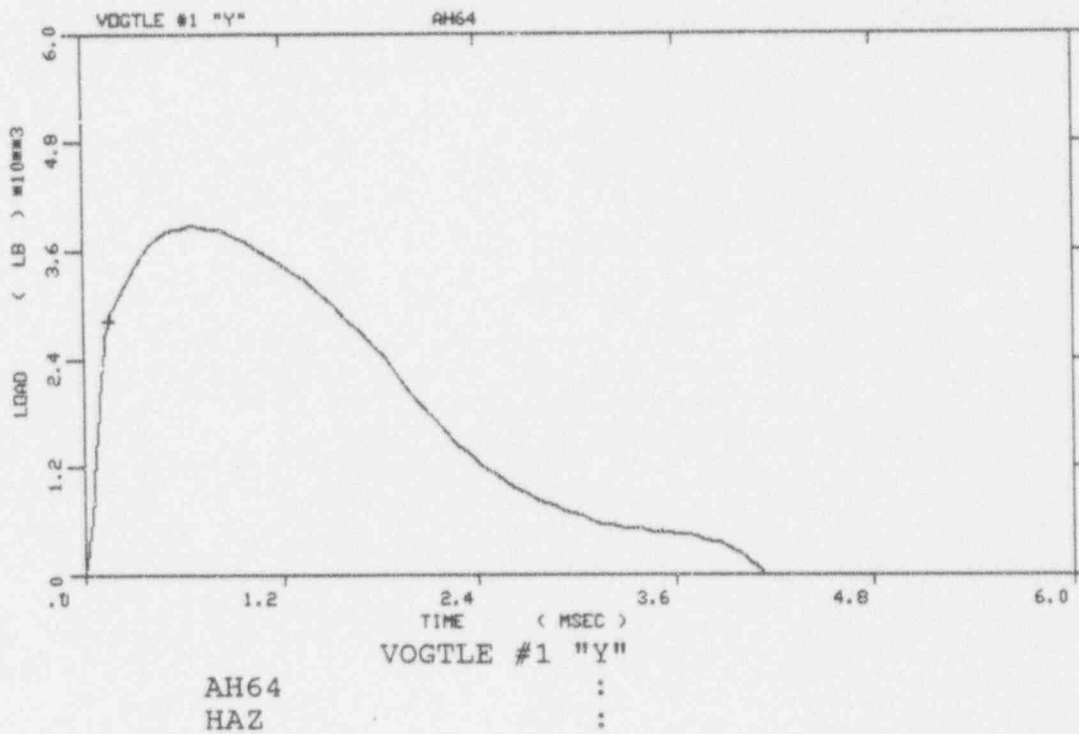
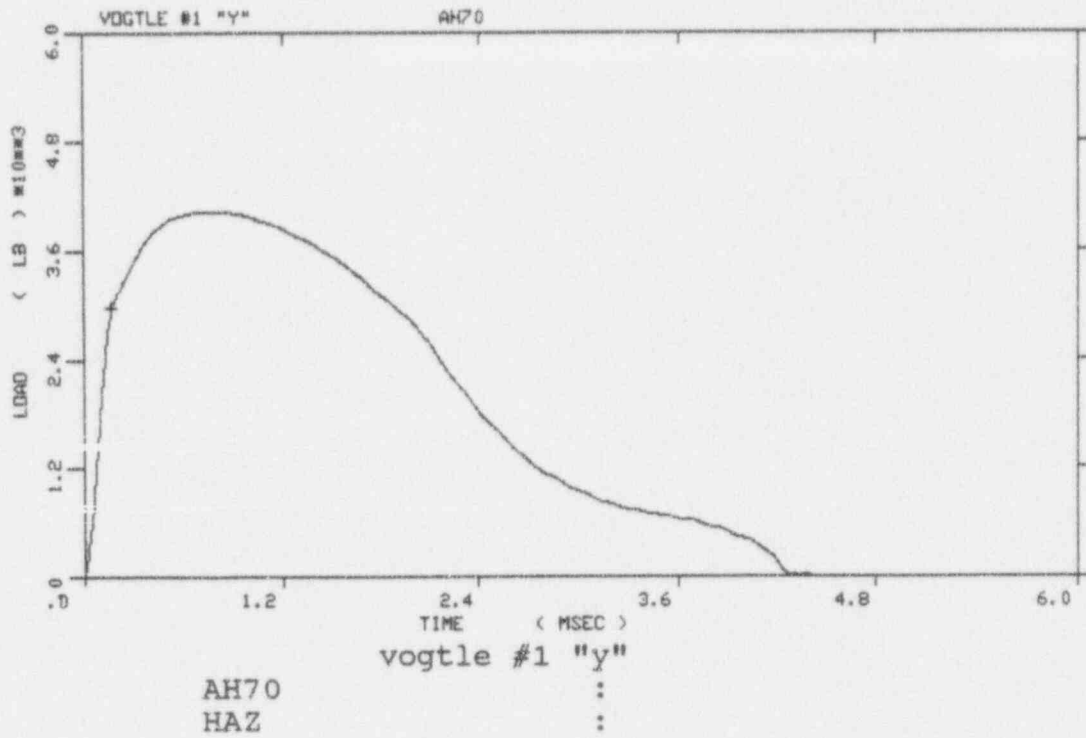


Figure A-31. Load-time records for Specimens AH70 and AH64

APPENDIX B

HEATUP AND COOLDOWN LIMIT CURVES
FOR NORMAL OPERATION OF THE
VOGTLE UNIT 1 REACTOR PRESSURE VESSEL

TABLE OF CONTENTS

<u>Section</u>	<u>Title</u>	<u>Page</u>
	LIST OF ILLUSTRATIONS	B-2
	LIST OF TABLES	B-2
B-1.	INTRODUCTION	B-4
B-2.	FRACTURE TOUGHNESS PROPERTIES	B-5
B-3.	CRITERIA FOR ALLOWABLE PRESSURE-TEMPERATURE RELATIONSHIPS	B-5
B-4.	CALCULATION OF ADJUSTED REFERENCE TEMPERATURE	B-8
B-5.	HEATUP AND COOLDOWN PRESSURE-TEMPERATURE LIMIT CURVES	B-9
B-6.	REFERENCES	B-22

LIST OF ILLUSTRATIONS

<u>Figure</u>	<u>Title</u>	<u>Page</u>
B-1	Vogtle Unit 1 Reactor Coolant System Heatup Limitations (Heatup rates up to 100°F/hr) Applicable for the First 16 EFPY (With Margins of 10°F and 60 psig for Instrumentation Errors, and Margin of 74 psig for Pressure Difference Between Pressure Instrumentation and Reactor Vessel Beltline Region) Including 10% Increase in Pressure for Temperatures Less than 200°F per ASME Code Case N-514	B-20
B-2	Vogtle Unit 1 Reactor Coolant System Cooldown Limitations (Cooldown rates up to 100°F/hr) Applicable for the First 16 EFPY (With Margins of 10°F and 60 psig for Instrumentation Errors, and Margin of 74 psig for Pressure Difference Between Pressure Instrumentation and Reactor Vessel Beltline Region) Including 10% Increase in Pressure for Temperatures Less than 200°F per ASME Code Case N-514	B-21

LIST OF TABLES

<u>Table</u>	<u>Title</u>	<u>Page</u>
B-1	Vogtle Unit 1 Reactor Vessel Toughness Table (Unirradiated)	B-12
B-2	Calculation of Average Copper and Nickle Weight Percent For Intermediate Shell Plates Using All Vogtle Unit 1 Chemistry Test Results	B-13
B-3	Calculation of Average Copper and Nickle Weight Percent For Lower Shell Plates Using All Vogtle Unit 1 Chemistry Test Results	B-14
B-4	Calculation of Average Copper and Nickle Weight Percent For Weld Metal Using All Vogtle Unit 1 Chemistry Test Results	B-15

LIST OF TABLES (cont.)

<u>Table</u>	<u>Title</u>	<u>Page</u>
B-5	Calculation of Chemistry Factors Using Surveillance Capsule Data	B-16
B-6	Summary of Adjusted Reference Temperatures (ART's) at 1/4-t and 3/4-t Locations for 16 EFPY	B-17
B-7	Calculation of Adjusted Reference Temperatures at 16 EFPY for the Limiting Vogtle Unit 1 Reactor Vessel Material - Intermediate Shell Plate B8805-2	B-18
B-8	Vogtle Unit 1 Heatup and Cooldown Data at 16 EFPY with Margins of 10°F and 60 psig for Instrumentation Errors	B-19

B-1. INTRODUCTION

Heatup and cooldown limit curves are calculated using the most limiting value of RT_{NDT} (reference nil-ductility transition temperature) corresponding to the limiting beltline region material for the reactor vessel. The most limiting RT_{NDT} of the material in the core region of the reactor vessel is determined by using the unirradiated reactor vessel material fracture toughness properties and estimating the radiation-induced ΔRT_{NDT} . The unirradiated RT_{NDT} is designated as the higher of either the drop weight nil-ductility transition temperature (NDTT) or the temperature at which the material exhibits at least 50 ft-lb of impact energy and 35-mil lateral expansion (normal to the major working direction) minus 60°F.

RT_{NDT} increases as the material is exposed to fast-neutron radiation. Therefore, to find the most limiting RT_{NDT} at any time period in the reactor's life, ΔRT_{NDT} due to the radiation exposure associated with that time period must be added to the original unirradiated RT_{NDT} . The extent of the shift in RT_{NDT} is enhanced by certain chemical elements (such as copper and nickel) present in reactor vessel steels. The Nuclear Regulatory Commission (NRC) has published a method for predicting radiation embrittlement in Regulatory Guide 1.99, Revision 2 (Radiation Embrittlement of Reactor Vessel Materials)^(B1). Regulatory Guide 1.99, Revision 2 is used for the calculation of adjusted reference temperature (ART) values (irradiated RT_{NDT} with margins for uncertainties) at 1/4-t and 3/4-t locations. "t" is the thickness of the vessel at the beltline region measured from the clad/base metal interface.

The pressure-temperature limit curves in Figures B-1 and B-2 of this report include margins of 10°F and 60 psig for instrumentation errors and include a pressure adjustment of 74 psig for the pressure difference between the wide-range pressure transmitter and the limiting reactor vessel pressure in the beltline region. In addition, the pressure-temperature limit curves contain the 10% relaxation in pressure for temperatures less than 200°F, per ASME Code Case N-514^(B25). The application of ASME Code Case N-514 increases the operating margin in the region of the pressure-temperature limit curves where the low temperature overpressure protection (LTOP) system is active. Although expected soon, use of the Code Case N-514 has not yet been formally approved by the NRC and therefore it is recommended that Georgia Power Company interface with the NRC to obtain their formal approval on this application of ASME Code Case N-514.

B-2. FRACTURE TOUGHNESS PROPERTIES

The fracture-toughness properties of the ferritic material in the reactor coolant pressure boundary are determined in accordance with the NRC Regulatory Standard Review Plan^[B2]. The pre-irradiation fracture-toughness properties of the Vogtle Unit 1 reactor vessel are presented in Table B-1. The irradiated fracture toughness properties of the reactor vessel beltline material were obtained directly from the Vogtle Unit 1 Reactor Vessel Radiation Surveillance Program. Credible surveillance data, as defined in Regulatory Guide 1.99 Rev. 2, is available from capsules U and Y.

B-3. CRITERIA FOR ALLOWABLE PRESSURE-TEMPERATURE RELATIONSHIPS

The ASME approach for calculating the allowable limit curves for various heatup and cooldown rates specifies that the total stress intensity factor, K_t , for the combined thermal and pressure stresses at any time during heatup or cooldown cannot be greater than the reference stress intensity factor, K_{IR} , for the metal temperature at that time. K_{IR} is obtained from the reference fracture toughness curve, defined in Appendix G of the ASME Code^[B3]. The K_{IR} curve is given by the following equation:

$$K_{IR} = 26.78 + 1.223 * e^{[0.0145 (T-RTNDT + 160)]} \quad (1)$$

where,

K_{IR} = reference stress intensity factor as a function of the metal temperature T and the metal reference nil-ductility transition temperature RTNDT

The governing equation for the heatup-cooldown analysis is defined in Appendix G of the ASME Code^[B3] as follows:

$$C * K_{IM} + K_{IT} \leq K_{IR} \quad (2)$$

where,

K_{IM} = stress intensity factor caused by membrane (pressure) stress

K_{IT} = stress intensity factor caused by the thermal gradients

K_{IR} = function of temperature relative to the RT_{NDT} of the material

C = 2.0 for Level A and Level B service limits

C = 1.5 for hydrostatic and leak test conditions when the reactor core is not critical

At any time during the heatup or cooldown transient, K_{IR} is determined by the metal temperature at the tip of the postulated flaw, the appropriate value for RT_{NDT} , and the reference fracture toughness curve. The thermal stresses resulting from the temperature gradients through the vessel wall are calculated and then the corresponding (thermal) stress intensity factors, K_{IT} , for the reference flaw are computed. From Equation 2, the pressure stress intensity factors are obtained and, from these, the allowable pressures are calculated.

For the calculation of the allowable pressure versus coolant temperature during cooldown, the reference flaw of Appendix G to the ASME Code is assumed to exist at the inside of the vessel wall. During cooldown, the controlling location of the flaw is always at the inside of the wall because the thermal gradients produce tensile stresses at the inside that increase with increasing cooldown rates. Allowable pressure-temperature relations are generated for both steady-state and finite cooldown rate situations. From these relations, composite limit curves are constructed for each cooldown rate of interest.

The use of the composite curve in the cooldown analysis is necessary because control of the cooldown procedure is based on the measurement of reactor coolant temperature, whereas the limiting pressure is actually dependent on the material temperature at the tip of the assumed flaw. During cooldown, the 1/4-t vessel location is at a higher temperature than the fluid adjacent to the vessel inner diameter. This condition, of course, is not true for the steady-state situation. It follows that, at any given reactor coolant temperature, the temperature difference across the wall developed during cooldown results in a higher value of K_{IR} at the 1/4-t location for finite cooldown rates than for steady-state operation. Furthermore, if conditions exist so that the increase in K_{IR} exceeds K_{IT} , the calculated allowable pressure during cooldown will be greater than the steady-state value.

The above procedures are needed because there is no direct control on temperature at the 1/4-t location

and, therefore, allowable pressures could be lower if the rate of cooling is decreased at various intervals along a cooldown ramp. The use of the composite curve eliminates this problem and ensures conservative operation of the system for the entire cooldown period.

Three separate calculations are required to determine the limit curves for finite heatup rates. As is done in the cooldown analysis, allowable pressure-temperature relationships are developed for steady-state conditions as well as finite heatup rate conditions assuming the presence of a 1/4-t defect at the inside of the wall. The heatup results in compressive stresses at the inside surface that alleviate the tensile stresses produced by internal pressure. The metal temperature at the crack tip lags the coolant temperature; therefore, the K_{IR} for the 1/4-t crack during heatup is lower than the K_{IR} for the 1/4-t crack during steady-state conditions at the same coolant temperature. During heatup, especially at the end of the transient, conditions may exist so that the effects of compressive thermal stresses and lower K_{IR} 's do not offset each other, and the pressure-temperature curve based on steady-state conditions no longer represents a lower bound of all similar curves for finite heatup rates when the 1/4-t flaw is considered. Therefore, both cases have to be analyzed in order to ensure that at any coolant temperature the lower value of the allowable pressure calculated for steady-state and finite heatup rates is obtained.

The third portion of the heatup analysis concerns the calculation of the pressure-temperature limitations for the case in which a 1/4-t deep outside surface flaw is assumed. Unlike the situation at the vessel inside surface, the thermal gradients established at the outside surface during heatup produce stresses which are tensile in nature and therefore tend to reinforce any pressure stresses present. These thermal stresses are dependent on both the rate of heatup and the time (or coolant temperature) along the heatup ramp. Since the thermal stresses at the outside are tensile and increase with increasing heatup rates, each heatup rate must be analyzed on an individual basis.

Following the generation of pressure-temperature curves for both the steady state and finite heatup rate situations, the final limit curves are produced by constructing a composite curve based on a point-by-point comparison of the steady-state and finite heatup rate data. At any given temperature, the allowable pressure is taken to be the lesser of the three values taken from the curves under consideration. The use of the composite curve is necessary to set conservative heatup limitations because it is possible for conditions to exist wherein, over the course of the heatup ramp, the controlling condition switches from the inside to the outside, and the pressure limit must at all times be based on analysis of the most critical situation.

Finally, the 1983 Amendment to 10CFR50^(B4) has a rule which addresses the metal temperature of the closure head flange and vessel flange regions. This rule states that the metal temperature of the closure flange regions must exceed the material unirradiated RT_{NDT} by at least 120°F for normal operation when the pressure exceeds 20 percent of the preservice hydrostatic test pressure (621 psig for Vogtle Unit 1).

Table B-1 indicates that the limiting unirradiated RT_{NDT} of 20°F occurs in the closure head flange of the Vogtle Unit 1 reactor vessel, so the minimum allowable temperature of this region is 150°F at pressures greater than 561 psig. These values include margins of 10°F and 60 psig for instrumentation errors. This limit is shown in Figures B-1 and B-2 wherever applicable.

B-4. CALCULATION OF ADJUSTED REFERENCE TEMPERATURE

From Regulatory Guide 1.99, Revision 2^(B1), the adjusted reference temperature (ART) for each material in the beltline region is given by the following expression:

$$ART = RT_{NDT} = \text{Initial } RT_{NDT} + \Delta RT_{NDT} + \text{Margin} \quad (3)$$

Initial RT_{NDT} is the reference temperature for the unirradiated material as defined in paragraph NB-2331 of Section III of the ASME Boiler and Pressure Vessel Code. If measured values of initial RT_{NDT} for the material in question are not available, generic mean values for that class of material are used if there are sufficient test results to establish a mean and standard deviation for the class.

ΔRT_{NDT} is the mean value of the adjustment in reference temperature caused by irradiation and is calculated as follows:

$$\Delta RT_{NDT} = CF * f^{(0.28 - 0.10 \log f)} \quad (4)$$

CF (°F) is the chemistry factor, obtained from the tables in Reference B1, using the average values of the copper and nickel content as reported in Tables B-1 through B-4. Some of the chemistry factors were also calculated using the surveillance capsule data in Table B-5.

To calculate ΔRT_{NDT} at any depth (e.g., at 1/4-t or 3/4-t), the following formula is used to attenuate the fluence at the specific depth.

$$f_x = f_{\text{surface}} * e^{(-0.24x)} \quad (5)$$

where x (in inches) is the depth into the vessel wall measured from the vessel clad/base metal interface. The resultant fluence is then put into equation (4) to calculate ΔRT_{NDT} at the specific depth. The calculated peak surface fluence for Vogtle Unit 1 intermediate and lower shell plates and circumferential weld at 16 EFY is 1.088×10^{19} n/cm² (E>1.0 MeV) as indicated in Section 6.0 of this report. The surface fluence for the longitudinal welds at 16 EFY is 6.216×10^{18} n/cm² (E>1.0 MeV) for weld seams located at 0° and 180°, and 6.897×10^{18} n/cm² (E>1.0 MeV) for weld seams located at 30°.

All materials in the beltline region of Vogtle Unit 1 reactor vessel were considered in determining the limiting material. The adjusted reference temperatures at 1/4-t and 3/4-t are summarized in Table B-6. From Table B-6, it can be seen that the limiting material is the Intermediate Shell Plate B8805-2 for heatup and cooldown curves applicable up to 16 EFY. Sample calculations to determine the ART values for intermediate shell plate B8805-2 at 16 EFY are shown in Table B-7.

B-5. HEATUP AND COOLDOWN PRESSURE-TEMPERATURE LIMIT CURVES

Pressure-temperature limit curves for normal heatup and cooldown of the primary reactor coolant system have been calculated for the pressure and temperature in the reactor vessel beltline region using the methods discussed in Sections B-3 and B-4 of this report^[B5]. Since indication of reactor vessel beltline pressure is not available on the plant, the pressure difference between the wide-range pressure transmitter and the limiting beltline region must be considered. Generic calculations have determined that the pressure indicated by the reactor coolant system wide-range instrumentation should be assumed to be 74 psig less than that at the reactor vessel beltline for Vogtle Unit 1^[B24]. The limit curves presented in Figures B-1 and B-2 include this pressure difference. In addition, at the request of Georgia Power Company, the heatup and cooldown curves herein were adjusted to incorporate a 10% increase in allowable pressure for temperatures less than 200°F, per ASME Code Case N-514. Code Case N-514 also requires LTOP systems to be effective at coolant temperatures less than 200°F or at coolant temperatures corresponding to a reactor vessel metal temperature less than 1/4-t $RT_{\text{NDT}} + 50^\circ\text{F}$, whichever is greater. This code case has been approved by ASME but has not yet been formally accepted by the NRC.

Figure B-1 presents the heatup curves with margins of 10°F and 60 psig for possible instrumentation

errors using a heatup rates up to 100°F/hr applicable for the first 16 EFPY. Figure B-2 presents the cooldown curves with margins of 10°F and 60 psig for possible instrumentation errors using cooldown rates up to 100°F/hr applicable for the first 16 EFPY. Allowable combinations of temperature and pressure for specific temperature change rates are below and to the right of the limit lines shown in Figures B-1 and B-2. This is in addition to other criteria that must be met before the reactor is made critical.

The reactor must not be made critical until pressure-temperature combinations are to the right of the criticality limit line shown in Figure B-1. The straight-line portion of the criticality limit is at the minimum permissible temperature for the 2485 psig inservice hydrostatic test as required by Appendix G to 10CFR Part 50^(B4). The governing equation for the hydrostatic test is defined in Appendix G to Section III of the ASME Code as follows:

$$1.5 K_{IM} \leq K_{IR} \quad (6)$$

where,

K_{IM} is the stress intensity factor covered by membrane (pressure) stress,

$$K_{IR} = 26.78 + 1.233 e^{[0.0145 (T - RTNDT + 160)]},$$

T is the minimum permissible metal temperature, and

RTNDT is the metal reference nil-ductility transition temperature.

The criticality limit curve shown in Figure B-1 specifies pressure-temperature limits for core operation to provide additional margin during actual power production as specified in Reference B4. The pressure-temperature limits for core operation (except for low power physics tests) require that the reactor vessel be at a temperature equal to or higher than the minimum temperature required for the inservice hydrostatic test, and at least 40°F higher than the minimum permissible temperature in the corresponding pressure-temperature curve for heatup and cooldown calculated as described in Section B-3. The minimum temperature for the inservice hydrostatic leak test for the Vogtle Unit 1 reactor vessel at 16 EFPY is 246°F. A vertical line drawn from these points on the pressure-temperature curve, intersecting a curve 40°F higher than the pressure-temperature limit curve, constitutes the limit for core operation for the reactor vessel. This curve includes margins of 10°F and 60 psig for instrumentation errors.

Figures B-1 and B-2 define all of the above limits for ensuring prevention of nonductile failure for the Vogtle Unit 1 reactor vessel. These figures include an instantaneous pressure change at 200°F, as a

result of applying ASME Code Case N-514, which could cause an additional pressure transient if the pressure-temperature limit curves were exactly followed. This transient can be avoided during normal heatup conditions by not exceeding the lower bound pressure value at 200°F until the reactor coolant system water temperature is greater than 200°F (i.e., using the 60°F/Hr heatup curve in Figure B-1, hold the pressure value of 837.97 psig constant for the temperature range between 189°F and 200°F). For normal cooldown conditions, the curves allow an increase in allowable pressure at temperatures below 200°F, therefore the pressure transient increases operating window margins and causes no adverse effect on cooldown operations. The data points used to develop the heatup and cooldown pressure-temperature limit curves shown in Figures B-1 and B-2 are presented in Table B-8.

Table B-1

Vogtle Unit 1 Reactor Vessel Toughness Table (Unirradiated)^(B7)

Material Description	Cu (%) *	Ni (%) *	Initial RT _{NDT} (°F) ^(a)
Closure Head Flange	--	0.70	20 ^(b)
Vessel Flange	--	0.71	0 ^(b)
Intermediate Shell Plate B8805-1	0.083	0.597	0
Intermediate Shell Plate B8805-2	0.083	0.610	20
Intermediate Shell Plate B8805-3	0.062	0.598	30
Lower Shell Plate B8606-1	0.053	0.593	20
Lower Shell Plate B8606-2	0.057	0.600	20
Lower Shell Plate B8606-3	0.067	0.623	10
Intermediate & Lower Shell Vertical Weld Seams and Girth Seam Weld	0.039	0.102	-80

(a) Initial RT_{NDT} values are measured values.

(b) These values are used for considering flange requirements for the heatup/cool-down curves^(B4).

* The average values of copper and nickel content determined as indicated in Tables B-2 through B-4 on the following pages.

Table B-2

Calculation of Average Copper and Nickel Weight Percent For Intermediate Shell Plates
Using All Vogtle Unit 1 Chemistry Test Results

Reference	Inter. Shell Plate B8805-1		Inter. Shell Plate B8805-2		Inter. Shell Plate B8805-3	
	Cu (wt%)	Ni (wt%)	Cu (wt%)	Ni (wt%)	Cu (wt%)	Ni (wt%)
Matl. Cert. Report ^[B8]	0.09	0.60				
Matl. Cert. Report ^[B8]	0.08	0.60				
Chemical Analysis ^[B9]	0.08	0.59				
Surveillance Program ^[B6]	0.08*	0.59*				
Matl. Cert. Report ^[B10]			0.09	0.64		
Matl. Cert. Report ^[B10]			0.08	0.60		
Chemical Analysis ^[B11]			0.08	0.59		
Surveillance Program ^[B6]			0.08*	0.59*		
Matl. Cert. Report ^[B12]					0.07	0.60
Matl. Cert. Report ^[B12]					0.07	0.61
Chemical Analysis ^[B13]					0.06	0.60
Surveillance Program ^[B6]					0.058	0.61
Surveillance Program ^[B6]					0.06*	0.60*
Capsule U Report ^[B7]					0.053	0.586
Capsule U Report ^[B7]					0.06*	0.60*
Capsule U Report ^[B7]					0.058*	0.61*
Chemical Analysis ^[B14]					0.061	0.584
Average	0.083	0.597	0.083	0.610	0.062	0.598

* Not used in average calculation since same as in other references; reported only for completeness.

Table B-3

Calculation of Average Copper and Nickel Weight Percent For Lower Shell Plates
Using All Vogtle Unit 1 Chemistry Test Results

Reference	Lower Shell Plate B8606-1		Lower Shell Plate B8606-2		Lower Shell Plate B8606-3	
	Cu (wt%)	Ni (wt%)	Cu (wt%)	Ni (wt%)	Cu (wt%)	Ni (wt%)
Matl. Cert. Report ^[B15]	0.06	0.61				
Matl. Cert. Report ^[B15]	0.05	0.58				
Chemical Analysis ^[B16]	0.05	0.59				
Surveillance Program ^[B6]	0.05*	0.59*				
Matl. Cert. Report ^[B17]			0.07	0.64		
Matl. Cert. Report ^[B17]			0.05	0.58		
Chemical Analysis ^[B18]			0.05	0.58		
Surveillance Program ^[B6]			0.05*	0.58*		
Matl. Cert. Report ^[B19]					0.07	0.60
Matl. Cert. Report ^[B19]					0.07	0.63
Chemical Analysis ^[B20]					0.06	0.64
Surveillance Program ^[B6]					0.06*	0.64*
Average	0.053	0.593	0.057	0.600	0.067	0.623

* Not used in average calculation since same as in other references; reported only for completeness.

Table B-4

Calculation of Average Copper and Nickel Weight Percent For Weld Metal
Using All Vogtle Unit 1 Chemistry Test Results

Reference	Weld Metal**	
	Cu (wt%)	Ni (wt%)
Surveillance Program ^[B6]	0.030	- -
Surveillance Program ^[B6]	0.040	0.100
Surveillance Program ^[B6]	0.037	0.100
Capsule U Report ^[B7]	0.035	0.091
Chemical Analysis ^[B14]	0.048	0.101
Chemical Analysis ^[B14]	0.040	0.117
Chemical Analysis ^[B14]	0.041	0.105
Chemical Analysis ^[B21]	0.040*	0.100*
Chemical Analysis ^[B22]	0.030*	- -*
Average	0.039	0.102

* Not used in average calculation since same as in other references; reported only for completeness.

** The surveillance weld is identical to that used in the core region for the longitudinal seam welds and the girth seam weld joining the intermediate and lower shells. All core region (beltline) welds were fabricated using Weld Wire Heat Number 83653, Linde 0091 Flux, Lot Number 3536.

Table B-5

Calculation of Chemistry Factors Using Surveillance Capsule Data

Material	Capsule	Fluence (n/cm ² , E>1.0 MeV)	FF	$\Delta RT_{NDT}^{(b)}$ (°F)	FF* ΔRT_{NDT} (°F)	FF ²
Inter. Shell Plate B8805-3 (Longitudinal)	U	3.437 x 10 ^{18 (a)}	0.706	15	10.585	0.498
	Y	1.242 x 10 ¹⁹	1.060	40	42.4	1.124
Inter. Shell Plate B8805-3 (Transverse)	U	3.437 x 10 ^{18 (a)}	0.706	0	0	0.498
	Y	1.242 x 10 ¹⁹	1.060	20	21.2	1.124
	Sum:				74.185	3.244
	Chemistry Factor = 74.185 ÷ 3.244 = 22.9					
Weld Metal	U	3.437 x 10 ^{18 (a)}	0.706	15	10.585	0.498
	Y	1.242 x 10 ¹⁹	1.060	0	0	1.124
	Sum:				10.585	1.622
	Chemistry Factor = 10.585 ÷ 1.622 = 6.5					

- (a) Original fluence value has been revised to be based on actual cycle burn up instead of predicted (original value = 3.41×10^{18} from capsule U report, WCAP-12256).
- (b) The weld metal ΔRT_{NDT} values contain no adjustment ratio per Regulatory Guide 1.99, Rev. 2 Position 2.1 since the surveillance weld is identical to that used in the core region of the longitudinal seams and the girth seam weld joining the intermediate and lower shells.

Table B-6

Summary of Adjusted Reference Temperatures (ART's)
at 1/4-t and 3/4-t Locations for 16 EFPY

Component	16 EFPY ART ^(a)	
	1/4-t (°F)	3/4-t (°F)
Intermediate Shell Plate B8805-1	80.7	64.1
Intermediate Shell Plate B8805-2	100.7 ^(b)	84.1 ^(b)
Intermediate Shell Plate B8805-3	97.5	76.4
Inter. Shell Plate B8805-3 Using S/C Data	67.1 ^(c)	57.6 ^(c)
Lower Shell Plate B8606-1	77.6	59.6
Lower Shell Plate B8606-2	81.9	62.5
Lower Shell Plate B8606-3	80.8	60.6
Circ. Weld 101-171	-21.7	-39.9
Circ. Weld Using S/C Data	-68.6 ^(c)	-72.2 ^(c)
Long. Weld 101-124A	-31.8	-48.5
Long. Weld 101-124B	-30.0	-47.0
Long. Weld 101-124C	-30.0	-47.0
Long. Weld 101-142A	-30.0	-47.0
Long. Weld 101-142B	-31.8	-48.5
Long. Weld 101-142C	-30.0	-47.0

- (a) Based on surface fluence of 1.088×10^{19} (n/cm², E>1.0 MeV).
- (b) These ART values are used to generate heatup and cooldown curves.
- (c) Numbers were calculated using a chemistry factor based on surveillance capsule data.

Table B-7

Calculation of Adjusted Reference Temperatures at 16 EFPY
for the Limiting Vogtle Unit 1 Reactor Vessel Material - Intermediate Shell Plate B8805-2

Parameter	ART Values	
Operating Time	16 EFPY	
Material	B8805-2	B8805-2
Location	1/4-t	3/4-t
Chemistry Factor, CF (°F)	53.1	53.1
Fluence/(10^{19} n/cm ² , E>1.0 MeV), f ^(a)	0.6485	0.2303
Fluence Factor, FF ^(b)	0.879	0.604
$\Delta RT_{NDT} = CF \times FF$ (°F)	46.653	32.056
Initial RT_{NDT} , I (°F)	20	20
Margin, M (°F) ^(c)	34	32.056
ART = I + (CFxFF) + M (°F) per Regulatory Guide 1.99, Revision 2 ^(B1)	100.7	84.1

- (a) Fluence, f, is based upon f_{surf} (10^{19} n/cm², E>1.0 MeV) = 1.088 at 16 EFPY. The Vogtle Unit 1 reactor vessel wall thickness is 8.625 inches at the beltline region.
- (b) Fluence Factor per equation (4) is defined by $FF = f^{(0.28 - 0.10 \log f)}$.
- (c) Margin is calculated as, $M = 2 \sqrt{(\sigma_i^2 + \sigma_{\Delta}^2)}$. The standard deviation for the initial RT_{NDT} margin term, σ_i , is 0°F since the initial RT_{NDT} is a measured value. The standard deviation for ΔRT_{NDT} term, σ_{Δ} , is 17°F for the plate, except that σ_{Δ} need not exceed 0.5 times the mean value of ΔRT_{NDT} . σ_{Δ} is 8.5°F for the plate (half the value) when surveillance data is used.

Table B-8

Vogtle Unit 1 Heatup and Cooldown Data at 16 EFPY with Margins of 10°F and 60 psig for Instrumentation Errors

Includes 1) 10% increase in pressure for temperatures less than 200°F per ASME code case N-514, 2) vessel flange requirements of 150°F and 561 psig per 10CFR50, and 3) pressure adjustment of 74 psig to account for pressure difference between the wide-range pressure transmitter and the limiting beltline region of the reactor vessel.

Steady State		20 CD		40 CD		60 CD		100 CD		60 HU		Criticality Limit		100 HU		Criticality Limit		Hydrostatic Leak Test	
T	P	T	P	T	P	T	P	T	P	T	P	T	P	T	P	T	P	T	P
70	492.57	70	449.33	70	405.48	70	360.87	70	269.82	70	460.15	246	0.00	70	424.95	246	0.00	225	2000
75	502.30	75	459.46	75	416.16	75	372.27	75	282.71	75	460.15	246	411.59	75	424.95	246	379.59	246	2485
80	512.62	80	470.45	80	427.77	80	384.57	80	296.62	80	460.15	246	411.59	80	424.95	246	379.59		
85	523.87	85	482.31	85	440.32	85	397.88	85	311.76	85	460.15	246	411.59	85	424.95	246	379.59		
90	535.96	90	495.06	90	453.81	90	412.12	90	328.02	90	460.15	246	411.59	90	424.95	246	379.59		
95	543.10	95	508.82	95	468.28	95	427.63	95	345.74	95	460.15	246	411.59	95	424.95	246	379.59		
100	543.10	100	523.47	100	483.98	100	444.34	100	364.79	100	461.72	246	413.02	100	424.95	246	379.59		
105	543.10	105	539.40	105	500.93	105	462.29	105	385.51	105	465.69	246	416.63	105	424.95	246	379.59		
110	543.10	110	543.10	110	519.02	110	481.76	110	407.88	110	472.04	246	422.40	110	424.95	246	379.59		
115	543.10	115	543.10	115	538.70	115	502.79	115	431.99	115	480.33	246	429.94	115	424.95	246	379.59		
120	543.10	120	543.10	120	543.10	120	525.29	120	458.10	120	490.67	246	439.34	120	426.75	246	381.23		
125	543.10	125	543.10	125	543.10	125	543.10	125	486.23	125	502.80	246	450.36	125	430.31	246	384.46		
130	543.10	130	543.10	130	543.10	130	543.10	130	516.56	130	516.66	246	462.96	130	435.65	246	389.32		
135	543.10	135	543.10	135	543.10	135	543.10	135	543.10	135	532.41	246	477.28	135	442.68	246	395.71		
140	543.10	140	543.10	140	543.10	140	543.10	140	543.10	140	543.10	246	487.00	140	451.44	246	403.67		
145	543.10	145	543.10	145	543.10	145	543.10	145	543.10	145	543.10	246	487.00	145	461.76	246	413.05		
150	543.10	150	543.10	150	543.10	150	543.10	150	543.10	150	543.10	246	487.00	150	473.93	246	424.12		
150	774.67	150	749.28	150	725.38	150	702.99	150	664.28	150	590.60	246	530.18	155	487.83	246	436.75		
155	805.46	155	782.19	155	760.80	155	741.02	155	708.71	155	613.84	246	551.31	160	503.52	246	451.02		
160	838.45	160	817.81	160	798.82	160	781.97	160	756.53	160	639.00	246	574.18	165	520.89	246	466.81		
165	874.18	165	855.93	165	839.76	165	826.30	165	808.15	165	666.42	246	599.11	170	540.32	246	484.47		
170	912.38	170	896.85	170	883.99	170	873.83	170	863.72	170	695.99	246	625.99	175	561.70	246	503.91		
175	953.37	175	940.88	175	931.41	175	924.99	175	923.59	175	727.87	246	654.97	180	585.03	246	525.12		
180	997.40	180	988.41	180	982.41	180	979.99	180	988.01	180	762.53	246	686.48	185	610.65	246	548.41		
185	1044.72	185	1039.34	185	1037.29	185	1039.18			185	799.65	246	720.23	190	638.42	246	573.65		
190	1095.77	190	1094.07							190	839.63	246	756.57	195	668.72	246	601.20		
195	1150.22									195	882.84	246	795.85	200	701.46	246	630.96		
200	1208.94									200	929.17	246	837.97	200	630.96	246	630.96		
200	1092.31									200	837.97	246	837.97	205	663.11	246	663.11		
205	1149.67									205	883.21	246	883.21	210	698.05	250	698.05		
210	1211.10									210	931.85	250	931.85	215	735.63	255	735.63		
215	1276.80									215	984.06	255	984.06	220	776.14	260	776.14		
220	1347.74									220	1039.90	260	1039.90	225	819.75	265	819.75		
225	1423.41									225	1100.16	265	1100.16	230	866.71	270	866.71		
230	1504.91									230	1164.70	270	1164.70	235	917.23	275	917.23		
235	1591.99									235	1233.69	275	1233.69	240	971.48	280	971.48		
240	1685.30									240	1308.02	280	1308.02	245	1029.79	285	1029.79		
245	1785.26									245	1387.43	285	1387.43	250	1092.22	290	1092.22		
250	1892.15									250	1472.31	290	1472.31	255	1159.47	295	1159.47		
255	2006.55									255	1563.28	295	1563.28	260	1231.28	300	1231.28		
260	2128.76									260	1660.77	300	1660.77	265	1308.60	305	1308.60		
265	2259.41									265	1765.08	305	1765.08	270	1391.31	310	1391.31		
270	2398.54									270	1876.53	310	1876.53	275	1479.80	315	1479.80		
										275	1995.33	315	1995.33	280	1574.52	320	1574.52		
										280	2122.41	320	2122.41	285	1675.74	325	1675.74		
										285	2257.67	325	2257.67	290	1783.98	330	1783.98		
										290	2401.70	330	2401.70	295	1899.51	335	1899.51		
														300	2023.06	340	2023.06		
														305	2154.59	345	2154.59		
														310	2294.65	350	2294.65		

MATERIAL PROPERTY BASIS

LIMITING MATERIAL: INTERMEDIATE SHELL PLATE B8805-2

LIMITING ART AT 16 EFPY: 1/4-t, 100.7°F

3/4-t, 84.1°F

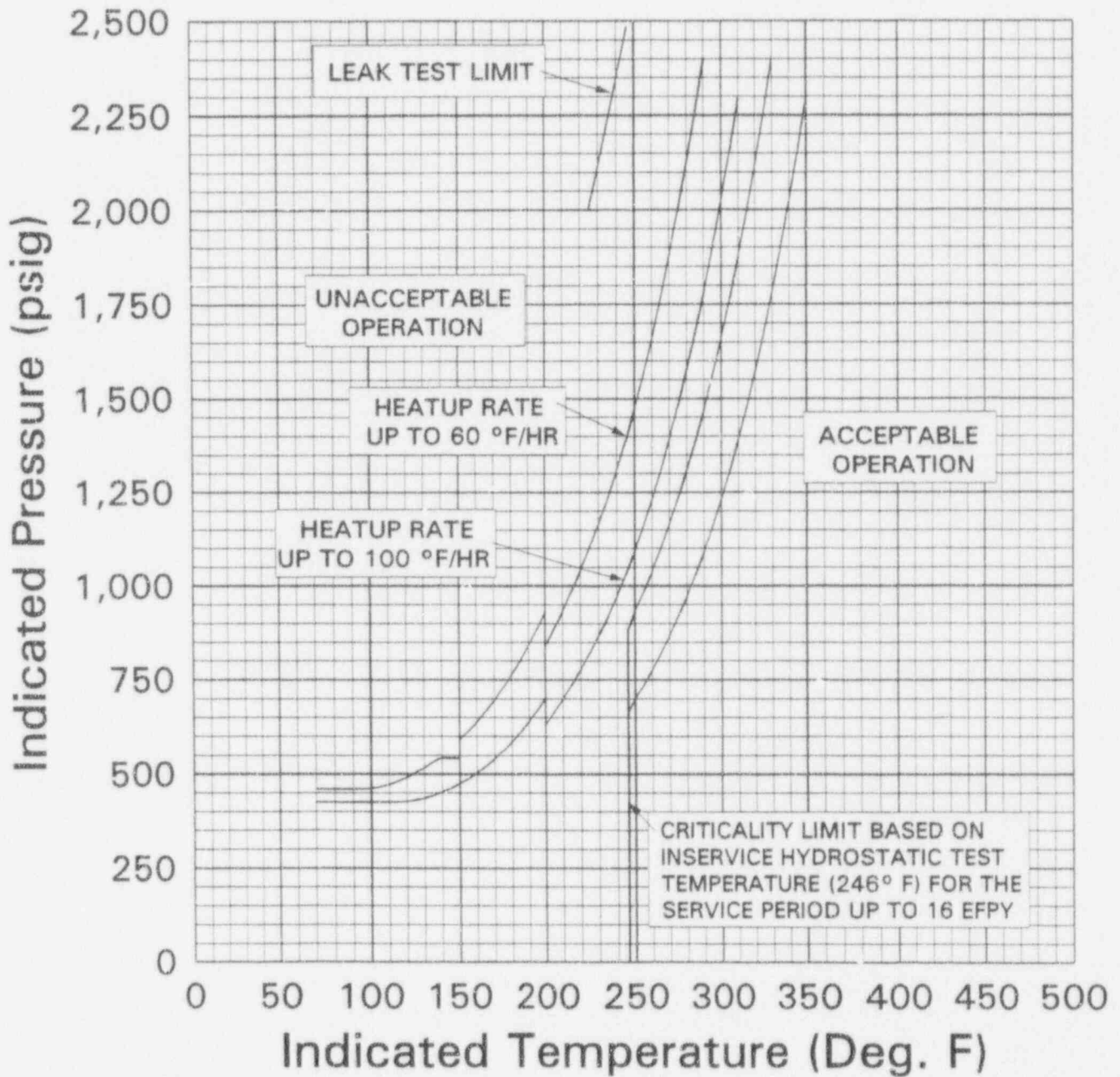


Figure B-1 Vogtle Unit 1 Reactor Coolant System Heatup Limitations (Heatup rates up to 100°F/hr) Applicable for the First 16 EFPY (With Margins of 10°F and 60 psig for Instrumentation Errors, and Margin of 74 psig for Pressure Difference Between Pressure Instrumentation and Reactor Vessel Beltline Region) Including 10% Increase in Pressure for Temperatures Less than 200°F per ASME Code Case N-514

MATERIAL PROPERTY BASIS

LIMITING MATERIAL: INTERMEDIATE SHELL PLATE B8805-2

LIMITING ART AT 16 EFPY: 1/4-t, 100.7°F

3/4-t, 84.1°F

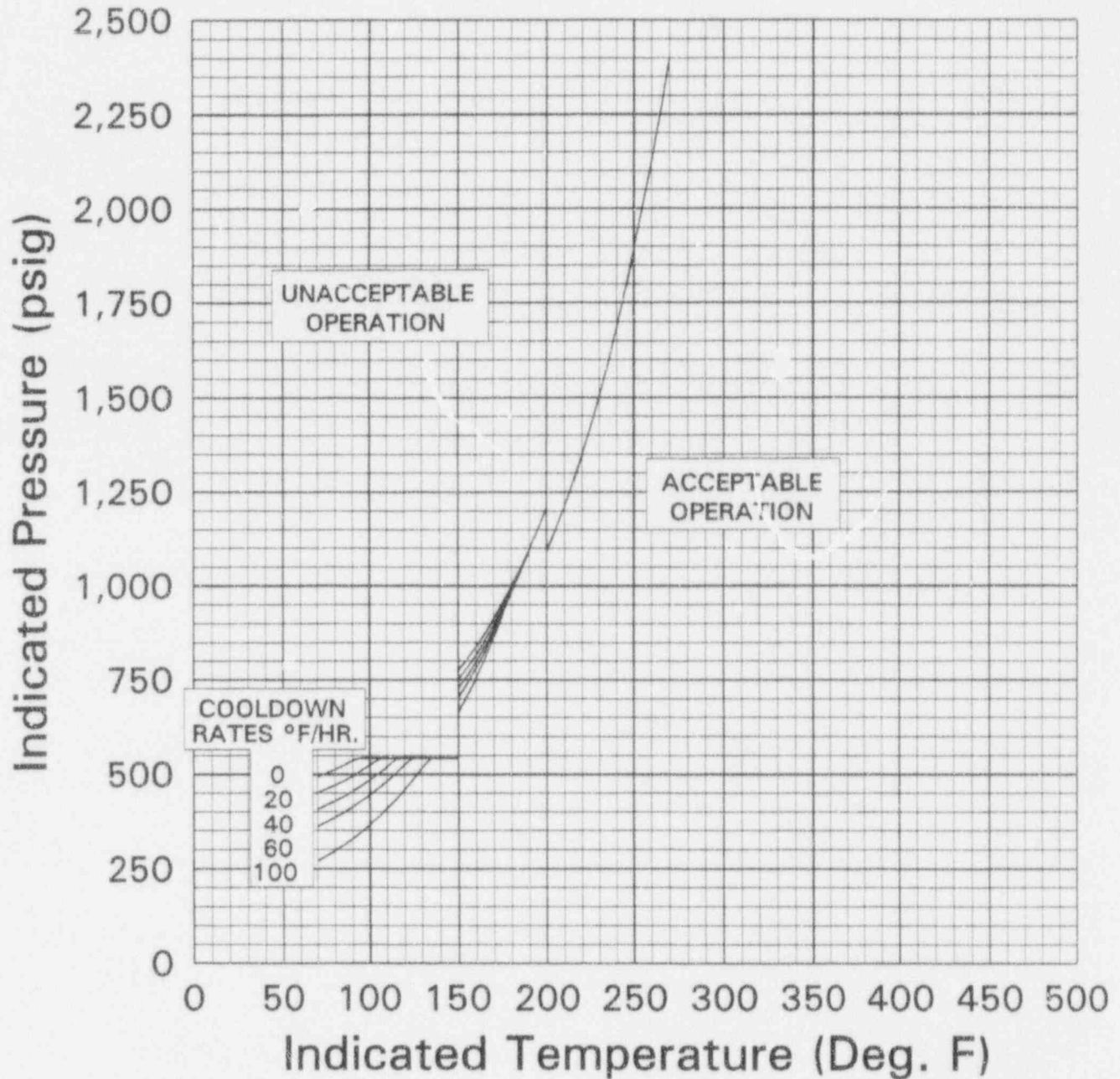


Figure B-2 Vogtle Unit 1 Reactor Coolant System Cooldown Limitations (Cooldown rates up to 100°F/hr) Applicable for the First 16 EFPY (With Margins of 10°F and 60 psig for Instrumentation Errors, and Margin of 74 psig for Pressure Difference Between Pressure Instrumentation and Reactor Vessel Beltline Region) Including 10% Increase in Pressure for Temperatures Less than 200°F per ASME Code Case N-514

B-6. REFERENCES

- [B1] Regulatory Guide 1.99, Revision 2, "Radiation Embrittlement of Reactor Vessel Materials", U.S. Nuclear Regulatory Commission, May, 1988.
- [B2] "Fracture Toughness Requirements", Branch Technical Position MTEB 5-2, Chapter 5.3.2 in Standard Review Plan for the Review of Safety Analysis Reports for Nuclear Power Plants, LWR Edition, NUREG-0800, 1981.
- [B3] ASME Boiler and Pressure Vessel Code, Section III, Division 1 - Appendices, "Rules for Construction of Nuclear Power Plant Components, Appendix G, Protection Against Nonductile Failure", pp. 558-563, 1986 Edition, American Society of Mechanical Engineers, New York, 1986.
- [B4] Code of Federal Regulations, 10CFR50, Appendix G, "Fracture Toughness Requirements", U.S. Nuclear Regulatory Commission, Washington, D.C., Federal Register, Vol. 48 No. 104, May 27, 1983.
- [B5] WCAP-7924-A, "Basis for Heatup and Cooldown Limit Curves", W. S. Hazelton, et al., April 1975.
- [B6] WCAP-11011, "Georgia Power Company Alvin W. Vogtle Unit No. 1 Reactor Vessel Radiation Surveillance Program", L. R. Singer, February 1986.
- [B7] WCAP-12256, "Analysis of Capsule U from the Georgia Power Company Vogtle Unit 1 Reactor Vessel Radiation Surveillance Program", S. E. Yanichko, et al., May 1989.
- [B8] Combustion Engineering Inc., Metallurgical Research and Development Materials Certification Report, Contract No. 8971, Job No. 708124-001, Code No. B-8805-1, Heat No. C0613-1, dated October 5, 1972 and Lukens Steel Company Test Certificate, Mill Order No. 10554-1, dated April 25, 1972.
- [B9] Combustion Engineering Power Systems Interoffice Correspondence to A.B. Harper from W.A. House, Lab No. P18955, Inter. Shell Code B8805-1, dated March 22, 1979.
- [B10] Combustion Engineering Inc., Metallurgical Research and Development Materials Certification Report, Contract No. 8971, Job No. 708124-003, Code No. B-8805-2, Heat No. C0613-2, dated October 5, 1972 and Lukens Steel Company Test Certificate, Mill Order No. 10554-1, dated May 9, 1972.
- [B11] Combustion Engineering Power Systems Interoffice Correspondence to A.B. Harper from W.A. House, Lab No. P18596, Inter. Shell Code B8805-2, dated March 22, 1979.
- [B12] Combustion Engineering Inc., Metallurgical Research and Development Materials Certification Report, Contract No. 8971, Job No. 708124-005, Code No. B-8805-3, Heat No. C0623-1, dated October 5, 1972 and Lukens Steel Company Test Certificate, Mill Order No. 10554-1, dated May 16, 1972.

- [B13] Combustion Engineering Power Systems Interoffice Correspondence to A.B. Harper from W.A. House, Lab No. P18957, Inter. Shell Code B8805-3, dated March 22, 1979.
- [B14] Analytical Request # 15177, "Alloy Analysis Irradiated Low Alloy Steel, Georgia Power Company Vogtle Unit 1 Nuclear Plant", Lawrence Kardos, 11/10/93.
- [B15] Combustion Engineering Inc., Metallurgical Research and Development Materials Certification Report, Revision 1, Contract No. 8971, Job No. 708142-007, Code No. B-8606-1, Heat No. C2146-1, dated March 29, 1974 and Lukens Steel Company Test Certificate, Mill Order No. 12517-2, dated March 23, 1973.
- [B16] Combustion Engineering Power Systems Interoffice Correspondence to A.B. Harper from W.A. House, Lab No. P15703, Code B8606-1, dated October 30, 1978.
- [B17] Combustion Engineering Inc., Metallurgical Research and Development Materials Certification Report, Revision 1, Contract No. 8971, Job No. 708142-013, Code No. B-8606-2, Heat No. C2146-2, dated March 29, 1974 and Lukens Steel Company Test Certificate, Mill Order No. 12517-2, dated March 23, 1973.
- [B18] Combustion Engineering Power Systems Interoffice Correspondence to A.B. Harper from W.A. House, Lab No. P13986, Code B8606-2, dated October 30, 1978.
- [B19] Combustion Engineering Inc., Metallurgical Research and Development Materials Certification Report, Revision 1, Contract No. 8971, Job No. 708142-011, Code No. B-8606-3, Heat No. C2085-2, dated March 29, 1974 and Lukens Steel Company Test Certificate, Mill Order No. 12517-1, dated March 30, 1973.
- [B20] Combustion Engineering Power Systems Interoffice Correspondence to A.B. Harper from W.A. House, Lab No. P15704, Code B8606-3, dated October 30, 1978.
- [B21] Combustion Engineering Power Systems Welding Material Qualification To Requirements of ASME Section III, Job No. D32255, Project Number 960009, dated November 6, 1972.
- [B22] Combustion Engineering Power Systems Interoffice Correspondence from P. C. Kiefer, Qualification Code G1.43, Job No. D32255, dated November 2, 1972.
- [B23] ASME Boiler and Pressure Vessel Code Case N-514, Section XI, Division 1, "Low Temperature Overpressure Protection", Approval date: February 12, 1992.
- [B24] Nuclear Safety Advisory Letter, NSAL-93-005A, "Cold Overpressure Mitigation System (COMS) Nonconservatism", 3-10-93.